Retention and toxicity of uremic solutes in chronic kidney disease

Rick Mutsaers

ISBN 978-94-6259-197-4

Cover and layout design
Promotie In Zicht, Arnhem

Cover art
Collin van der Sluijs

Print
Ipskamp Drukkers, Enschede

The research presented in this thesis was performed at the departments of Pharmacology and Toxicology, Physiology and Pediatrics, Radboud University Medical Center, Nijmegen, the Netherlands and financially supported by the Dutch Kidney Foundation, grant IK08.03.

Financial support for the printing of this thesis by the Radboud University, Nijmegen, the Netherlands is gratefully acknowledged.

Retention and toxicity of uremic solutes in chronic kidney disease

Proefschrift

ter verkrijging van de graad van doctor
aan de Radboud Universiteit Nijmegen
op gezag van de rector magnificus prof. mr. S.C.J.J. Kortmann,
volgens besluit van het college van decanen
in het openbaar te verdedigen op donderdag 4 september 2014
om 12.30 uur precies

door

Henricus Antonius Maria Mutsaers
Geboren op 14 februari 1985
te Oss

Promotoren

Prof. dr. J.G.J. Hoenderop
Prof. dr. L.P.W.J. van den Heuvel

Copromotor

Dr. R. Masereeuw

Manuscriptcommissie

Prof. dr. D.M. Burger *(voorzitter)*
Prof. dr. A.J. van Gool
Prof. dr. G.J. Navis *(UMCG)*

CONTENTS

LIST OF ABBREVIATIONS

[^{3}H]-E1S	[^{3}H]-estrone sulfate
[^{3}H]-MTX	[^{3}H]-methotrexate
1-MH	1-methylhistidine
2-HIBA	2-hydroxyisobutyric acid
3-MH	3-methylhistidine
7-OHC	7-hydroxycoumarin
7-OHCG	7-hydroxycoumarin glucuronide
AA	antimycin A
ABC	ATP-binding cassette
AhR; AHR	aryl hydrocarbon receptor
AMP	adenosine monophosphate
ANOVA	analysis of variance
ARNT	AhR nuclear translocator
ATP	adenosine-5′-triphosphate
BCRP	breast cancer resistance protein
BioKid	bioartificial kidney
CAPD	continuous ambulatory peritoneal dialysis
ciPTEC	conditionally immortalized human renal proximal tubule epithelial cells
ciPTEC-T	ciPTEC isolated from renal tissue
CKD	chronic kidney disease
C_m	concentration determined in this study
C_{max}	maximal uremic concentrations
CMPF	3-carboxy-4-methyl-5-propyl-2-furanpropanoic acid
CRF	chronic renal failure
Ct	cycle threshold
C_u	mean/median uremic concentration
CYP	cytochrome p450
$DMSO_2$	dimethyl sulphone
E; ETS	electron transport system
E1S	estrone sulfate
EDX	energy-dispersive X-ray
eGFR	estimated glomerular filtration rate
ELISA	enzyme-linked immunosorbent assay
EM	electron microscopy
EMT	epithelial-to-mesenchymal transition
ER	endoplasmic reticulum
ESRD	end-stage renal disease
EUTox	European Uremic Toxin Workgroup

EYFP; eYFP	enhanced yellow fluorescent protein
FCCP	p-trifluoromethoxy carbonyl cyanide phenyl hydrazone
FCS	fetal calf serum
FVB	friend leukemia virus B
GAPDH	glyceraldehyde-3-phosphate dehydrogenase
GST	glutathione S-transferase
h	hour
HA	hippuric acid
HD	hemodialysis
HE	hematoxylin and eosin
HEK293	human embryonic kidney cells
HP	high protein
HPLC	high-performance liquid chromatography
Hsp	heat shock protein
I3A; IAA	indole-3-acetic acid
IDO	indoleamine 2,3-dioxygenase
IS	indoxyl sulfate
KA	kynurenic acid
Ki	inhibition constant
KIM-1	kidney injury molecule-1
L	LEAK
LC-MS/MS	Liquid chromatography-tandem mass spectrometry
LN	natural logarithm
M	medium
m/z	mass-to-charge ratio
MATE	multidrug and toxin extrusion protein
MDRD	Modification of Diet in Renal Disease
min	minute
MRP4	multidrug resistance protein 4
MTT	3-[4,5-dimethylthiazol-2-yl]-2,5-diphenyl tetrazolium bromide
MTX	methotrexate
N	normal
N2a	malignant neuroblastoma cells
NA	not applicable
NAD+	nicotinamide adenine dinucleotide
NAT	N-acetyltransferase
ND	not determined
Ngal	neutrophil gelatinase-associated lipocalin
NMDA	*N*-methyl-d-aspartate
NMR	nuclear magnetic resonance
OAT	organic anion transporter
OCT	organic cation transporter
omy	oligomycin A
Ox	oxalate
OXPHOS	oxidative phosphorylation
pC; PC	*p*-cresol
PCA	perchloric acid
pCG	*p*-cresyl glucuronide
pCS	*p*-cresyl sulfate
P-gp	P-glycoprotein
PHA; PhA; PA	phenylacetic acid
PhG	phenyl glucuronide
PhS	phenyl sulfate
PTA	*p*-toluenesulfonic acid
PTEC	proximal tubule epithelial cells
Pu	putrescine
QA	quinolinic acid
R	Routine
ROT	rotenone
ROX	residual oxygen consumption
RT	room temperature
SCr	serum creatinine
SD	standard deviation
SEM	standard error of the mean
SLC	solute carrier family
SLCO4C1	organic anion transporting polypeptide 4C1
SNP	single nucleotide polymorphisms
SRM	selected reaction monitoring
SULT	sulfotransferase
TCDD	2,3,7,8-tetrachlorodibenzo-*p*-dioxin
TSP	trimethylsilyl-2,2,3,3-tetradeuteropropionic acid
UDPGA	UDP-glucuronic acid
UGT	UDP-glucuronosyltransferases
URAT1	urate transporter 1
WT	wild type
ZO-1	tight junction protein 1
α7nAch	α7-nicotinic-acetylcholine

1

General introduction

In part published as:
The kidney and uremic toxin removal: glomerulus or tubule?

Rosalinde Masereeuw, Henricus A.M. Mutsaers, Takafumi Toyohara, Takaaki Abe, Sachin Jhawar, Douglas H. Sweet and Jerome Lowenstein

Seminars in Nephrology, Volume: 34, Issue: 2, Page: 191-208, 2014

Throughout history, ancient tribes and civilizations have displayed a clear understanding of the essential role the kidney plays in sustaining life. For instance, the Aborigines of Australia believe that the kidney houses the kurrunpa or spirit, and it is reported that they wore a piece of kidney as an amulet around the neck to protect themselves against harmful spells [1]. In ancient Egypt, the heart and kidney were the only organs not removed from the body during mummification, indicating that they were considered important, although it is still unclear what mythical significance was bestowed upon the kidney [2]. Moreover, in the Bible (*i.e.* the Christian Old Testament), the kidney is mentioned over 30 times, often in conjunction with the heart, whereas the brain is never mentioned [1,3]. Of note, in the scriptures the kidney is regarded as the seat of conscience, emotions and wisdom [3]. And in the Talmud, the presence of two kidneys is explained as there being one to give good and the other bad advice [3]. Moreover, in the teachings from Saint Ephrem the Syrian (ca. 306 to 373 AD) it is stated that: "In the kidneys are seated reasonings, and there dwells in them the faculty of discernment; they distinguish truth from falsehood, and judge what is base and what is noble". Eloquently summarizing the current understanding of normal renal functioning.

Uremia

The main role of the kidney is recycling nutrients and removing endogenous and exogenous waste products, and for this seemingly easy task the kidney is equipped with an ingenious system of filters and smart plumbing, the so-called nephrons. When the kidneys fail, patients will develop uremia – a term generally used to describe the illness accompanying kidney failure – due to the accumulation of organic waste products normally cleared by the kidney [4]. Approximately 10% of the adult population in the developed countries suffers from chronic kidney disease (CKD) [5], and in half of these patients the diagnosis of CKD is based on the presence of a reduced kidney function defined by a reduction in estimated glomerular filtration rate (eGFR). Although features of uremic illness are most pronounced in patients with end-stage renal disease (ESRD; Stage 5 CKD: eGFR < 15 ml/min/1.73 m^2), symptoms associated with uremia may be present to a lesser extent in people with a GFR that is barely below 50% of the normal rate, which ranges between 100 – 120 ml/min/1.73 m^2, at 30 years of age [4]. Uremic illness is a complex disorder illustrated by the diverse clinical signs and symptoms associated with the disease, such as fatigue, cognitive impairment, insulin resistance, bone disease and anemia [6-11]. Thus, it is not surprising that the quality of life is very low in CKD patients. Due to a lack of donor kidneys, uremia treatment is currently dominated by dialysis. The concept of dialysis was first devised by the Scottish chemist Thomas Graham who, in 1861, observed that by using vegetable parchment as a semipermeable membrane, colloid and crystalloid substances contained in fluids could be separated by diffusion [12]. In 1945, Kolff reported for the first time the successful implementation of hemodialysis to treat acute renal failure using the "rotating drum kidney" (developed in Kampen, the Netherlands) with cellophane

as dialysis membrane [13], and in 1960, Scribner first described the use of hemodialysis for the treatment of ESRD [14,15]. Although hemodialysis treatment has been highly effective in relieving the symptoms of uremic illness, it has become increasingly clear that patients undergoing chronic dialysis treatment – either hemodialysis or peritoneal dialysis – have a markedly reduced survival attributable to accelerated cardiovascular disease and to progressive renal disease [16]. Due to the view that uremia is caused by small, dialyzable solutes, modifications of dialysis membranes, frequency of dialysis, and duration of dialysis treatments have been extensively studied. Although progress has been made regarding dialysis adequacy, there has been little impact on the renal and cardiovascular comorbities associated with dialysis treatment, often, incorrectly, termed "renal replacement " therapy [17]. Regarding uremic illness, Homer Smith wrote in 1951 "Death, if not caused by intercurrent infection or other extrarenal disturbance, occurs from severe imbalance in the composition of body fluids (edema, acidosis, hyponatremia, hyperkalemia, hyperphosphatemia, etc.) complicated by anemia, circulatory disturbances, and other factors of unknown nature" [18]. Several years later, Kolff wrote "What uremic toxin is and what it really does is something which still worries a number of scientists … For a physician engaged in dialysis treatment such as is the writer, it is wise to assume that uremia is caused by an aggregate of many products that are normally excreted but which are now being retained, and it behooves him to remove them all" [19].

Uremic solutes

For a long time it was unclear whether the uremic syndrome and the associated alterations in biochemical and physiological functions could be attributed to one or more uremic retention solutes [20]. In 1999, the European Uremic Toxin Workgroup (EUTox; www.uremic-toxins.org) was launched in order to find biomarkers for different stages of CKD as well as identifying solutes that accumulate during renal failure. At present, over 150 compounds have been found at higher concentrations in the plasma of patients with uremia as compared to healthy individuals [21,22]. These uremic retention solutes compromise a heterogeneous multiplicity of compounds, and although many of these solutes can evoke symptoms seen in CKD patients, identifying responsible retention solutes remains problematic [4]. Currently, uremic solutes are divided into three classes based on the chemical properties that influence the capacity to clear these solutes during dialysis [23]. The first group consists of small water-soluble compounds (≤500 Da) with limited toxicity that are easily cleared by standard dialysis treatment. Urea, one of the earliest identified uremic solutes, is archetypical for this class and although dialysis is still adjusted to eliminate approximately two thirds of the total-body urea content [4], it has been long since recognized that urea contributes little to the pathophysiology of CKD [24]. The second group are the middle molecules (>500 Da) for which filtration during conventional dialysis is limited due to their size. β2-microglobulin is a prototype for this class of uremic solutes [25], and in an analysis from the Hemodialysis (HEMO) study, serum β2-microglobulin levels were associated with both all-cause mortality and infectious mortality in the studied patient population [26,27]. The third, and final group, are the protein-bound solutes, compounds in this class are very difficult to eliminate using standard dialysis modalities as well as high-flux dialysis [23,28]. Clearance of these compounds is not limited due to their size but because they bind to albumin or other plasma proteins, and as a result only the free, unbound fraction contributes to the gradient driving solutes across the dialysis membrane [4]. Indoxyl sulfate is probably the most studied solute belonging to this class, and recently also *p*-cresyl sulfate has gained much attention from the scientific community [29,30]. Of note, indoxyl sulfate is one of the solutes that has been almost exclusively studied in the context of uremic illness and while in 1990 no publication was devoted to this compound, since 2011 the number of papers exceeds 60 per year [29]. Indoxyl sulfate is a small organic aromatic polycyclic anion (average molecular weight: 213.21, chemical formula: $C_8H_7NO_4S$, [31]) derived from dietary tryptophan that is mainly studied in conjunction with CKD-associated cardiovascular disease, and it is reported that this uremic solute can induce vascular calcification and correlates with coronary artery disease and mortality [32-34]. Furthermore, it has been shown that indoxyl sulfate can induce free radical formation in several cell types [35,36], disrupt adherens junctions of endothelial cells [37], promote smooth muscle cell proliferation [38], is toxic for renal tubular cells as well as osteoblasts [39,40], and stimulates renal and cardiac fibrosis [41,42]. Congruous effects have been reported for *p*-cresyl sulfate and it known that this solute is pro-inflammatory and is a predictor of mortality in dialysis patients [43-46]. Moreover, both indoxyl sulfate and *p*-cresyl sulfate are associated with CKD progression [47].

Due to technical advances in analytical approaches the bewildering list of solutes implicated in uremic illness will only lengthen, yet novel therapeutics resulting in an improved removal of uremic retention solutes are lacking. Hopefully, better understanding of both the formation and the physiological clearance of these compounds will reveal new avenues to achieve a more effective therapy.

Metabolism in CKD patients

A hallmark of uremic illness are changes in drug disposition, partially caused by a reduction in glomerular filtration and active tubular secretion of xenobiotics, as well as due to a direct effect of uremic solutes on the expression level and activity of drug metabolism enzymes [48,49]. During the process of drug metabolism, three phases can be distinguished: Phase I reactions, mainly occurring in the liver, are oxidation reactions mediated by cytochrome P450 enzymes. Phase II reactions are conjugation reactions encompassing methylation involving methyltransferase, acetylation by N-acetyltransferases, sulfation mediated by sulfotransferases and glucuronidation via UDP-glucuronosyltransferases, these reactions primarily take place in the liver, kidney and gastro-intestinal tract. Finally, Phase III is the active efflux of xenobiotics by a multitude of transport proteins

[50], which will be described in more detail below. Next to drugs, uremic solutes are also subjected to enzymatic metabolism, and the most straight-forward example of uremic solute formation can be illustrated by the process of *p*-cresol metabolism. As depicted in Figure 1, *p*-cresol is formed by colonic bacteria from dietary tyrosine and this parent compound is either conjugated to sulfate or glucuronic acid giving rise to circulating *p*-cresyl sulfate (~95% of total *p*-cresol) or *p*-cresyl glucoronide (~5% of total *p*-cresol), respectively [51]. In an analogous fashion, tryptophan can give rise to a multitude of indolic uremic solutes, including indoxyl sulfate and indoxyl glucuronide [52,53]. Of note, one could argue that tryptophan is the kingpin of uremic toxin precursors, since this amino acid is also metabolized via the kynurenine pathway – responsible for ~99% of non-protein tryptophan metabolism – resulting in the formation of, amongst others, melatonin, kynurenic acid and quinolinic acid [54,55]. All compounds with distinct neuroactive properties as well as major contributors to immune responses [55]. For more information regarding the complex pathways of tryptophan metabolism and the biological responses elicited by endogenous kynurenines the interested reader is referred to the review by Stone and Darlington [55]. Taken together, there is a clear link between enzyme activity and uremic solutes, yet the repercussion of elevated metabolite levels on the functionality of drug metabolism enzymes is still unknown.

Renal handling of uremic solutes

For a long time, renal function has been solely assessed by means of serum creatinine in order to calculate the eGFR, disregarding the important role of active tubular secretion in the clearance of waste products. Already in 1959, Homer Smith put forward that toxins might be secreted rather than filtered, this suggestion arose from his observation that prochordates living in osmotic equilibrium with their salt water habitat did not have glomeruli and disposed of wastes via tubules which drained into the coelomic cavity. He pointed out that though glomeruli evolved when life moved into fresh water in the Cambrian era 500 million years ago, aglomerular species of fish have persisted throughout evolution up to the present [56]. Micropuncture studies in glomerular teleosts have demonstrated that the importance of tubular secretion is not limited to aglomerular fish [57]. The renal proximal tubules are equipped with a range of transporters, consisting of multiple carriers with overlapping substrate specificities that cooperate in basolateral uptake and luminal excretion. We can distinguish the organic anion and the organic cation systems, each comprising transporters belonging to the organic cation/anion/zwitterion solute carrier family (*SLC*; *e.g.* Organic Cation Transporter 2 (OCT2; *SLC22A2*), Organic Anion Transporter 1 and 3 (OAT1/3; *SLC22A6* and *SLC22A8*), Organic Anion Transporting Polypeptide 4C1 (OATP4C1; *SLCO4C1*), the Multidrug and Toxin Extrusion proteins (MATEs; *SLC47A1/2*)) and the ATP-binding cassette transporter family (P-glycoprotein (P-gp also termed MDR1; *ABCB1*) Multidrug Resistance Protein 2 and 4 (MRP2/4; *ABCC2/4*), and Breast Cancer Resistance Protein (Bcrp; *ABCG2*)), as schematically

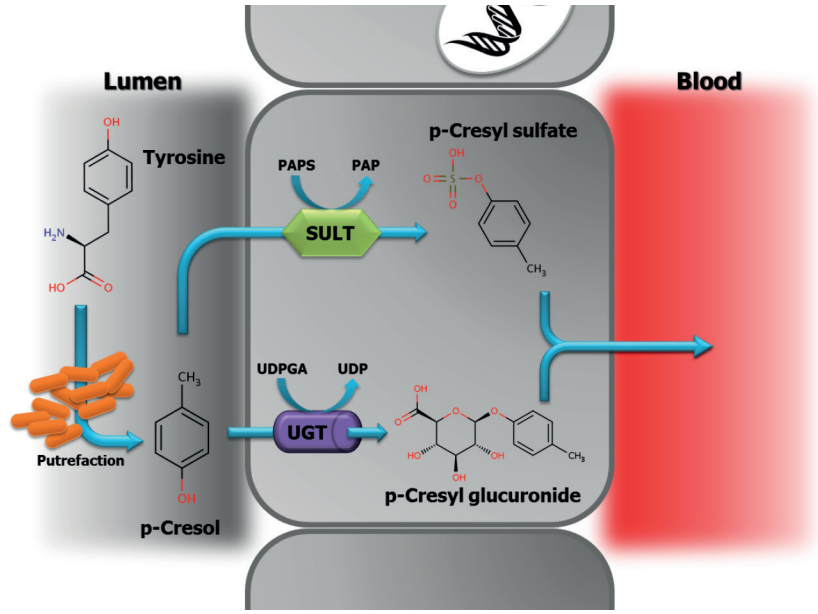

Figure 1 Colonic formation of p-cresol and its metabolites.
The dietary amino acid tyrosine is fermented by the intestinal flora resulting in the formation of *p*-cresol. Subsequently, this parent compound is metabolized into either *p*-cresyl sulfate or *p*-cresyl glucuronide which enter the systemic circulation. Chemical structures were obtained from the Human Metabolome Database (www.hmdb.ca). PAP, 3'-phosphoadenosine-5'-phosphate; PAPS, 3'-phosphoadenosine-5'-phosphosulfate; SULT, sulfotransferase; UDP, Uridine 5'-diphosphate; UDPGA, UDP-glucuronic acid; UGT, UDP-glucuronosyltransferase

depicted in Figure 2 [58-61]. However, the importance of these systems in uremic toxin removal is for a part still unknown.

Already in the 1960's it was demonstrated that serum isolated from uremic rats or patients could hamper accumulation of the prototypical organic anion substrate, *p*-aminohippurate (PAH), in rat renal cortical slices [62,63], implicating the classical organic anion transport system in the renal elimination of uremic toxins. Since then, OAT1 (*SLC22A6*), OAT2 (*SLC22A7*), OAT3 (*SLC22A8*), OAT4 (*SLC22A11*) and URAT1 (*SLC22A12*) all have been shown to contribute, at least to some degree, to the renal handling of uremic solutes [39,64-71]. Up to now, OAT1 and OAT3 have been studied most extensively with regard to the transport of uremic solutes, and a multitude of uremic toxins have been shown to be either a substrate or inhibitor for these OATs, including 3-carboxy-4-methyl-5-propyl-2-furanpropanoic acid (CMPF), hippuric acid, indole-3-acetic acid, indoxyl sulfate and kynurenic acid

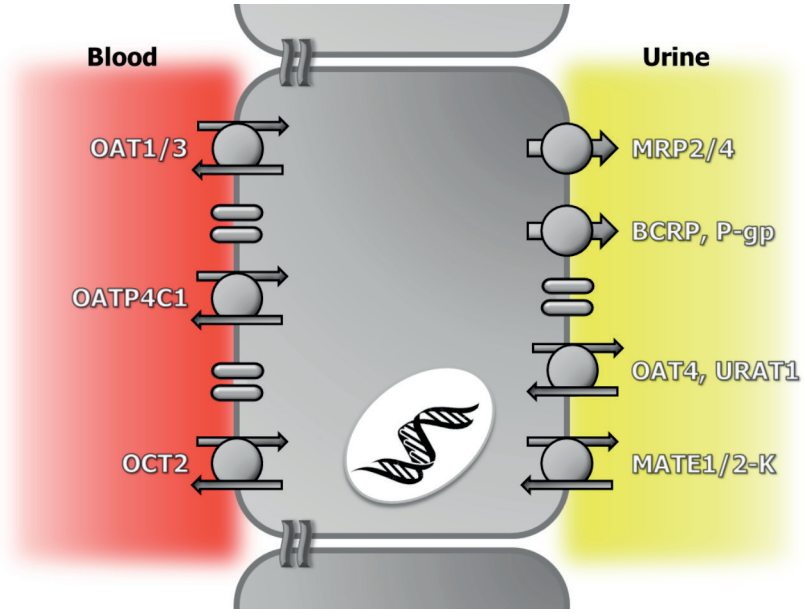

Figure 2 Renal tubular transport systems.
Schematic presentation of transporters present in the renal proximal tubule and potentially relevant for tubular uremic toxin handling. See text for details.

[64,72-74]. Another transporter suspected to aid in the renal clearance of uremic solutes is member 4C1 of the organic anion transporting polypeptide family (OATP4C1), classified within the *SLCO* solute carrier superfamily family. Members of the OATP/*SLCO* family are expressed in various organs and their substrates also range in a broad spectrum from endogenous compounds to xenobiotics [75,76]. Interestingly, OATP4C1 is the only OATP/*SLCO* member expressed in the human kidney, where it is found at the basolateral side of proximal tubules [76]. Recently, Toyohara *et al.* demonstrated that OATP4C1 facilitates the removal of several uremic solutes, including guanidino succinate and asymmetric dimethylarginine [60]. Moreover, they reported that the promoter region of OATP4C1 contains xenobiotic responsive element motifs and that statins, via interplay with the aryl hydrocarbon receptor, can be used to increase the expression and thus activity of the uptake transporter [60]. This suggests that it might be feasible to directly influence renal handling of uremic solutes by medication. Next to the organic anion system, the human kidney is also equipped with transporters to handle organic cations, of which OCT2 (*SLC22A2*) is the predominant transporter present in proximal tubules [77]. Recently, it was reported that the polyamine uremic toxins, cadaverine, putrescine, spermine and

spermidine, the polyamine breakdown product acrolein, and the guanidino compounds guanidine and methylguanidine inhibited substrate-specific transport by OCT2 [78,79]. In addition, two single nucleotide polymorphisms (SNPs) of OCT2, *e.g.* rs3127573 and rs316009, were associated with an increased risk for ESRD [80]. Thus, progress has been made in identifying the transport systems involved in the basolateral uptake of uremic toxins, yet, transport of uremic solutes over the apical membrane into urine remains to be elucidated.

Various transporters expressed at the apical membrane of renal proximal tubule cells are suspected to play a role in the urinary efflux of uremic solutes (Figure 2). The multidrug and toxic compound extrusion (MATE) family of transporters is the latest addition to the pack of multidrug transporter families [81]. MATE1 and its isoforms (MATE2 and MATE2-K), are encoded by the *SLC47A* gene family and they function as secondary-active antiporters [58,82]. MATE1 is expressed throughout the body, but predominantly in the liver and kidney, whereas MATE2-K is exclusively located in renal proximal tubules [83]. Up to now, only a limited number of MATE substrates have been identified and their contribution to uremic solute clearance remains unknown. Another important congregate of efflux transporters is the family of ATP-binding cassette (ABC) transporters, a group of transmembrane proteins – including P-gp, MRP2, MRP4 and BCRP – that are involved in the urinary excretion of a multitude of endogenous compounds and drugs [84]. P-gp is the best characterized transporter, originally discovered in drug-resistant tumor cells, but now recognized as crucial component of tissues with a barrier function [85]. The efflux pump has a preference for uncharged and cationic compounds and was found to be differentially regulated in CKD rats [49], but evidence of its involvement in renal uremic toxin excretion are lacking. MRPs are highly promiscuous transporters and a multitude of substrates have been identified [59]. In addition, MRP2 expression was demonstrated to be elevated in uremic conditions suggesting a protective function for this transporter [49,86]. More importantly, both MRP4 and BCRP are known to transport the uremic solute urate [87,88], making them likely candidates involved in the tubular excretion of uremic solutes.

AIMS OF THE THESIS

A key feature of CKD is the retention and subsequent accumulation of a great array of metabolites that are normally excreted by the healthy kidney. The chemical diversity of these uremic retention solutes likely contributes to the complex pathophysiology that defines uremic illness. In this thesis we strived to lift the uremic veil in order to gain more insight on the multiplicity of uremic retention solutes – by using and improving both untargeted and targeted analytical techniques – as well as the possible detrimental impact of these solutes on xenobiotic elimination pathways in renal proximal tubule cells.

In **Chapter 2** we describe the successful use of ^{1}H-nuclear magnetic resonance spectroscopy, an untargeted metabolomic approach, following different deproteinization techniques to detect both known and previously unidentified uremic retention solutes (*e.g.* dimethyl sulfone and 2-hydroxyisobutyric acid). Moreover, we tested the nephrotoxic potential of these two newly detected solutes using human conditionally immortalized renal proximal tubule epithelial cells (ciPTEC).

Chapter 3 details the interaction between several uremic solutes, including indoxyl sulfate and kynurenic acid, and the renal efflux pumps BCRP and MRP4. These pumps were selected for scrutinization since they were known to transport urate, as described above, and because of the wide availability of models for these transporters in our lab. In this chapter, we demonstrated that uremic solutes can inhibit substrate-specific transport mediated by both transporters at clinically relevant concentrations, indicating that uremic solutes can augment retention of potential toxic metabolites in CKD patients.

The transporters involved in the renal handling of *p*-cresyl sulfate and *p*-cresyl glucuronide are, as of yet, unknown. Moreover, due to a recent paradigm shift [30], both solutes have gained much attention as key uremic solutes. Therefore, **Chapter 4** investigates the interaction between the two *p*-cresol metabolites and the ABC-transporters BCRP and MRP4. In addition, this chapter delineates the negative impact of both uremic solutes on ciPTEC, illustrating the nephrotoxic potential of both compounds.

It is still a debate whether uremic retention solutes are simply a result of CKD or if these compounds can also be a causative agent of uremia. Using a murine model of hyperuricemia, **Chapter 5** shows that elevated levels of uric acid in lieu of kidney damage instigate accumulation of the tryptophan metabolites kynurenine and kynurenic acid. In addition, we identified the transporters involved in the renal clearance of kynurenic acid.

A hallmark of CKD are the alterations in drug disposition and kinetics observed in dialysis patients. **Chapter 6** describes the effect of a myriad of uremic retention solutes on a specific class of phase II drug metabolism enzymes present in renal tubule cells, namely UGTs, in addition to the mitochondria. Moreover, we studied the potential contribution of the proximal tubule in the formation of uremic solutes.

Chapter 7 provides a general discussion of the findings described in this thesis, placing them in the framework of our current understanding of uremic illness and details the future perspectives. The results detailed in this thesis are summarized in **Chapter 8**.

2

Optimized metabolomic approach to identify uremic solutes in plasma of stage 3-4 chronic kidney disease patients

Henricus A.M. Mutsaers, Udo F.H. Engelke, Martijn J.G. Wilmer,
Jack F.M. Wetzels, Ron A. Wevers, Lambertus P. van den Heuvel, Joost G. Hoenderop
and Rosalinde Masereeuw

PLoS ONE, Volume: 8, Issue: 8, e71199, 2013

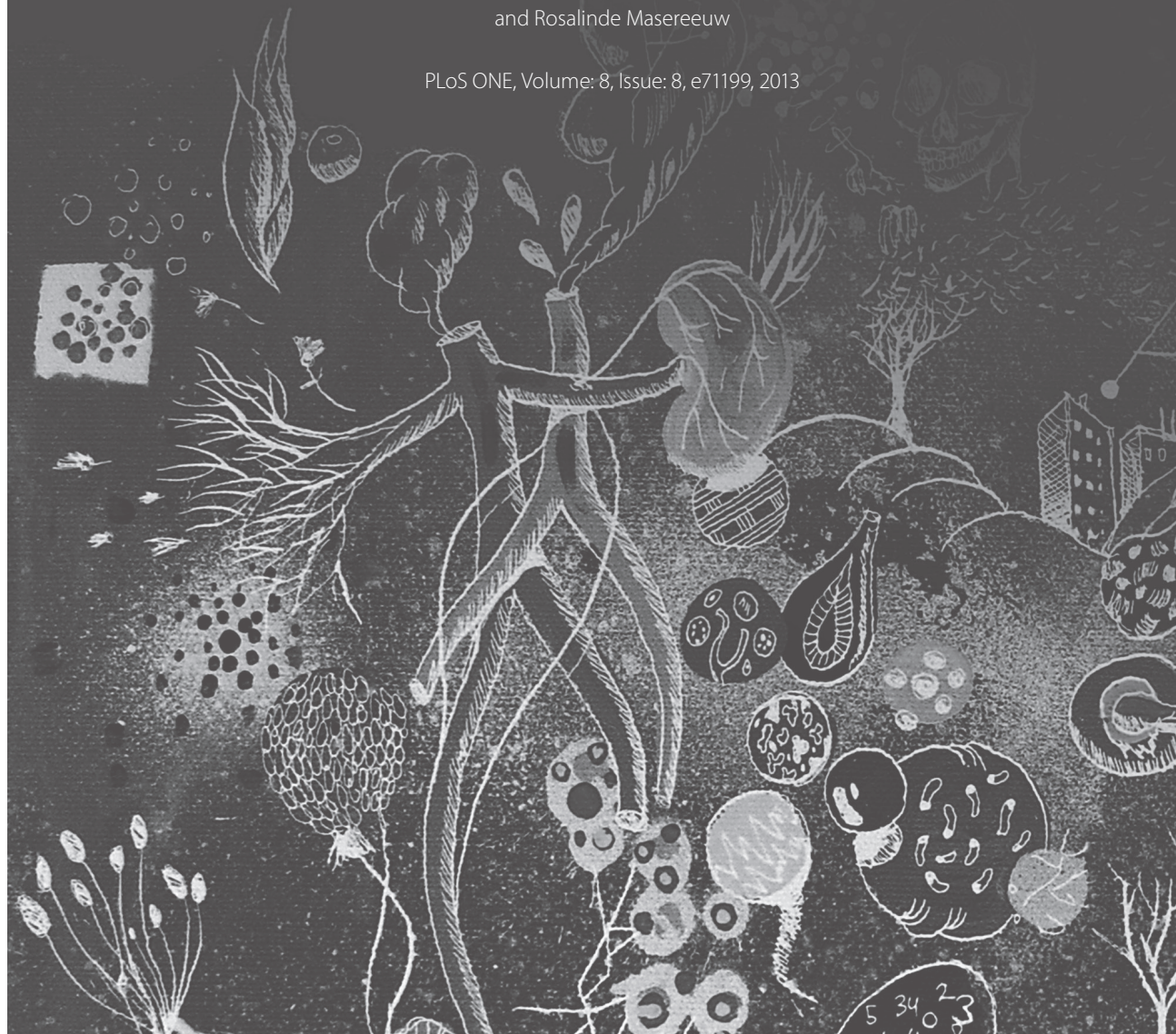

ABSTRACT

Chronic kidney disease (CKD) is characterized by the progressive accumulation of various potential toxic solutes. Furthermore, uremic plasma is a complex mixture hampering accurate determination of uremic toxin levels and the identification of novel uremic solutes. In this study, we applied ^{1}H-nuclear magnetic resonance (NMR) spectroscopy, following three distinct deproteinization strategies, to determine differences in the plasma metabolic status of stage 3-4 CKD patients and healthy controls. Moreover, the human renal proximal tubule cell line (ciPTEC) was used to study the influence of newly indentified uremic solutes on renal phenotype and functionality. Protein removal via ultrafiltration and acetonitrile precipitation are complementary techniques and both are required to obtain a clear metabolome profile. This new approach, revealed that a total of 14 metabolites were elevated in uremic plasma. In addition to confirming the retention of several previously identified uremic toxins, including p-cresyl sulphate, two novel uremic retentions solutes were detected, namely dimethyl sulphone ($DMSO_2$) and 2-hydroxy-isobutyric acid (2-HIBA). Our results show that these metabolites accumulate in non-dialysis CKD patients from 9 ± 7 µM (control) to 51 ± 29 µM and from 7 (0-9) µM (control) to 32 ± 15 µM, respectively. Furthermore, exposure of ciPTEC to clinically relevant concentrations of both solutes resulted in an increased protein expression of the mesenchymal marker vimentin with more than 10% ($p<0.05$). Moreover, the loss of epithelial characteristics significantly correlated with a loss of glucuronidation activity (Pearson $r = -0.63$; $p<0.05$). In addition, both solutes did not affect cell viability nor mitochondrial activity. This study demonstrates the importance of sample preparation techniques in the identification of uremic retention solutes using ^{1}H-NMR spectroscopy, and provide insight into the negative impact of $DMSO_2$ and 2-HIBA on ciPTEC, which could aid in understanding the progressive nature of renal disease.

INTRODUCTION

The kidneys play an important role in maintaining total body homeostasis by facilitating the urinary secretion of both endogenous and exogenous waste products. Chronic kidney disease (CKD) affects approximately 10% of the adult population in developed countries. In half of these patients the diagnosis of CKD is based on the presence of a reduced kidney function (chronic renal failure; CRF). In CKD patients adequate renal clearance is compromised resulting in the accumulation of a plethora of uremic solutes [5]. Nowadays, over 140 uremic toxins have been reported, divided into three distinct classes based on their physico-chemical properties. It is well documented that uremic toxins accumulate in dialysis patients and several biomarkers of CKD have been identified [21,22,89,90]; yet, less is known about the retention of possible toxic solutes in other patients with a compromised kidney function. Herget-Rosenthal *et al.*, reported that several uremic toxins are retained during acute kidney injury including β_2-microglobulin, hippuric acid and 3-carboxyl-4-methyl-5-propyl-2-furan-propionic acid [91]. Furthermore, our group previously demonstrated that plasma levels of hippuric acid, indole-3-acetic acid, indoxyl sulphate and kynurenic acid are elevated in non-dialysis CRF patients compared with healthy controls [89].

Although the retention of uremic toxins in dialysis patients is widely studied, there is a large variation in blood levels reported for uremic toxins. These discrepancies can be due to differences in the study population with respect to diet, colonic microbial metabolism and endogenous metabolism [92,93]. Moreover, precise determination of uremic toxin concentrations is cumbersome and dependent on the physico-chemical characteristics of these solutes, such as protein-binding, which can result in insufficient extraction of compounds from body fluids, leading to an underestimation of the true values [30,51]. In addition, plasma is a complex mixture of proteins, molecules and ions that together can undergo a myriad of molecular interactions [94]. During ^{1}H-nuclear magnetic resonance (NMR) spectroscopy, the abundance of proteins in complete plasma results in broad overlapping signals that obscure resonances of low-molecular-weight metabolites and quantification of these compounds is hampered due to T_2-relaxation processes [94]. Therefore, deproteinization is required when studying small organic molecules in plasma, and it is required to optimize analytical techniques and/or sample preparation methods to obtain a reliable overview of uremic toxin levels in CKD patients.

In metabolomics studies, generally two analytical approaches are used: mass spectrometry-based methods and NMR [95]. Recently, Shah *et al.*, reported the plasma metabolite profiles of stage 2-4 CKD patients using gas and liquid chromatography coupled to mass spectrometry [96]. Therefore, we investigated whether NMR could be used as a complementary tool to elucidate novel biomarkers in kidney disease. The metabolic status of stage 3-4 CKD patients was determined using one-dimensional ^{1}H-NMR spectroscopy following three previously described deproteinization strategies [94], namely ultrafiltration, protein precipitation via perchloric acid or via acetonitrile extraction.

MATRIALS AND METHODS

Ethics statement

The ethical committee of the Radboud University Nijmegen Medical Centre on research involving human subjects approved this study, and written informed consent was obtained from each patient and each healthy volunteer.

Chemicals

All chemicals were obtained from Sigma (Zwijndrecht, the Netherlands) unless stated otherwise. Stock solutions of uremic toxins were prepared in milli-Q and stored at -20 ºC. The reference standard of p-cresyl sulphate, kindly provided by Prof. R. Vanholder (University Hospital Ghent, Belgium), was synthesized as a potassium salt as described previously [97].

Patients and sample preparation

Blood samples were obtained from ten patients with CKD stage 3-4 (eGFR: 14-36 ml/min/1.73 m^2) during regular check-up and four adult controls. Clinical characteristics of study subjects are listed in Table 1. None of the subjects had been fasting at the time of blood sampling. Blood was collected in an Heparin Vacutainer and was immediately centrifuged at 3,000 x g for 10 min. Subsequently, plasma was collected and stored at -20 °C. Before analysis, each patient sample was deproteinized via three distinct methods: (1) ultrafiltration; plasma samples were deproteinized using a 10 kD filter (Sartorius). Before use, the filter was washed twice by centrifugation of water to remove glycerol. (2) perchloric acid (PCA) extraction; 100 µl of 20% (v/v) PCA was added to 500 µl plasma, samples were then vortexed and placed on ice for 5 min. Next, samples were centrifuged at 12,000 x g for 3 min and the clear supernatant was used for spectroscopy. (3) acetonitrile extraction; 1.5 ml of acetonitrile was added to 0.5 ml plasma, mixed thoroughly, followed by centrifugation (3,000 x g for 5 min). Subsequently, the supernatant was dried by heating at 40 ºC under N_2 flow and finally resuspended in 700 µl milli-Q. The control samples were deproteinized via ultrafiltration or acetonitrile extraction. Following protein removal via the different methods, 20 µl of 20.2 mM trimethylsilyl-2,2,3,3-tetradeuteropropionic acid (TSP, sodium salt) in ^2H_2O was added to the sample, providing a chemical shift reference (δ=0.00), a concentration reference and a deuterium lock signal. The pH of the ultrafiltrate was adjusted to 2.50 ± 0.05 with concentrated hydrogen chloride. Finally, 650 µl of the sample was placed in a 5 mm NMR tube (Wilmad Royal Imperial).

One-dimensional ^{1}H-NMR spectroscopy

Plasma was measured at 500 MHz on a Bruker DRX 500 spectrometer equipped with a triple-resonance inverse (TXI) ^{1}H [^{15}N, ^{13}C] probe head and equipped with x,y,z gradient coils. ^{1}H spectra were acquired as 256 transients in 32K data points with a spectral width of 6002 Hz. Sample temperature was 298 K and the H_2O resonance was pre-saturated by

Table 1 Characteristics of study subjects

	Patients	Controls[a]
Number	10	4
Age (years)	55 ± 12	40 ± 12
Women (%)	33	50
Urea (mmol/l)	20 ± 9	ND
Creatinine (µmol/l)	227 ± 56	20-90
Albumin (g/l)	37 ± 4	ND
eGFR (ml/min/1.73 m^2)[b]	26 ± 7	ND

Values are shown as mean ± SD. ND, not determined.
[a] Control metabolite levels were similar as compared to an established database (n=50) from the Radboud University Nijmegen.
[b] eGFR was calculated using the Modification of Diet in Renal Disease (MDRD) equation (www.nkdep.nih.gov).

single-frequency irradiation during a relaxation delay of 10 s, and a 90° excitation was used. Automated tuning and matching (ATMA) and shimming (Topshim) was performed on all plasma samples. The resonances from the metabolites in Table 2 and the TSP singlet (nine equivalent protons) were fitted semi-automatically with Lorentzian line shapes. The concentration of the metabolites was calculated from the relative integrals of the fitted lineshapes using the known concentration of TSP.

Cell culture

The human conditionally immortalized proximal tubule epithelial cell (ciPTEC) line was generated as previously described by Wilmer *et al.* [98]. The cells were cultured in phenol red free DMEM/F12 medium (Gibco/Invitrogen, Breda, the Netherlands) containing 10% (v/v) fetal calf serum (MP Biomedicals, Uden, the Netherlands), insulin (5 µg/ml), transferrin (5 µg/ml), selenium (5 ng/ml), hydrocortisone (36 ng/ml), epithelial growth factor (10 ng/ml), and tri-iodothyronine (40 pg/ml) at 33 ºC in a 5% (v/v) CO_2 atmosphere. Propagation of cells was maintained by subculturing the cells at a dilution of 1:3 to 1:6 at 33 °C. For experiments, cells were cultured at 33 ºC to 40% confluency, followed by maturation for 7 days at 37 ºC. Experiments were performed on the cells between passages 30 and 40, during which proximal tubule characteristics, such as albumin uptake and phosphate reabsorption, were maintained [98].

Flow cytometry

In this study, flow cytometry was used to study both cell viability and the expression of vimentin, a mesenchymal cell marker. ciPTEC were seeded at 40% confluence in 12-well

plates and allowed to adhere over night at 33 ºC followed by maturation for 7 days at 37 ºC, before being treated for 48 h with clinically relevant uremic toxin concentrations. In addition, ciPTEC were also exposed for 48 h to 1 mM 1-methylhistidine, 3-methylhistidine (both as negative control) or indoxyl sulphate as a positive control. After incubation, cells were harvested using trypsin-EDTA and centrifuged at 600 x g during 5 min. Subsequently, supernatant was removed and the cell pellet was resuspended in 100 µL PBS containing 1 µL mouse-α-human Vimentin-PE (Abcam, Cambridge, UK) followed by 30 min incubation at RT. Samples were acquired with a BD FACSCalibur (Becton Dickinson, Breda, the Netherlands) using channel FL-2. Analysis was performed using Flow Jo software (TreeStar, Ashland, USA), gating on live cells.

High-performance liquid chromatography (HPLC)

HPLC was used to measure UDP-glucuronosyltransferase (UGT) activity via the glucuronidation of 7-hydroxycoumarin (7-OCH), as described previously [99,100]. Following exposure to uremic toxins at clinically relevant concentrations for 48 h, ciPTEC were incubated with 10 µM 7-OCH for 3 h at 37°C. Before chromatography, an aliquot of culture medium was collected and centrifuged at 12,000 x g for 3 min and 50 µl of the supernatant was injected into the HPLC-system (Spectra-Physics Analytical, Spectrasystem SCM400). To measure 7-OCH and 7-OCH glucuronide (7-OCHG) the HPLC was equipped with a C18 HPLC column (GraceSmart RP 18 5u 150 x 4.6 mm; Grace, Breda, the Netherlands). Separation was performed at a flow rate of 1 ml/min with eluent A (95% (v/v) H_2O, 5% (v/v) methanol and 0.2% (v/v) acetic acid) and eluent B (50% (v/v) H_2O, 49% (v/v) acetonitrile and 1% (v/v) tetrahydrofuran) under the following gradient conditions: 0-3 min, 80-50% eluent A; 3-8 min, 50% eluent A; 8-9 min, 50-80% eluent A; 9-14 min, 80% eluent A. The compounds were detected at a wavelength of 316/382 nm. Standards of the compounds were also run in order to quantify the amount of metabolites found in the samples. Acquired data were processed with PC1000 software (Spectrasystem).

3-[4,5-dimethylthiazol-2-yl]-2,5-diphenyl tetrazolium bromide (MTT) assay

Mitochondrial succinate dehydrogenase activity was assessed using the MTT assay. ciPTEC were cultured in a 96 well culture plate and exposed to $DMSO_2$ or 2-HIBA for 48 h. Next, medium was removed and 40 µl preheated (37ºC) MTT-solution (5 mg 3-[4,5-dimethylthiazol-2-yl]-2,5-diphenyl tetrazolium bromide/ml ciPTEC medium) was added and incubated for 4 h at 37ºC. Afterwards, MTT-solution was removed, followed by the addition of 150 µl DMSO to dissolve produced formazan crystals. The extinction of the solution was measured at 570 nm using a Benchmark Plus Microplate Spectrophotometer (Bio-rad).

Statistics

Statistics were performed using GraphPad Prism 5.02 via one-way analysis of variance (ANOVA) followed by Dunnett's Multiple Comparison Test. Differences between groups

were considered to be statistically significant when $p<0.05$. The software was also used to perform linear regression analysis and correlation analysis (Spearman and Pearson). Raw data files are available upon request.

RESULTS

Influence of deproteinization on ^{1}H-NMR spectra

Figure 1 shows the deproteinized ^{1}H-NMR plasma spectrum following ultrafiltration (Figure 1A), acetonitrile precipitation (Figure 1B) and PCA extraction (Figure 1C). Citric acid is clearly detected following ultrafiltration with a symmetrical quadruplet, generally referred to as an AB-system, at 2.94 ppm; whereas, resonance signals are low in the spectral region δ 7.00-8.00 (Figure 1A). In contrast, high-resonance signals were observed in this part of the ^{1}H-NMR spectrum after acetonitrile treatment (Figure 1B). Hippuric acid showed a triplet at both 7.54 ppm and 7.62 ppm, and a doublet at 7.82 ppm. The other resonance signals were assigned to p-cresyl sulphate. Moreover, Figure 1B also shows that the citric acid peak observed following ultrafiltration is lost by acetonitrile deproteinization. Furthermore, PCA extraction resulted in an overall decreased sensitivity, a poor signal-to-noise ratio and shifts in peak position (Figure 1C), making this method unsuitable for metabolite identification and quantification. To our knowledge, this is the first report to demonstrate the presence of p-cresyl sulphate in plasma using ^{1}H-NMR spectroscopy. Therefore, we aimed to verify the identity of the detected metabolite using a reference standard. ^{1}H-NMR of the authentic compound p-cresyl sulphate in H_2O at pH 2.5 (Figure 2A) showed a singlet at 2.33 ppm (CH_3 group) and a doublet at both 7.19 ppm and 7.27 ppm (aromatic ring protons). A similar resonance profile was observed in acetonitrile-treated plasma from a CKD patient (Figure 2B), indicating that p-cresyl sulphate is indeed retained in patients with kidney failure. The absence of both hippuric acid and p-cresyl sulphate in plasma following ultrafiltration is most likely due to the strong protein binding of these solutes. Thus, ultrafiltration and acetonitrile extraction are complementary deproteinization strategies and both methods are required to obtain a clear overview of the metabolic status of non-dialysis CKD patients.

Accumulation of uremic toxins in patients with CKD stage 3-4

^{1}H-NMR spectroscopy revealed that a plethora of uremic compounds are elevated in CKD patients as compared with healthy controls (Figure 3). Resonance assignments were based on previously recorded spectra and a total of 14 solutes could be assigned. As expected, creatinine was elevated in all patients. Moreover, the well-known toxins 3-methylhistidine, hippuric acid, p-cresyl sulphate, *N,N*-dimethylglycine, betaine and *myo*-inositol were detected in all patients. In all ten patient samples we also detected the hitherto unknown toxins $DMSO_2$ and 2-HIBA. 1-methylhistidine was detected in nine patients, trigonelline

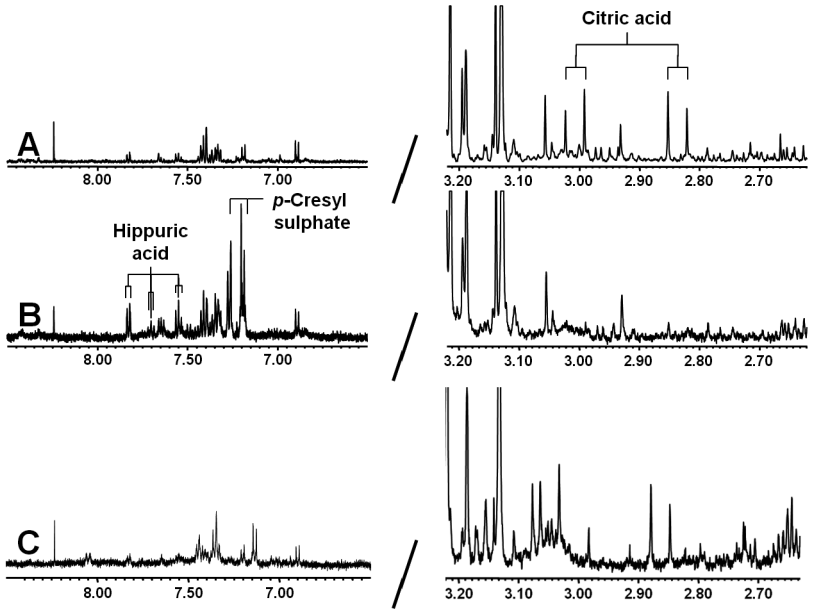

Figure 1 Comparison of deproteinization methods.

500 MHz ^{1}H-NMR spectrum of plasma from CKD patient following **(A)** ultrafiltration, **(B)** acetonitrile precipitation or **(C)** PCA extraction.

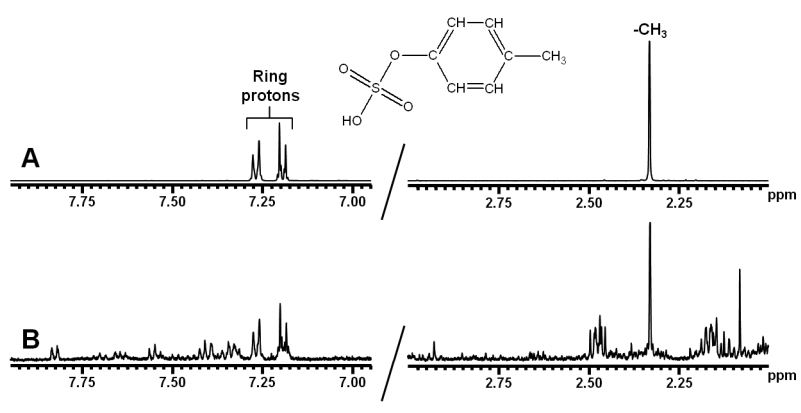

Figure 2 500 MHz ^{1}H-NMR spectra: region δ 7.00-7.80 and 3.00-2.00.

(A) Authentic reference solution of p-cresyl sulphate with chemical structure and assignments. **(B)** Plasma (acetonitrile precipitation) from CKD patient. The spectrum shows resonances of p-cresyl sulphate. These resonances were not observed in plasma from controls.

and trimethylamine *N*-oxide were found in six patients and pseudouridine was found in five patients; whereas, dimethylamine was only detected in one individual. Resonance assignments and concentrations of uremic toxins measured by ^{1}H-NMR are summarized in Table 2 and chemical structures can be found in Figure S1.

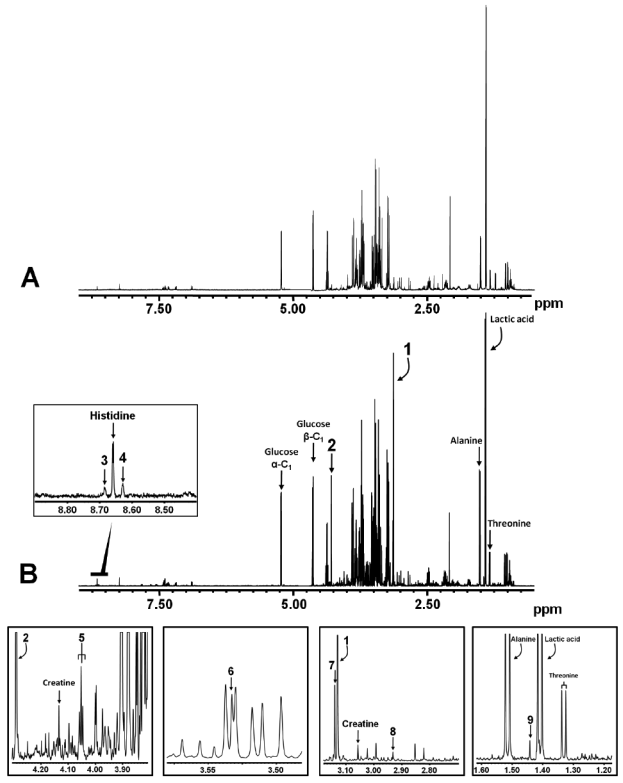

Figure 3 Accumulation of uremic solutes.

500 MHz ^{1}H-NMR spectrum of plasma (ultrafiltrate) from **(A)** a healthy control and **(B)** a CKD patient. Insets show 5 regions of interest in greater detail. Metabolite abnormalities: Creatinine (1 and 2), 1-methylhistidine (3), 3-methylhistidine (4), *myo*-Inositol (5), trimethylamine *N*-oxide (6), dimethyl sulphone (7), *N,N*-dimethylglycine (8) and 2-hydroxyisobutyric acid (9).

Comparison with normal concentrations

To evaluate the relative solute retention in stage 3-4 CKD patients, the ratio of the mean of all uremic concentrations (M) determined were calculated to the normal concentration (N) reported in literature (M/N), as described previously [22]. The solute solely retained in one patient (*i.e.* dimethylamine), trigonelline (due to lack of reference value) and creatinine

Table 2 [1]H resonance assignments and plasma concentrations of uremic solutes in stage 3-4 CKD patients

Metabolite	Peak no.[a]	C_u (μM)	C_{max}[b] (μM)	Control (μM)	Literature[c] (μM)
1-Methylhistidine	3	34 ± 26	87	< 5	4 ± 8
3-Methylhistidine	4	38 ± 25	89	ND	2.7 (0-6)
Hippuric acid		134 ± 111	357	ND	3 (0-5)
p-Cresyl sulphate		289 ± 132	552	ND	15 ± 9
Creatinine	1,2	590 ± 276	1143	20-90	72 (57-93)
Dimethyl sulphone	7	51 ± 29	108	< 30	9 ± 7
2-Hydroxyisobutyric acid	9	32 ± 15	61	ND	7 (0-9)
N,N-Dimethylglycine	8	23 ± 11	46	< 5	2.6 (1.8-3.7)
trigonelline		28 ± 24	76	ND	ND
Pseudouridine		48 ± 15	79	ND	3.2 ± 1
Betaine		83 ± 34	150	< 50	34.6 (24-42)
myo-Inositol	5	499 ± 170	838	ND	30 (21-49)
Dimethylamine		17[d]	NA	ND	3.3 ± 1.5
Trimethylamine *N*-oxide	6	88 ± 42	172	ND	38 ± 20

Values are shown as mean (C_u) ± SD or range (μM) and maximal uremic concentration (C_{max}). ND, not detected; NA, not applicable.
[a]Numbers correspond to peaks in Figure 3.
[b]Hypothetical C_{max} calculated as $C_{max} = C_u + 2$ SD, as previously described [21,89].
[c]Data obtained from the Human Metabolome Database (www.hmdb.ca) [31].
[d]Only detected in one patient.

were excluded from this analysis. The M/N ratio ranged from 2.3 for trimethylamine *N*-oxide to 44.7 for hippuric acid (Figure 4). In the case of five metabolites, the uremic concentration was more than 10 times higher than normal. A moderate degree of retention was observed for four solutes for which the M/N ratio ranged between 4 and 10.

Correlation between eGFR and retention of $DMSO_2$ and 2-HIBA

Next, we investigated whether the plasma concentration of $DMSO_2$ and 2-HIBA in non-dialysis CKD patients correlated with a decline in kidney function as represented by the eGFR. As shown in both Figure 5 and Figure S2, there is no association between the parameters studied as concluded from a Spearman correlation analysis (r<0.2 for both solutes).

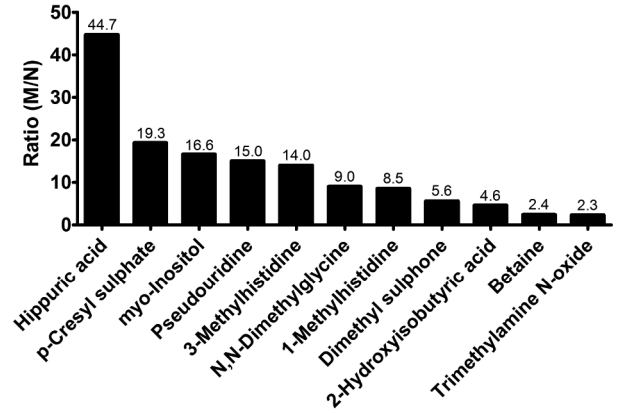

Figure 4 Relative retention of uremic solutes in stage 3-4 CKD patients.
The M/N index is the ratio of the mean uremic concentration (M) found in the present study to the normal concentration (N) measured in healthy controls reported in literature.

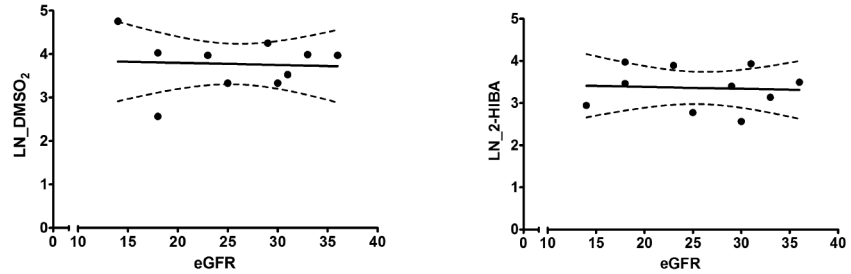

Figure 5 Correlation between plasma solute levels and eGFR.
Dots represent the natural logarithm (LN) of individual concentrations of **(A)** $DMSO_2$ and **(B)** 2-HIBA and the lines the best fit linear regression line with the 95% confidence interval.

Influence of uremic solutes on ciPTEC phenotype

The impact of the novel uremic retention solutes on proximal tubular epithelium was investigated using a unique human proximal tubule cell line, demonstrated to be a valid model to study nephrotoxicity and renal cell metabolism [100-102]. Exposure of ciPTEC to the C_{max} of $DMSO_2$ or 2-HIBA, determined in this study (Table 2), resulted in an increase in vimentin expression by 12% and 30%, respectively (Figure. 6A). Moreover, at the highest concentration tested (10x $C_{max,}$) these toxins increased vimentin expression by 26% and 55%, respectively. In comparison, both 1-methylhistidine and 3-methylhistidine did not

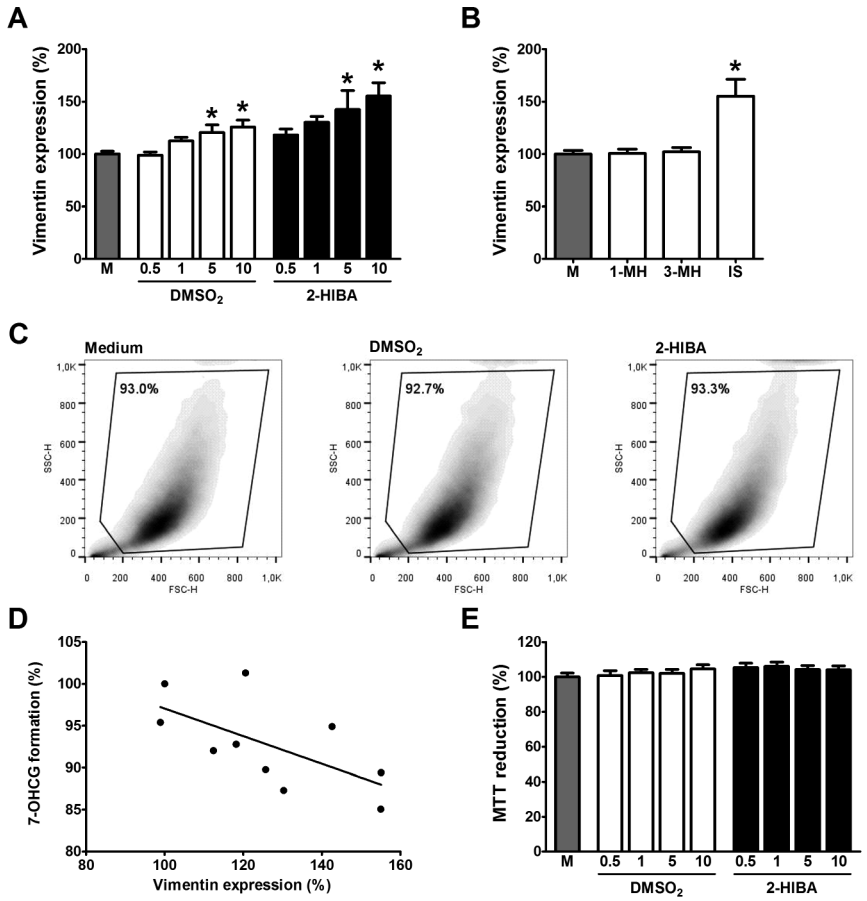

Figure 6 Impact of $DMSO_2$ and 2-HIBA on ciPTEC.

Cells were exposed for 48 h to ciPTEC medium (gray bar), $DMSO_2$ or 2-HIBA (concentration range: ½ C_{max} – 10x C_{max}). **(A)** Following treatment, cells were harvested and stained with mouse-α-human Vimentin-PE. Quantification of staining was done with a BD FACSCalibur flow cytometer using channel FL-2, and analyzed with FlowJo software, gating on live cells. Statistical analysis was performed via a One-way ANOVA followed by the Dunnett's Multiple Comparison Test for each toxin. Results are presented as mean ± SEM of three independent experiments performed in duplicate or triplicate. * indicates $p<0.05$ compared with control. **(B)** Vimentin expression following exposure to 1 mM 1-methylhistidine (1-MH), 3-methylhistidine (3-MH; both negative control) or indoxyl sulphate (IS; positive control) for 48 h. Results are presented as mean ± SEM of three independent experiments performed in duplicate or triplicate. * indicates $p<0.05$ compared with control. **(C)** Cells were exposed for 48 h to ciPTEC medium, $DMSO_2$ or 2-HIBA (both 10x C_{max}). Representative density plots with percentage of gated (*i.e.* living) cells of three independent experiments, performed in duplicate or triplicate

(D) Following treatment, ciPTEC were incubated for 3 h with 10 µM 7-OHC. Afterwards, an aliquot of culture medium was collected and injected into the HPLC-system. Standards of 7-OHCG were also analyzed in order to quantify the amount of glucuronide found in the samples. Acquired HPLC data were processed with PC1000 software (Spectrasystem). Pearson correlation analysis revealed a significant association between the expression of vimentin and glucuronidation ($r = -0.63$; $p<0.05$). **(E)** The MTT assay was used to study the impact of $DMSO_2$ and 2-HIBA on mitochondrial metabolism. Cells were exposed for 48 h to both solutes as described above. Afterwards, cells were incubated for 4 h with MTT-solution at 37 °C. Subsequently, produced formazan crystals were dissolved in DMSO and extinction was measured at 570 nm. Results are presented as mean ± SEM of three independent experiments performed minimally in triplicate.

affect vimentin expression; whereas the positive control (indoxyl sulphate) increased vimentin expression by 55% (Figure 6B). Flow cytometry revealed that exposure to the highest concentration of both solutes did not affect cell morphology nor the percentage of living cells as compared to untreated cells (Figure 6C). Furthermore, when ciPTEC were exposed to the C_{max}, UGT activity was reduced by 8% and 13%, respectively. And we observed a clear correlation between vimentin expression and UGT activity with a calculated Pearson r of -0.63 ($p<0.05$; Figure 6D). In addition, $DMSO_2$ and 2-HIBA did not impede mitochondrial succinate dehydrogenase activity as demonstrated with the MTT assay (Figure 6E). Taken together, our findings suggest that both solutes induce a loss of epithelial characteristics and reduce renal glucuronide formation, indicating changes in cell metabolism without affecting cell viability.

DISCUSSION

Accumulation of uremic toxins due to inadequate renal clearance is a hallmark of CKD. Uremic retention solutes are associated with disease progression and the myriad of pathologies observed in dialysis patients. In this study, ^{1}H-NMR spectroscopy was successfully used to indentify multiple uremic toxins in the plasma of stage 3-4 CKD patients.

Our results revealed that ultrafiltration and acetonitrile extraction are complementary deproteinization techniques and both are required as sample preparation methods for the proper detection of uremic retention solutes using ^{1}H-NMR spectroscopy. In the study of Tiziani *et al.*, it was demonstrated that ultrafiltration was the best deproteinization strategy to remove proteins from serum samples resulting in a high metabolite retainment and reproducibility [103]. Furthermore, they reported that following acetonitrile extraction most of the metabolites were maintained, although with a reduced signal intensity compared to ultrafiltration [103]. In contrast, Daykin *et al.*, demonstrated that deproteinization using acetonitrile at physiological pH resulted in an increased detection of low-mo-

lecular-weight metabolites and a improved signal-to-noise ratio [94]. These studies corroborate our notion that multiple deproteinization strategies are needed when investigating the metabolome.

Here, we report for the first time that $DMSO_2$ and 2-HIBA are retained in CKD patients. Moreover, both solutes were demonstrated to negatively influence renal cell physiology using ciPTEC. Already in 1966, Williams *et al.* reported the presence of $DMSO_2$ in urine [104]. Yet, it took several decades to establish that $DMSO_2$ is a common metabolite present in blood and cerebrospinal fluid [105,106]. $DMSO_2$ can originate from dietary sources such as, milk and port wine [106-108]. Moreover, it can be formed during bacterial metabolism of methanethiol in the gut or endogenous human methanethiol metabolism [106,109]. Recently, it has been described that $DMSO_2$ attenuated both constitutive as well as IL-1β-induced IL-6 and IL-8 production in human chondrocyte cell line, possibly by inhibiting the ERK1/2 signaling pathway [110]. Older studies indicated that $DMSO_2$ inhibited oxidant production in activated neutrophils and diminished the proliferation of vascular smooth muscle cells and endothelial cells [111,112]. Regarding 2-HIBA, two recent studies reported that this compound is constitutively present in human urine and serum [113,114]. Moreover, 2-HIBA is the major urinary metabolite in humans following exposure to the gasoline additives methyl-*tert*.butyl ether and ethyl-*tert*.butyl ether [115,116]. Elevated plasma concentrations of 2-HIBA were observed in patients with type 2 diabetes mellitus, possibly due to disturbances in fatty acid metabolism [117]. Moreover, a recent genome-wide association study revealed a significant negative association with urinary 2-HIBA levels and SNP rs830124, an intronic SNP of the *WDR66* gene on chromosome 12, which is closely associated with mean platelet volume [118,119]. At present, little is known regarding the biological activity of $DMSO_2$ and 2-HIBA. Our results provide the first proof that these metabolites induce a loss of defined renal epithelial features and are possibly involved in the progression of CKD. However, more research is necessary to definitely label these solutes as uremic toxins.

It is known that uremic toxin levels rise in concordance with CKD severity [2]. Therefore, it is suggested that eGFR, as a marker of kidney function, should reflect retention state and the levels of uremic solutes in CKD patients. In this study, we did not observe any correlation between eGFR and plasma concentration of $DMSO_2$ or 2-HIBA, which suggests that eGFR is a poor marker for the accumulation of these solutes. These findings are in agreement with previous studies demonstrating that eGFR is an unsuitable tool to predict levels of uremic toxins from different classes (*e.g.* middle weight and protein-bound) in CKD patients [120,121]. Furthermore, these results suggest that the renal clearance of both metabolites is mainly dependent on active tubular transport, possibly due to binding of the compounds to plasma proteins. Yet, more research is needed to fully elucidate the chemical properties, including protein-binding, of $DMSO_2$ and 2-HIBA.

Next to $DMSO_2$ and 2-HIBA, the present study showed that 1-methylhistidine, 3-methylhistidine, hippuric acid, p-cresyl sulphate, *N,N*-dimethylglycine, pseudouridine, betaine,

myo-inositol and trimethylamine *N*-oxide were elevated in stage 3-4 CKD patients. Previously, Choi *et al.*, used ^{1}H-NMR spectroscopy to study the metabolic status of dialysis patients [122]. They reported that a multitude of uremic toxins were retained including *myo*-inositol and 3-methylhistidine, similar to our findings in non-dialysis CKD patients. In addition, Rhee *et al.* studied the metabolomic profile of 44 hemodialysis patients using three different LC-MS methods [90]. In total, 40 metabolites were elevated at baseline in patients, compared to healthy controls. In concordance with our results, they demonstrated retention of hippuric acid, trimethylamine *N*-oxide and dimethylglycine. Both studies did not report the retention of 1-methylhistidine, pseudouridine and betaine. However, accumulation of 1-methylhistidine in patients treated with hemodialysis has been demonstrated by HPLC previously [123]. And Niwa *et al.*, reported that pseudouridine levels were increased in both CRF and dialysis patients compared with controls [124]. Taken together, there is a clear overlap in the solutes retained in both the early stages of CKD and patients with end-stage renal disease.

Previously, using HPLC and LC-MS/MS, our group demonstrated that indole-3-acetic acid, indoxyl sulfate and kynurenic acid accumulated in CRF patients with mean concentrations of 4.4 μM, 67 μM and 0.6 μM, respectively [89]. These compounds were not identified during the present study due to the limited sensitivity of proton NMR spectroscopy. Other widely deployed techniques, such as HPLC and LC-MS/MS, have a higher sensitivity with detection limits in the nano- or even picomolar range although the sensitivity highly varies depending on the compound of interest. The present study was an initial proof-of-concept study to determine whether ^{1}H-NMR spectroscopy could be used as a tool to expand our knowledge about uremic retention solutes and if this technique can be utilized in the search for CKD biomarkers. As such, a small number of CKD patients was included, which limited our power to identify uremic retention solutes for which levels greatly differ among individual patients. Still, the current study is the first to provide an overview of the metabolome of non-dialysis CKD patients by means of NMR spectroscopy. One has to take into account that, due to the reasons stated above, not all of the potential toxic solutes retained in stage 3-4 CKD patients are identified. Further studies with additional subjects and analytical techniques should provide a more complete overview of metabolites retained in CKD patients.

In conclusion, a hallmark of renal failure is the retention of a plethora of metabolites, belonging to multiple physico-chemical classes, with potential deleterious effects on total body homeostasis. In this study, we have demonstrated that both ultrafiltration and acetonitrile extraction are required as deproteinization methods to elucidate the metabolomic profile of stage 3-4 CKD patients by means of ^{1}H-NMR spectroscopy. Moreover, using this technique, we have successfully identified a total of 14 metabolites, including 2 novel uremic solutes, that possibly contribute to the co-morbidity and mortality in CKD patients. These results might aid in revealing new biomarkers for CKD and possibly contribute to a better understanding of the progressive character of renal disease.

ACKNOWLEDGEMENTS

The authors would like to thank P.H.H. van den Broek for assisting with the HPLC measurements and A. Bilos for advice regarding sample preparation methods.

Supplementary data

Supporting information is available online at www.plosone.org.

3

Uremic toxins inhibit transport by Breast Cancer Resistance Protein and Multidrug Resistance Protein 4 at clinically relevant concentrations

Henricus A.M. Mutsaers, Lambertus P. van den Heuvel, Lauke H.J. Ringens, Anita C.A. Dankers, Frans G.M. Russel, Jack F.M. Wetzels, Joost G. Hoenderop and Rosalinde Masereeuw

PLoS ONE, Volume: 6, Issue: 4, e18438, 2011

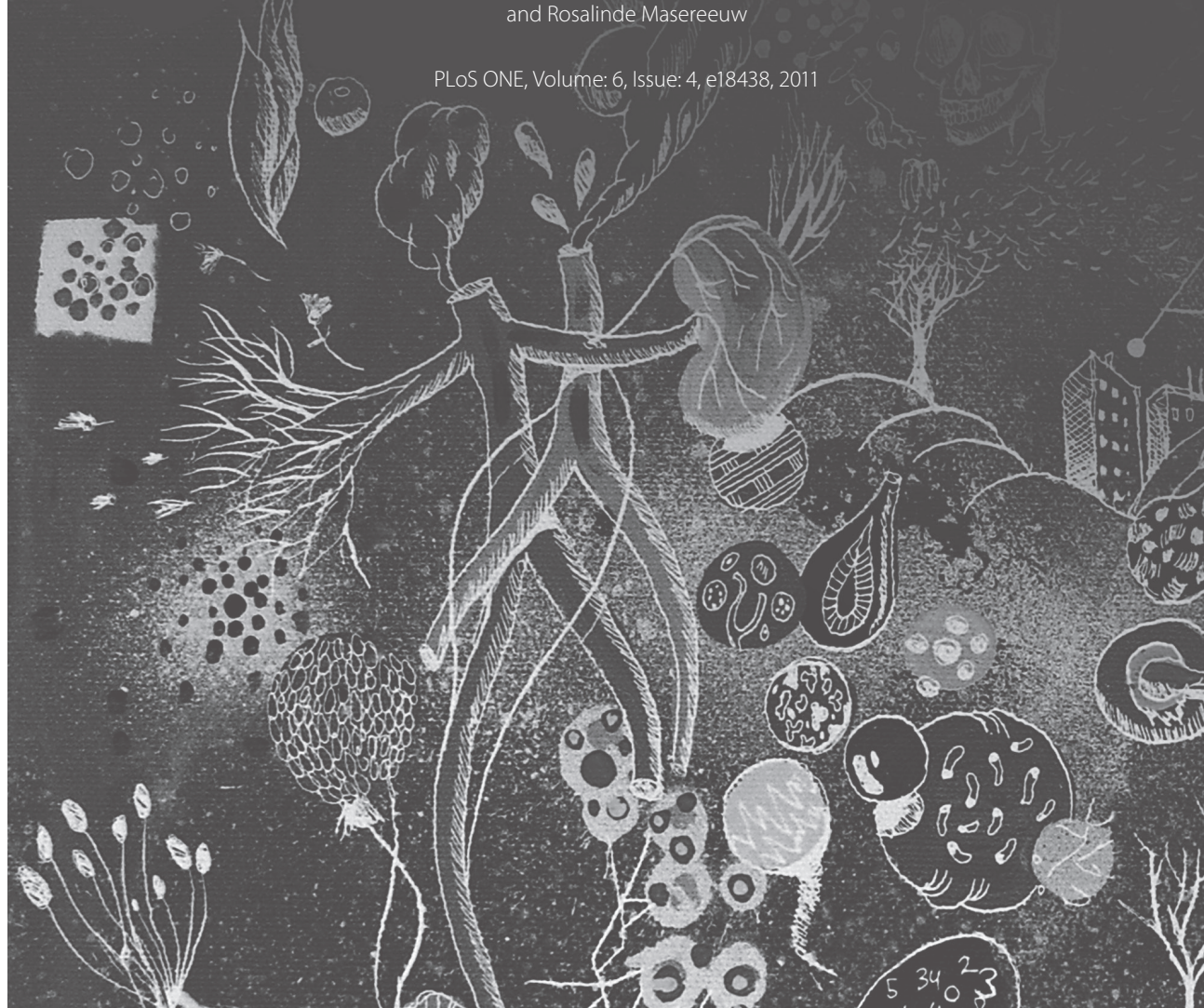

ABSTRACT

During chronic kidney disease (CKD), there is a progressive accumulation of toxic solutes due to inadequate renal clearance. Here, the interaction between uremic toxins and two important efflux pumps, *viz.* multidrug resistance protein 4 (MRP4) and breast cancer resistance protein (BCRP) was investigated. Membrane vesicles isolated from MRP4- or BCRP-overexpressing human embryonic kidney cells were used to study the impact of uremic toxins on substrate specific uptake. Furthermore, the concentrations of various uremic toxins were determined in plasma of CKD patients using high performance liquid chromatography and liquid chromatography/tandem mass spectrometry. Our results show that hippuric acid, indoxyl sulfate and kynurenic acid inhibit MRP4-mediated [^{3}H]-methotrexate ([^{3}H]-MTX) uptake (calculated Ki values: 2.5 mM, 1 mM, 25 µM, respectively) and BCRP-mediated [^{3}H]-estrone sulfate ([^{3}H]-E1S) uptake (Ki values: 4 mM, 500 µM and 50 µM, respectively), whereas indole-3-acetic acid and phenylacetic acid reduce [^{3}H]-MTX uptake by MRP4 only (Ki value: 2 mM and IC_{50} value: 7 mM, respectively). In contrast, p-cresol, p-toluenesulfonic acid, putrescine, oxalate and quinolinic acid did not alter transport mediated by MRP4 or BCRP. In addition, our results show that hippuric acid, indole-3-acetic acid, indoxyl sulfate, kynurenic acid and phenylacetic acid accumulate in plasma of end-stage CKD patients with mean concentrations of 160 µM, 4 µM, 129 µM, 1 µM and 18 µM, respectively. Moreover, calculated Ki values are below the maximal plasma concentrations of the tested toxins. In conclusion, this study shows that several uremic toxins inhibit active transport by MRP4 and BCRP at clinically relevant concentrations.

INTRODUCTION

Approximately 5% of the adult population in the developed countries suffers from chronic kidney disease (CKD) stage III-V, which is defined by a decreased estimated glomerular filtration rate (eGFR) [5]. A main feature at this stage of CKD is the accumulation of solutes that are normally excreted in urine. These uremic retention solutes, also known as uremic toxins, are a heterogeneous group of organic compounds. Currently, 110 compounds are considered to be uremic toxins and they are classified into three groups depending on their chemical properties that largely influence the possibility to remove these toxins using current dialysis strategies, namely size and solubility. The currently defined groups, as described by Vanholder *et al.* 2008, are: (1) the small water-soluble compounds, with a molecular weight (MW) arbitrarily set at ≤ 500 Da, for example, urea and creatinine; these compounds are easily removed via dialysis and their toxic potential is limited. (2) The middle molecules, with a MW > 500 Da, such as β_2-microglobulin; due to their size, these retention solutes can only be cleared using dialyzer membranes with large pores, which focus on filtration via convection instead of diffusion. (3) The protein-bound solutes; the compounds in this group mostly have a small MW and prototypes include indoxyl sulfate and p-cresyl sulfate. Solutes belonging to this group are very difficult to clear using current dialysis strategies and they exhibit toxic effects [23]. Uremic toxins are thought to contribute to the plethora of pathologies observed in patients with CKD, including anemia, bone disorders, renal fibrosis and cardio-vascular disease. Administration of the oral sorbent AST-120 is currently the only therapy to prevent accumulation of protein-bound uremic toxins in patients with CKD. Unfortunately, AST-120 prevents no more than the uptake of indoxyl sulfate and p-cresol in the intestinal tract [125]. Understanding the endogenous clearance of protein-bound solutes could lead to the development of novel therapeutic strategies for the removal of uremic toxins.

In the healthy population, uremic toxins are cleared by the kidney and this process is largely dependent on glomerular filtration and tubular secretion via a multitude of transport proteins expressed in renal proximal tubules. Moreover, it has been demonstrated that both organic anion transporter (OAT) 1 and OAT3 play important roles in the renal tubular uptake of uremic toxins and organic anions [64,72,126]. Both transporters show overlapping substrate specificities, but differential contributions to uremic toxin clearance have been reported as well. For example, indoxyl sulfate is equally transported by OAT1 and OAT3, but indole-3-acetic acid and hippuric acid are preferable substrates for OAT1, and uptake of 3-carboxy-4-methyl-5-propyl-2-furanpropionate is mediated by OAT3 solely [72]. In addition, using a rat model of renal failure, the basolaterally expressed kidney-specific organic anion transporting polypeptide 4C1 (SLCO4C1) was recently shown to facilitate the removal of several uremic toxins, including guanidino succinate, in the proximal tubule [60]. Thus, basolateral uptake of uremic toxins in renal proximal tubules cells is fairly well characterized, however, little is known about the transport of

uremic toxins over the apical membrane into urine. Two important renal efflux pumps at the apical membrane are multidrug resistance protein 4 (MRP4) and breast cancer resistance protein (BCRP) [127,128]. Both MRP4 and BCRP are known to transport urate, [87,88] a uremic toxin involved in the pathogenesis of gout and cardiovascular disease [129]. Furthermore, functional and nonfunctional mutations in the BCRP gene cause hyperuricemia-based gout, supporting the importance of the efflux pump in urate secretion [88,130]. Therefore, it seems likely that both MRP4 and BCRP are involved in the transport of uremic toxins into the proximal tubule lumen.

The present study was designed to investigate the interaction between several uremic toxins, mainly belonging to the group of protein-bound solutes, and MRP4- and BCRP-mediated transport. Our results show that hippuric acid, indoxyl sulfate and kynurenic acid inhibit substrate specific uptake by both MRP4 and BCRP, whereas indole-3-acetic acid and phenylacetic acid only reduce transport by MRP4. Moreover, inhibition of transport by multiple uremic toxins mainly occurs at clinically relevant concentrations, suggesting that uremic toxins may contribute to the many complications of CKD.

MATERIALS AND METHODS

Ethics Statement

The ethical committee of the Radboud University Nijmegen Medical Centre on research involving human subjects approved this study, and oral informed consent was obtained from each patient and each healthy volunteer.

Chemicals

All chemicals were obtained from Sigma (Zwijndrecht, the Netherlands) unless stated otherwise. Stock solutions of uremic toxins were prepared as previously described [131], and stored at -20 ºC. [3',5',7'-^{3}H(*n*)]-methotrexate disodium salt ([^{3}H]-MTX) with a specific activity ranging between 13.4 and 25.3 Ci/mmol was purchased from Moravek (Brea, USA) and [6',7'-^{3}H(*n*)]-estrone-sulfate ammonium salt ([^{3}H]-E1S) with a specific activity of 54.26 Ci/mmol was obtained from Perkin Elmer (Groningen, the Netherlands).

Cell culture and transfection

Human embryonic kidney (HEK293; purchased at American Type Culture Collection, Manassas, VA) cells were cultured in Dulbecco's modified Eagle's medium (Invitrogen life sciences, Breda, the Netherlands) containing 10% (v/v) fetal calf serum (MP Biomedicals, Uden, the Netherlands) at 37 ºC in a 5% (v/v) CO_2 atmosphere. To functionally overexpress MRP4 and BCRP, HEK293 cells were transduced with baculoviruses of human MRP4, BCRP

or enhanced yellow fluorescent protein (EYFP), generated via the Bac-to-Bac system (Invitrogen) as previously described [132]. To transduce HEK293 cells, they were cultured in 500 cm^{2} flasks until 70% confluence. Subsequently, medium was removed and 10 ml of virus and 25 ml of medium were added and incubated for 30 min at 37 ºC. Next, 50 ml of medium was added and after 2 h of transduction 5 mM sodium butyrate was added.

Membrane vesicle preparation

Three days after transduction, cells were harvested and pelleted by centrifugation (30 min at 4,000 x g). Afterwards, the cells were resuspended in ice-cold hypotonic TS buffer (0.5 mM sodium phosphate, 0.1 mM EDTA, pH 7.0) containing protease inhibitors (100 µM phenylmethylsulfonyl fluoride, 5 µg/ml aprotinin, 5 µg/ml leupeptin, 1 µg/ml pepstatin and 1 µg/ml E-64) and shaken for 30 min at 4 ºC. Cells were then centrifuged at 100,000 x g for 30 min at 4 ºC. Subsequently, pellet was resuspended in ice-cold isotonic buffer (10 mM Tris-HEPES and 250 mM sucrose, pH 7.4, adjusted with HEPES) supplemented with protease inhibitors and homogenized using a tight fitting Dounce homogenizer followed by centrifugation (1,000 x g, 20 min, 4 ºC). Afterwards, supernatant was centrifuged at 100,000 x g for 1 h at 4 ºC. The resulting pellet was resuspended in isotonic buffer and passed through a 27-gauge needle 25 times to obtain crude membrane vesicles. The protein content of samples was determined using the Bio-Rad protein assay (Veenendaal, the Netherlands), according to manufacturers recommendations. Vesicles were frozen in liquid nitrogen and stored at -80 ºC until use. The orientation of the membrane vesicles was not determined, since ATP-dependent uptake occurs only in inside-out vesicles.

Western blotting

Overexpression of MRP4 or BCRP in membrane vesicles was studied using the Odyssey western blotting technique. Total protein (15 µg) was separated via SDS/PAGE using a 10% (w/v) gel, and blotted onto nitrocellulose membranes using the iBlot dry blotting system (Invitrogen). Afterwards, the membrane was blocked using Odyssey Blocking Buffer, (1:1 diluted with PBS; Westburg BV, Leusden, the Netherlands) for 1 hour at RT. The membrane was then incubated overnight at 4 ºC with rabbit-α-MRP4 (1:5,000; van Aubel *et al.* [127]) or mouse-α-BCRP (1:200; Clone BXP-21; Kamiya Biomedical, Seattle, USA) in Odyssey Blocking Buffer containing 0.1% (v/v) Tween-20. Afterwards, the membrane was thoroughly washed three times during 10 min with PBS containing 0.1% (v/v) Tween-20. The secondary antibodies, goat-α-rabbit IRDye 800 (1:10,000; Sigma) and goat-α-mouse Alexa Fluor 680 (1:10,000; Rockland, Heerhugowaard, the Netherlands), were incubated for 1 hour at RT in Odyssey Blocking Buffer containing 0.1% (v/v) Tween-20 and 0.01% (w/v) SDS. The membrane was thoroughly washed, as described above, and then scanned using the Odyssey Infrared Imaging System (LI-COR Biotechnology). Expression of MRP4 was assessed using channel 800 and BCRP expression was determined using channel 700.

Membrane vesicle transport inhibition assay

A rapid filtration technique was used to study the uptake of [^{3}H]-MTX and [^{3}H]-E1S into MRP4 or BCRP membrane vesicles, as previously described [133]. In short, 25 µl of TS buffer containing 4 mM ATP, 10 mM $MgCl_2$ and radiolabeled substrate was added to 5 µl of the membrane vesicles (1.5 mg/ml). The transport assay was performed in the absence or presence of various concentrations of uremic toxins to evaluate the inhibitory effects of these compounds on MRP4-mediated [^{3}H]-MTX uptake and BCRP-mediated [^{3}H]-E1S uptake. Transport was started by incubating the mixture at 37 ºC for 1 min (BCRP) or 10 min (MRP4), time points at which substrate uptake was previously shown to be linear [132,134]. Uptake was stopped by placing the samples on ice and the addition of 150 µl ice cold TS buffer. Subsequently, the samples were transferred to a 96 well filter plate (Millipore, Etten-leur, the Netherlands) pre-incubated with TS buffer and filtered using a Multiscreen HTS-Vacuum Manifold filtration device (Millipore). Afterwards, 2 ml of scintillation liquid was added to each filter and radioactivity was determined using liquid scintillation counting. As negative controls ATP was substituted for AMP and EYFP-membrane vesicles were used. Each experiment was performed in triplicates.

High-performance liquid chromatography (HPLC)

Blood samples were obtained from 4 patients with chronic renal failure (CRF) during regular check-up, 6 patients with end-stage renal disease (ESRD) before hemodialysis and 4 healthy controls. Clinical characteristics of study subjects are listed in Table 1. None of the subjects had been fasting at the time of blood sampling. Blood was collected in an EDTA Vacutainer and was immediately centrifuged at 3,000 x g for 10 min. Subsequently, plasma was collected and stored at -20 °C. Before chromatography an aliquot of plasma was diluted in H_2O (1:1) and deproteinized with perchloric acid (final concentration 3.3% (v/v)). Next, samples were centrifuged at 12,000 x g for 3 min and 50µl of the supernatant was injected into the HPLC-system (Spectra-Physics Analytical, Spectrasystem SCM400). To measure indole-3-acetic acid, indoxyl sulfate and hippuric acid, the HPLC was equipped with a C18 HPLC column (GraceSmart RP 18 5u 150 x 4.6 mm; Grace, Breda, the Netherlands). Separation was performed at a flow rate of 1 ml/min with eluent A (95% (v/v) H_2O, 5% (v/v) acetonitril and 0.1% (v/v) heptafluorobutyric acid) and eluent B (50% (v/v) H_2O, 50% (v/v) acetonitrile and 0.1% (v/v) heptafluorobutyric acid) under the following gradient conditions: 0-1 min, 100% eluent A; 1-15 min, 100-25% eluent A; 15-17 min, 25% eluent A; 17-18 min, 0-100% eluent A; 18-23 min, 100% eluent A. The compounds were detected at a wavelength of 230 nm. For the detection of phenylacetic acid, chromatography was performed on a C18 HPLC column (Polaris 3 C18-A 150 x 4.6 mm; Varian, Middelburg, the Netherlands) with eluent A (97% (v/v) 50 mM sodium phosphate buffer [pH 6.5] and 3% (v/v) methanol) and eluent B (50% (v/v) H_2O, 49% (v/v) acetonitrile and 1% (v/v) tetrahydrofuran) using the following gradient: 0-1 min, 100% eluent A; 1-15 min, 100-90% eluent A; 15-18 min, 10-100% eluent B; 18-22 min, 100% eluent B; 22-25 min, 0-100% eluent A; 25-30 min, 100% eluent A. The flow rate was 1 ml/min and phenylacetic acid was measured at a wavelength of 215 nm. Standards of the compounds were also run in order to quantify the amount of toxins found in the samples. Acquired data were processed with PC1000 software (Spectrasystem).

Table 1 Characteristics of study subjects

	CRF	ESRD	Control
Number	4	6	4
Age (years)	54 ± 20	58 ± 13	34 ± 10
Women (%)	25	33	25
Ureum (mmol/l)	32 ± 6	21 ± 6	ND
Creatinine (µmol/l)	510 ± 210	720 ± 90	ND
Dialysis strategy	NA	4 HD, 2 CAPD	NA

Values are shown as mean ± SD. CRF, chronic renal failure; ESRD, end-stage renal disease; ND, not determined; NA, not applicable; HD, hemodialysis; CAPD, continuous ambulatory peritoneal dialysis.

Liquid chromatography-tandem mass spectrometry (LC-MS/MS)

To determine the levels of kynurenic acid, blood was collected from CRF patients and processed as described above. Subsequently, 10 µl of the clear supernatant was injected into the LC-MS/MS system that consisted of an Accela HPLC system (Thermo scientific, Breda, the Netherlands) equipped with a C18 HPLC column (VisionHT C18 B 100x2 mm, 1.5 µm; Grace). Separation was performed at a flow rate of 150 µl/min with eluent A (5mM ammonium formate + 0.01% (v/v) trifluoroacetic acid) and eluent B (50% acetonitrile) under the following gradient conditions: 0-10 min, 98-50% eluent A; 10-15 min, 50% eluent A; 15-16 min, 50-98% eluent A; 16-21 min, 98% eluent A. The fractions eluted were directly passed through a TSQ Vantage tandem mass spectrometer (Thermo scientific) equipped with an electro-spray ionization source operating in the positive ion mode. The ion spray voltage was 4 kV, source temperature was 350 ºC and collision gas pressure was 1.5 bar. Kynurinic acid and the internal standard 1-methyl-tryptophan were quantified by selected reaction monitoring (SRM). The following SRM transitions were used: *m/z* 190 (parent ion) to *m/z* 89 and 144 (both product ions) for kynurenic acid and *m/z* 219.1 (parent ion) to *m/z* 160 and 202.1 (product ions) for methyl-tryptophan. A calibration curve of kynurenic acid was made to quantify the amount of toxin found in the samples and the results were corrected using the internal standard. Acquired data were processed with Thermo Xcaliber software (Thermo scientific).

Kinetic analysis and statistics

Statistics were performed using GraphPad Prism 5.02 via an unpaired t test or a Kruskal-Wallis test followed by a Dunn's Multiple Comparison test. Differences between groups were considered to be statistically significant when $p < 0.05$. The software was also used to perform (non-)linear regression analysis, curve fitting details are summarized in Table S1. The mean IC_{50} and IC_{20} values were calculated from the inhibition curves used for the Dixon analysis and to determine the inhibition constant (Ki) from the Dixon plots. Transport inhibition studies were performed in triplicate and repeated at least three times.

RESULTS

Selection of uremic toxins

The number of solutes that are considered to be uremic toxins is constantly increasing [135]. As stated before, protein-bound toxins are difficult to eliminate via dialysis and, therefore, these toxins accumulate and become players in the multitude of pathologies observed in uremic patients. In our study, ten toxins were selected containing one water-soluble solute (oxalate) and nine protein-bound solutes. The latter group contained four indoles (indoxyl sulfate, indole-3-acetic acid, kynurenic acid and quinolinic acid), three phenols (phenylacetic acid, p-cresol and p-toluenesulfonic acid as a model compound for p-cresyl sulfate), one hippurate (hippuric acid) and one polyamine (putrescine). Chemical characteristics of the solutes studied are depicted in Figure 1.

Expression of MRP4 and BCRP, and uptake of [^{3}H]-MTX and [^{3}H]-E1S by membrane vesicles

Human embryonic kidney (HEK293) cells were transduced using a baculovirus system to overexpress human MRP4, BCRP or enhanced yellow fluorescent protein (EYFP; negative control). Using the Odyssey Western blot technique, MRP4 and BCRP were detected in membrane vesicles isolated from MRP4- and BCRP-overexpressing HEK293 cells at 150 kD and 75 kD, respectively. Protein expression of the transporters was absent in EYFP-transduced cells, indicating that endogenous expression was undetectable. For functionality of MRP4, the uptake of methotrexate (MTX) was investigated by using a radiotracer of the drug [133]. Figure 2A shows that the ATP-dependent uptake of [^{3}H]-MTX in MRP4-over-expressing vesicles is 11-fold higher as compared to EYFP vesicles with an average rate of 1.3 pmol/mg*min. To determine the transport activity of BCRP, radioactively labeled estrone sulfate (E1S) was used as typical substrate [134]. BCRP-overexpressing vesicles showed 24-fold higher ATP-dependent uptake of [^{3}H]-E1S, compared to EYFP controls with an average rate of 15.5 pmol/mg*min (Figure 2B). Furthermore, Figure 2 demonstrates that for both transporters non-specific, AMP-dependent, uptake is very low. Therefore, AMP-corrected uptake is shown in subsequent figures. These results support the functional expression of the transporters.

Solute	Structure	Group	Solute	Structure	Group
hippuric acid	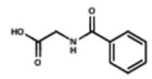	hippurates	p-cresol	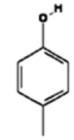	phenols
indole-3-acetic acid	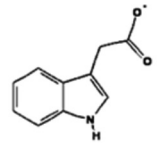	indoles	phenylacetic acid	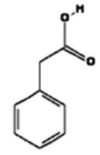	phenols
indoxyl sulfate	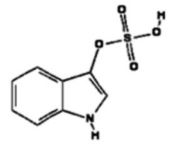	indoles	p-toluenesulfonic acid	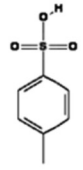	phenols
kynurenic acid	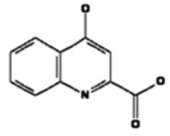	indoles	putrescine	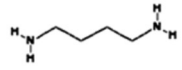	polyamines
oxalate	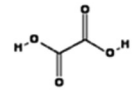		quinolinic acid	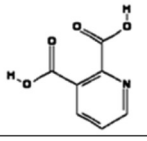	indoles

Figure 1 Selected uremic toxins.

p-toluenesulfonic acid was used as a model compound for p-cresyl sulfate.

Uremic toxins inhibit transport

Using membrane vesicles overexpressing either transport protein, the interaction between ten uremic toxins and substrate specific transport by MRP4 and BCRP was studied. Hippuric acid dose-dependently inhibited MRP4-mediated [^{3}H]-MTX uptake (Figure 3) and BCRP-mediated [^{3}H]-E1S uptake (Figure 4) in a concentration range of 0.1 mM to 3.5 mM. The compound did not completely inhibit transport by MRP4, as depicted by the plateau at 50% of the inhibition curve, whereas uptake of [^{3}H]-E1S by BCRP was completely blocked by hippuric acid. Indoxyl sulfate inhibited transport by both MRP4 and BCRP at concentrations ranging from 0.1 mM to 4 mM and 50 µM to 3 mM, respectively. Kynurenic acid inhibited substrate specific uptake by both MRP4 and BCRP in a concentration range of 0.1 µM to 1 mM. In addition, our results illustrate that indole-3-acetic acid and phenylacetic acid only reduced [^{3}H]-MTX uptake by MRP4 both at concentrations ranging from 0.1 mM to 5 mM. Differences in initial substrate uptake arose from batch-to-batch variations of the membrane vesicles, however, all vesicles used

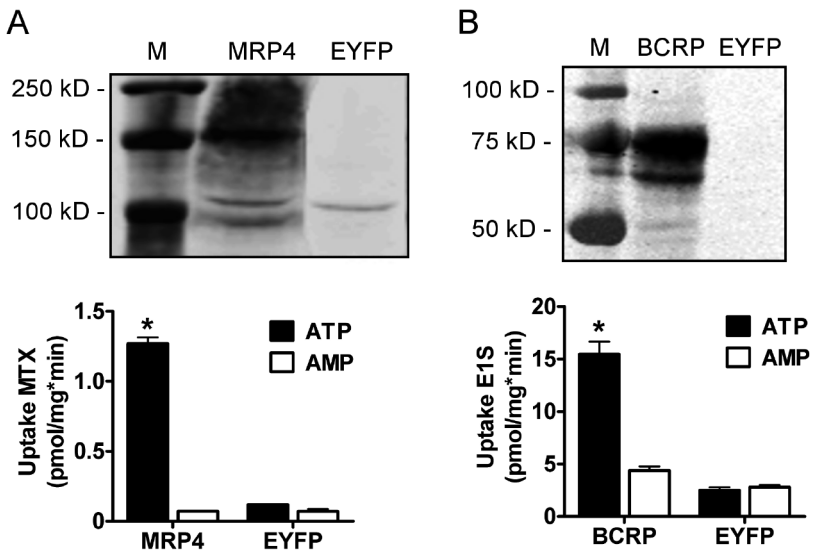

Figure 2 Transport expression and activity in isolated membrane vesicles.

HEK293 cells were transfected with a baculovirus of either human MRP4 or BCRP. Cells transfected with EYFP were used as a negative control. Subsequently, membranes were isolated and vesicles were prepared. Proteins were separated via SDS/PAGE and blotted onto nitrocellulose membranes. Blots were incubated with an antibody against MRP4 or BCRP and the appropriated fluorescently labeled secondary antibodies. MRP4 was detected at 150 kD **(upper panel A)** and BCRP was detected at 75 kD **(upper panel B)**. A rapid filtration technique was used to study the ATP-dependent uptake of [^{3}H]-MTX into MRP4- overexpressing membrane vesicles **(lower panel A)** and [^{3}H]-E1S into BCRP membrane vesicles **(lower panel B)**. As negative control ATP was substituted for AMP. Results are presented as mean ± SEM of one representative experiment performed in triplicate. M = marker, * indicates $p < 0.0001$ compared to EYFP. Experiments were performed at least three times.

demonstrated high substrate-specific uptake. The other toxins tested, *viz.* oxalate, p-cresol, p-toluenesulfonic acid, putrescine and quinolinic acid, did not decrease transport mediated by MRP4 or BCRP with more than 10% at a concentration of 1 mM, compared to control (Figure S1).

To investigate the mode of interaction, the uptake of three different concentrations of substrate in the absence and presence of uremic toxin was studied. The resulting inhibition curves were transformed to a Dixon plot and analyzed by linear regression. As depicted in the Dixon plots, most curves intersect with the x-axis, indicating non-competitive inhibition. Figures 5 and 6 show that hippuric acid and indoxyl sulfate inhibited MRP4-mediated transport in a non-competitive manner, with a Ki of 25 µM and 1 mM, respectively. Both toxins also inhibited transport by BCRP in a non-competitive fashion

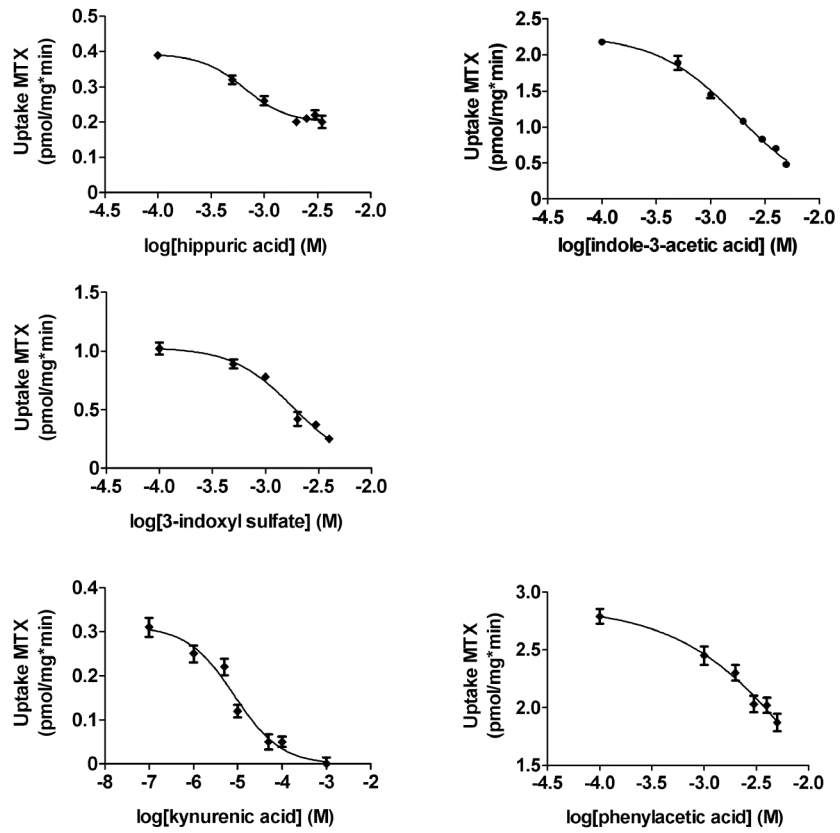

Figure 3 Uremic toxins inhibit MRP4-mediated transport.

A rapid filtration technique was used to study uptake of [^{3}H]-MTX into MRP4 membrane vesicles in the presence of various concentrations of uremic toxins. Radioactivity was determined using liquid scintillation counting. Nonlinear regression analysis was performed using Graphpad Prism 5.02. Results are presented as mean ± SEM of one representative experiment performed in triplicate. Experiments were performed at least three times.

with a Ki of 4 mM and 0.5 mM, respectively. Furthermore, our results indicated non-competitive inhibition of MRP4-mediated transport by indole-3-acetic acid (Ki: 2mM) and kynurenic acid (Ki: 25 µM), while the latter compound acted as a mixed inhibitor for [^{3}H]-E1S transport by BCRP. Mixed inhibition is considered to be composed of competitive and non-competitive inhibition. The mode of inhibition induced by phenylacetic acid, could not be elucidated due to incomplete inhibition of MRP4-mediated transport by this toxin. The kinetic analysis is summarized in Table 2.

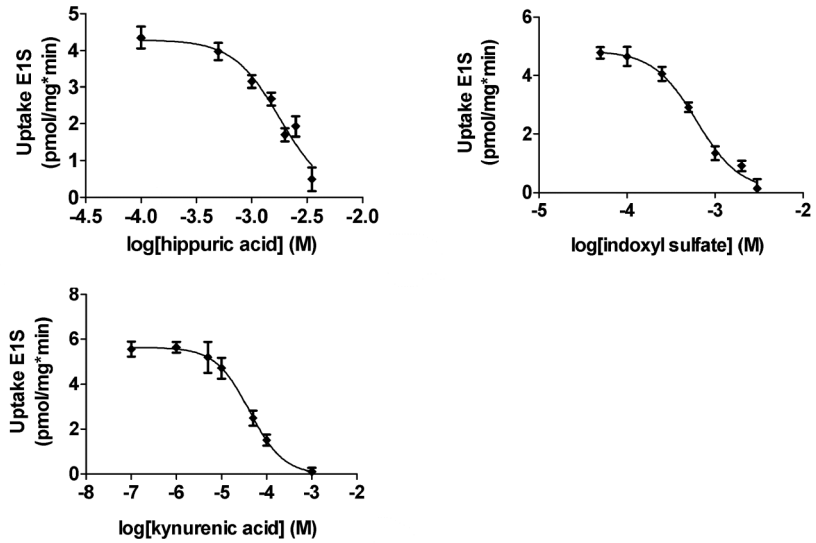

Figure 4 Uremic toxins inhibit BCRP-mediated transport.

A rapid filtration technique was used to study uptake of [^{3}H]-E1S into BCRP membrane vesicles in the presence of various concentrations of uremic toxins. Radioactivity was determined using liquid scintillation counting. Nonlinear regression analysis was performed using Graphpad Prism 5.02. Results are presented as mean ± SEM of one representative experiment performed in triplicate. Experiments were performed at least three times.

Accumulation of uremic toxins in plasma

To investigate whether the observed transport inhibition induced by several uremic toxins occurs at clinically relevant concentrations, the plasma levels of these toxins were measured in CRF and ESRD patients using HPLC and LC-MS/MS. Figure 7 illustrates that mean hippuric acid levels increased from 2.2 µM to 25 µM in CRF patients and to 160 µM in patients with ESRD. Furthermore, it was observed that indoxyl sulfate concentrations markedly increased from 13 µM (control) to 65 µM (CRF) and 129 µM (ESRD). The levels of indole-3-acetic acid significantly increased in patients with renal failure compared to control (2 µM), however, no differences were observed between patients with CRF (4 µM) or ESRD (4 µM). Furthermore, mean kynurenic acid levels significantly increased from 0.05 µM to 0.6 µM in CRF patients and to 1 µM in patients with ESRD. The mean plasma concentrations of phenylacetic acid slightly increased during CKD (CRF: 4 µM, ESRD: 18 µM), compared to control levels (5 µM), although not significantly. Hence, the interindividual variability increased with disease severity, with maximum concentrations reaching 9 µM in CRF patients and 83 µM in patients with ESRD.

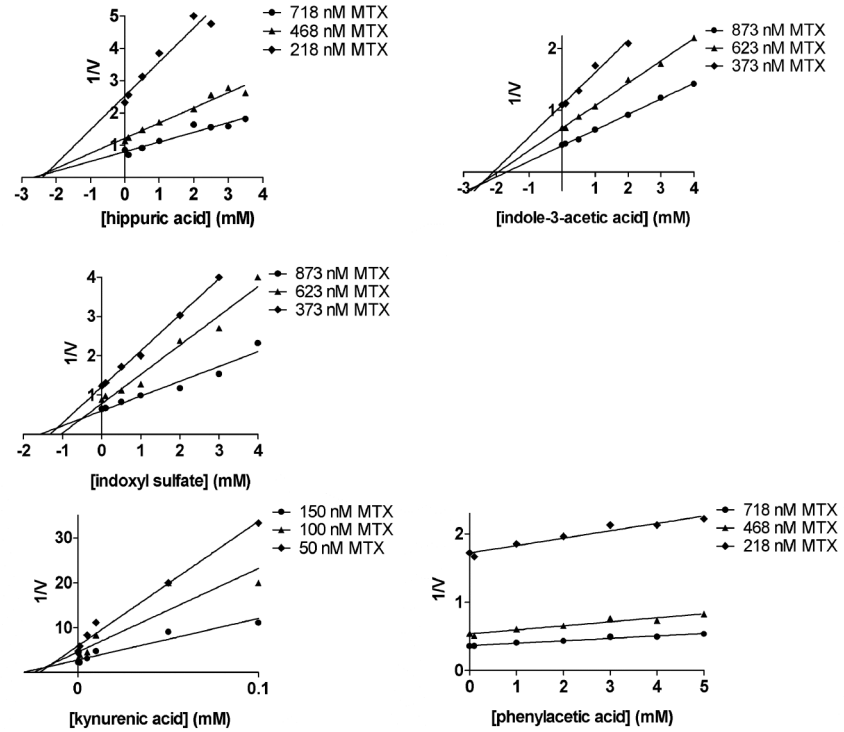

Figure 5 Uremic toxins inhibit MRP4-mediated transport mainly in a non-competitive fashion.

A rapid filtration technique was used to study substrate specific uptake by MRP4 membrane vesicles in the presence of various concentrations of uremic toxins. Radioactivity was determined using liquid scintillation counting. Three independent dose-response experiments were performed, each in triplicate, using different concentrations of [^{3}H]-MTX. A Dixon plot of the reciprocal of velocity was plotted against the concentration of different uremic toxins.

Inhibition of MRP4- and BCRP-mediated transport occurs at clinical relevant concentrations

The calculated Ki and IC_{20} values were compared with the mean plasma concentrations measured in ESRD patients during this study (C_m), the highest mean/median (C_u) and the highest maximal plasma concentrations (C_{max}) measured in the literature in patients with CKD are also shown. The IC_{20} value was used since we believe that a 20% decrease in transport can already have a clinical impact. The C_u and C_{max} values were obtained from the online database of the European Uremic Toxin (EUTox) Work Group (www.

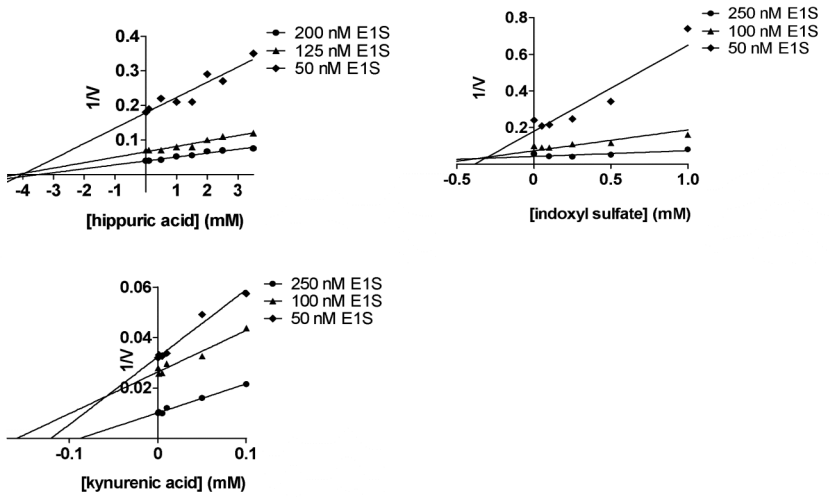

Figure 6 Uremic toxins inhibit BCRP-mediated transport mainly in a non-competitive fashion.

A rapid filtration technique was used to study substrate specific uptake by BCRP membrane vesicles in the presence of various concentrations of uremic toxins. Radioactivity was determined using liquid scintillation counting. Three independent dose-response experiments were performed, each in triplicate, using different concentrations of [^{3}H]-E1S. A Dixon plot of the reciprocal of velocity was plotted against the concentration of different uremic toxins.

uremic-toxins.org; [21]), unless stated otherwise. The results are summarized in Table 2. Kynurenic acid potently inhibited transport by MRP4, the Ki (25 µM) being notably lower than C_{max} (50 µM) and the IC_{20} (1.5 µM) similar to the mean concentration of this compound. Furthermore, our results indicated that 50% of MRP4-mediated uptake was inhibited by 2.5 mM hippuric acid, which is lower than the C_{max} of this solute (2.6 mM) and the IC_{20} (0.35 mM) is four times lower than the C_u. Phenylacetic acid inhibited 50% of the transport by MRP4 at a concentration lower than the C_{max} (7 mM vs. 7.7 mM), whereas, 20% of the transport was inhibited at a concentration lower than the highest median plasma concentration (1.6 mM vs. 3.5 mM). Moreover, the Ki of indoxyl sulfate is almost similar to the C_{max} of this solute (1 mM vs. 940 µM), whereas, the IC_{20} (530 µM) is approximately two-times below the maximal concentration. Indole-3-acetic acid is the least potent inhibitor of MRP4-mediated transport, with both the Ki (2 mM) and the IC_{20} (570 µM) noticeably higher than the C_{max} (52 µM). BCRP-mediated transport is significantly inhibited by kynurenic acid, with the Ki (50 µM) comparable to the peak uremic toxin concentration (50 µM) and the IC_{20} (10 µM) lower than the C_{max}. Indoxyl sulfate acid inhibited 50% of the

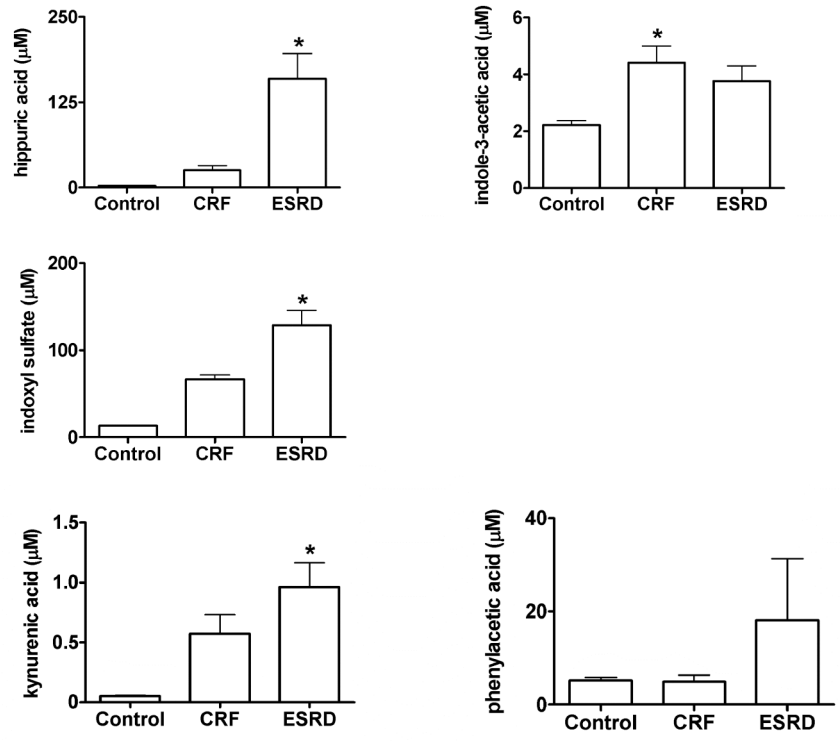

Figure 7 Accumulation of uremic toxins during CKD.

HPLC was used to measure the total plasma concentrations of hippuric acid, indole-3-acetic acid, indoxyl sulfate and phenylacetic acid. LC-MS/MS was used to measure kynurenic acid. Plasma samples were obtained from healthy volunteers (n=4) and patients with CRF (n=4) or ESRD (n=6). Standards of the compounds were also analyzed in order to quantify the amount of toxins found in the samples. Acquired HPLC data were processed with PC1000 software (Spectrasystem) and LC-MS/MS data were processed with Xcaliber software (Thermo scientific). Results are presented as mean ± SEM. * indicates $p < 0.05$ compared to control.

uptake by BCRP at a concentration below the maximal uremic concentration (500 µM vs. 940 µM). Furthermore, hippuric acid inhibited 20% of the [^{3}H]-E1S uptake by BCRP at a concentration almost two-fold lower than the highest median uremic concentration (690 µM vs. 1.4 mM), whereas the Ki (4 mM) was higher than the C_{max} (2.6 mM).

Table 2 Transport inhibition occurs at clinically relevant concentrations

MRP4						
Uremic toxin	**IC_{50} (μM)**	**IC_{20} (μM)**	**Ki (μM)**	**C_m (μM)**	**C_u (μM)**	**C_{max} (μM)**
kynurenic acid	8 ± 1	1.5 ± 0.3	25 ± 2	1	-	50
hippuric acid	990 ± 180	350 ± 20	2500 ± 50	160	1380	2631
phenylacetic acid	7100 ± 1600	1600 ± 170	-	18	3490[a]	7664[b]
indoxyl sulfate	1750 ± 110	530 ± 70	1000 ± 90	129	211	940
indole-3-acetic acid	1795 ± 8	570 ± 30	2000 ± 70	4	5	52

BCRP						
Uremic toxin	**IC_{50} (μM)**	**IC_{20} (μM)**	**Ki (μM)**	**C_m (μM)**	**C_u (μM)**	**C_{max} (μM)**
kynurenic acid	40 ± 1	10 ± 1	50[c]	1	-	50
hippuric acid	3670 ± 170	690 ± 70	4000 ± 100	160	1380	2631
indoxyl sulfate	770 ± 120	390 ± 30	500	129	211	940

Values are shown as mean (C_m; concentration determined in this study), highest mean/median (C_u) and maximal uremic concentration (C_{max}). Both C_u and C_{max} were obtained from www.uremic-toxins.org, unless stated otherwise. IC_{50} and IC_{20} values are shown as mean ± SEM of three separate experiments performed in triplicate.

[a] C_u obtained from literature [136].
[b] Hypothetical C_{max}, calculated as $C_{max} = C_u + 2$ SD, as previously described [21].
[c] Ki for competitive inhibition

DISCUSSION

This study reports, for the first time, that several uremic toxins directly inhibit transport by two important efflux pumps, *viz*. MRP4 and BCRP, at clinically relevant concentrations. Since MRP4 and BCRP are located at the apical membrane of proximal tubule cells, transport activity depends on the intracellular levels of substrates rather than substrate concentrations in the blood. Previously, Masereeuw *et al*. demonstrated that methyl hippuric acids accumulate during secretory transport in the isolated perfused rat kidney [137,138]. Furthermore, they showed that 2-methyl hippuric acid levels were 175-times higher in kidney tissue compared to the perfusate and 4-methyl hippuric acid concentrations were even 600-times higher. Thus, it is likely that intracellular uremic toxin concentrations are much higher than total plasma concentrations. This indicates that our results probably underestimate the potential inhibitory effect of uremic toxins on MRP4- and BCRP-mediated transport *in vivo*.

Both MRP4 and BCRP belong to the superfamily of ATP-binding cassette (ABC) transporters, a family of transmembrane proteins involved in the efflux of endo- and xenobiotics [58]. They are expressed in several tissues including liver, intestine, brain and the kidney [58,139]. In addition to their contribution to the renal secretion of endogenous compounds, MRP4 and BCRP are involved in the extrusion of a broad range of drugs [58]. Despite their importance, little is known about the expression and activity of both MRP4 and BCRP during renal disease. Lu *et* al. showed, in a rat model of CKD, that BCRP gene expression decreased in correlation with disease severity in male rats. In contrast, both gene and protein expression of MRP4 remained unaltered [140]. Furthermore, it was demonstrated that following acute kidney injury in mice the gene expression of MRP4 increased whereas the expression of BCRP decreased. Conversely, protein expression of both transporters showed an opposite effect [141]. The impact of kidney disease on transporter expression and the inhibition of transport activity by uremic toxins, as described in this study, indicates that during CKD drug disposition may be altered leading to an increased risk of adverse drug reactions.

Other transporters of the ABC family are P-glycoprotein (P-gp) and MRP2. These transporters are also expressed in the apical membrane of proximal tubule cells, amongst other tissues, and, similar to MRP4 and BCRP, they are involved in the urinary excretion of drugs [58]. It was described that the activity of P-gp in rat kidneys decreased following glycerol-induced acute kidney injury, whereas, P-gp expression increased [142]. In addition, it was demonstrated in rats that CRF induced the expression of MRP2 in the kidney while P-gp expression remained unaltered [86]. Although P-gp and MRP2 have not been associated with uremic toxin clearance, these reports further support the hypothesis that pharmacokinetics can be altered during kidney disease due to alterations in expression and activity of transporters.

Competition for renal excretion by different compounds with similar structural characteristics has been demonstrated decades ago in canine models [143]. These classic experiments used *in vivo* models to investigate the effect of certain compounds on the renal clearance of an entity with a similar chemical structure. However, these models do not allow to distinguish between competitive or non-competitive inhibition, but merely showed an overall effect on renal clearance which includes various kinetic steps. Nowadays, by applying molecular tools such as the membrane vesicle transport assay, the interaction between substrates/inhibitors and a transporter of interest can be studied in detail without the interference of other transporters and metabolizing enzymes present in available *in vivo* and *in vitro* models. However, the membrane vesicle transport assay is based on the premise that *in vitro* uptake is similar to *in vivo* efflux. Nevertheless, the use of isolated membrane vesicles to study transport by efflux transporters has been proven to be suitable in both fundamental science and drug discovery [58].The uremic toxins inhibit transport predominantly in a non-competitive fashion, suggesting that the toxins tested may use a different binding site than [^{3}H]-MTX or [^{3}H]-E1S for either MRP4 or BCRP, or that

the toxins are not a substrate for the efflux pumps. It is known that MRP4 has multiple binding sites and simultaneously transports urate and cAMP or cGMP [87]. Moreover, there is also evidence suggesting that BCRP contains multiple binding regions [144,145]. These findings suggest that the toxins tested may show different inhibition profiles when studied with other substrates for the transporters. Therefore, it is still possible that the tested uremic toxins are also substrates for MRP4 and BCRP. Evidently, more research is needed to fully elucidate the molecular interaction of uremic toxins with MRP4 and BCRP.
Our study further demonstrates that uremic toxins accumulate in patients with renal failure. We hypothesize that increasing MRP4- and BCRP-mediated transport activity is an important therapeutic target to prevent or reduce the accumulation of uremic toxins in dialysis patients. This hypothesis is supported by the study of Toyohara *et al.* who showed that overexpression of SLCO4C1 in the kidney reduces plasma levels of several uremic toxins in nephrectomized rats. Furthermore, they demonstrated that the transcription of SLCO4C1 is regulated by a xenobiotic responsive core element and that several statins induced the transcription of SLCO4C1 [60]. It would be interesting to examine whether statins, or drugs with a similar safety and tolerability profile, affect the expression and activity of MRP4 and BCRP.
In the present study the concentrations of five uremic toxins were measured in patients with CRF and ESRD. The CRF patients have severe renal insufficiency but were not yet on dialysis. The ESRD patients were treated with either peritoneal dialysis or hemodialysis. Plasma levels of urea and creatinine, substances not actively secreted to a considerable extent, were quite comparable between the groups. Still, our results indicate that the levels of several uremic toxins were higher in the ESRD patients as compared to the CRF patients. These results are in line with previous studies demonstrating that blood levels of indoxyl sulfate, p-cresol and uric acid are lower in patients with residual renal function [146,147]. Thus, residual renal function importantly contributes to the clearance of uremic toxins, supporting the hypothesis that active transport is a necessity for the removal of uremic toxins.
Importantly, the mean concentrations of hippuric acid, indoxyl sulfate and phenylacetic acid reported in this study are lower than the mean/median concentrations in patients reported in literature [21,136]. In contrast, the fold-increase of these toxins in ESRD patients compared to healthy controls, are higher in our study than in a preceding study [90]. Previously, Vanholder *et al.* noted that many discrepancies exist in the reported blood levels of uremic toxins in patients with renal failure [21]. These authors proposed several causes for these differences, including technical reasons (*e.g.* incomplete elution of compounds during chromatography or insufficient extraction of compounds from blood) and deviations in study population. Furthermore, it is important to notice that the largest variations were found in the concentrations of solutes derived from dietary intake. For example, hippuric acid is a metabolite of phenolic compounds found in tea, wine and fruit juices and phenylacetic acid is present in many fruits. Thus, it is likely that differences in diet between the study populations contribute largely to the observed variations in uremic toxin levels.
CKD is characterized by progressive and irreversible loss of renal function and the patho-physiological mechanisms underlying the progression of renal failure remain elusive. Concluding, several uremic toxins inhibit substrate-specific transport by MRP4 and BCRP at clinically relevant concentrations. Our results depict a novel pathway via which uremic toxins impede kidney excretory function and can contribute to accumulation of these potentially toxic uremic retention solutes.

ACKNOWLEDGEMENTS

The authors would like to thank J.J.M.W. van den Heuvel and P.H.H. van den Broek for excellent technical support regarding the transport inhibition assay and the HPLC and LC-MS/MS measurements of uremic toxins in plasma.

Supplementary data

Supporting information is available online at www.plosone.org.

4

Proximal tubular transporters involved in renal excretion of *p*-cresyl sulfate and *p*-cresyl glucuronide: implications for CKD pathophysiology

In part published as:
Basolateral transport of the uraemic toxin p-cresyl sulfate: role for organic anion transporters?

Henricus A.M. Mutsaers, Martijn J.G. Wilmer, Lambertus P. van den Heuvel, Joost G. Hoenderop and Rosalinde Masereeuw

Nephrology Dialysis Transplantation, Volume: 26, Issue: 12, Page: 4149, 2011

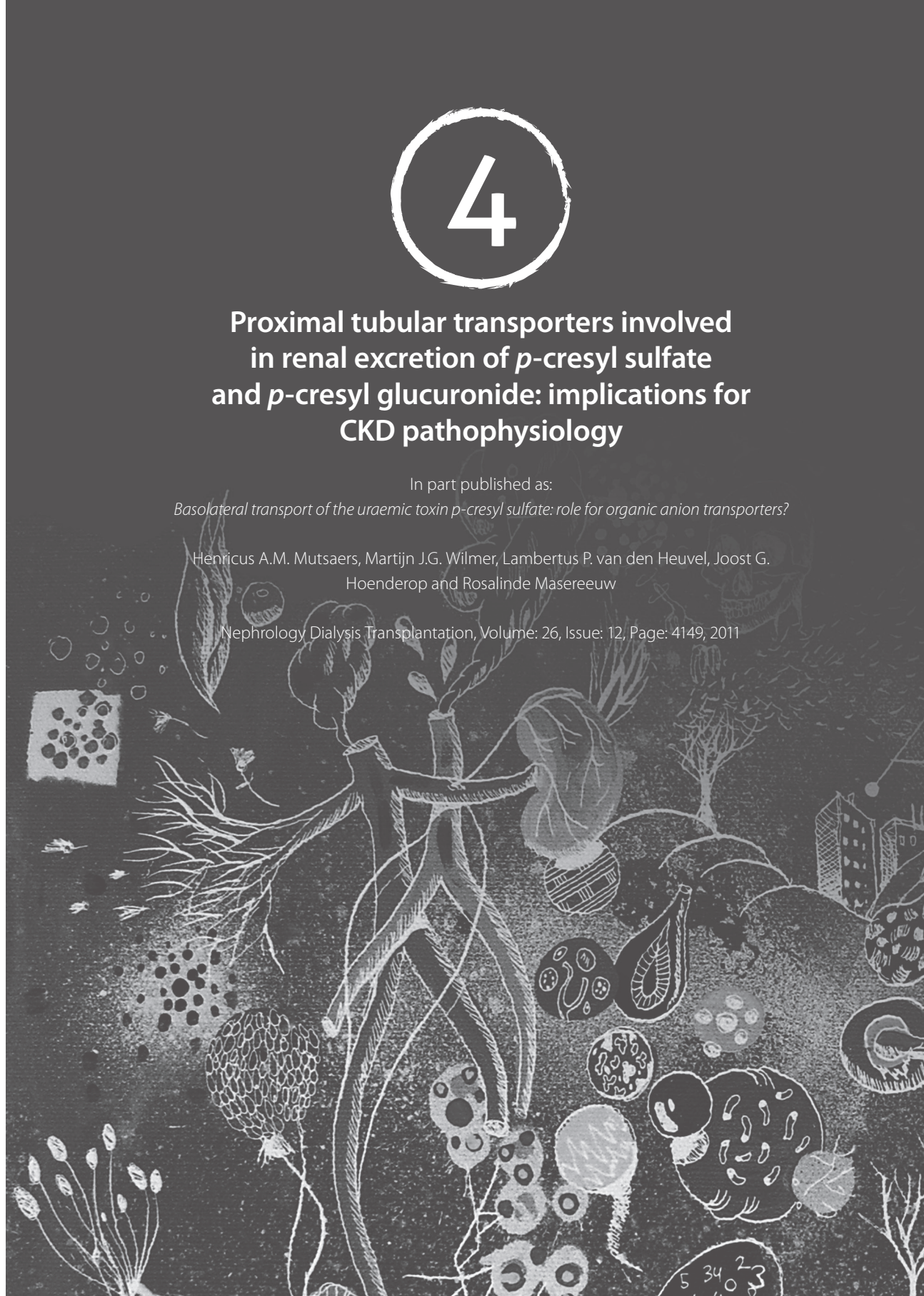

ABSTRACT

Chronic kidney disease (CKD) is characterized by the progressive accumulation of potential toxic metabolites due to impaired renal clearance. Here, we studied the retention of *p*-cresyl sulfate (pCS) and *p*-cresyl glucuronide (pCG) in different stages of CKD, and we aimed to identify the transporters involved in the tubular excretion of pCS and pCG. Moreover, the nephrotoxic activity of both solutes was investigated using human conditionally immortalized renal proximal tubule epithelial cells (ciPTEC). Our results show that pCS and pCG accumulate in plasma of end-stage CKD patients with mean concentrations of 161 µM and µM 46, respectively. Moreover, pCS inhibited multidrug resistance protein 4 (MRP4)-mediated [^{3}H]-methotrexate ([^{3}H]-MTX) uptake with 40% and breast cancer resistance protein (BCRP)-mediated [^{3}H]-estrone sulfate uptake with 25%, whereas pCG only reduced [^{3}H]-MTX uptake by MRP4 with 75%. Exposure of ciPTEC to pCG caused a 1.4-fold increased protein expression of the mesenchymal marker, vimentin, and a 1.5-fold induction of Bcl-2 gene expression, suggesting epithelial-to-mesenchymal transition (EMT). This process was associated with changes in the expression of key tubular transporters as demonstrated by decreased mRNA levels of organic anion transporting polypeptide 4C1 (33-fold) and elevated BCRP expression, with a fold change of 2.2. Moreover, both solutes did not induce tubular damage as observed by the gene expression of the biomarkers kidney injury molecule-1 and vanin-1. In conclusion, this study shows that pCS and pCG plasma levels are elevated during uremia. Moreover, we demonstrated that MRP4 and BCRP are likely involved in the renal excretion of both solutes. In addition, pCS was shown to lack biological activity in ciPTEC, whereas pCG induced cell stress and EMT.

INTRODUCTION

A hallmark of chronic kidney disease (CKD) is the retention and accumulation of a wide variety of potential toxic metabolites [21,22], associated with the plethora of pathologies observed in uremic patients, including renal fibrosis and cardio-vascular disease [23,135]. In the healthy population, these so-called uremic toxins are cleared via the kidney by means of glomerular filtration and transporter-mediated tubular excretion. In the early days of uremic toxin research, *p*-cresol, a phenol derived from tyrosine metabolism, was widely studied and a broad array of pathophysiological effects observed in CKD patients were contributed to this compound, including endothelial and immunological dysfunction [30]. However, several years ago it was demonstrated, by several groups, that not *p*-cresol but the metabolites, *p*-cresyl sulfate (pCS) and *p*-cresyl glucuronide (pCG), are retained during CKD [51,148,149]. *P*-cresol is formed in the gut during protein fermentation and is subsequently conjugated to either sulfate or glucuronic acid in the intestinal wall resulting in the formation of pCS or pCG, respectively [125]. In a study by Aronov *et al.*, it was elegantly demonstrated that the colon indeed plays a key role in the production of pCS [92]. In addition, our group recently showed renal *p*-cresol metabolism and subsequent formation of pCG in human proximal tubular cells [100]. Thus, the origin of pCS and pCG is reasonably well understood; however the molecular transport mechanisms involved in physiological urinary excretion of both solutes are not fully elucidated. Two pumps that likely contribute to the renal excretion of the *p*-cresol metabolites are multidrug resistance protein 4 (MRP4) and breast cancer resistance protein (BCRP). Both pumps are trans-membrane proteins belonging to the superfamily of ATP-binding cassette (ABC) transporters. They are expressed in several tissues with a barrier function, including liver, intestine, brain and kidney, and both transporters are known to transport a wide variety of drugs and endogenous compounds against steep concentration gradients [58,150]. Previously, we reported that several uremic toxins, such as kynurenic acid, hippuric acid and indoxyl sulfate, inhibited substrate-specific transport by MRP4 and BCRP at clinically relevant concentrations [89]. Since pCS and pCG share structural characteristics with the previously studied uremic solutes, we hypothesized that both pumps are also involved in the transport of pCS and pCG into the proximal tubule lumen.

Ever since it has been reported that pCS accumulates in CKD patients, this compound has been widely used as a model solute to elucidate the capacity of different dialysis modalities to remove protein-bound uremic toxins from the circulation of CKD patients [149]. In addition, several studies have shown that pCS can contribute to the pathophysiology of CKD. For instance, pCS can increase the shedding of endothelial micro particles by endothelial cells *in vitro*, indicating that pCS is involved in endothelial dysfunction [151]. Moreover, pCS can contribute to inflammation [43], suppresses the expression of the renoprotective antiaging gene Klotho both *in vitro* and *in vivo* [152], and causes insulin resistance and metabolic disturbances associated with CKD in mice by activating the

ERK1/2 pathway [8]. Furthermore, pCS is often studied in conjunction with indoxyl sulfate, a protein-bound uremic toxin derived from tryptophan, and it was recently reported by Kim *et al.* that this solute induces epithelial-to-mesenchymal transition (EMT) in proximal tubular cells [153]. Conversely, little is known about the biological activity of pCG and the nephrotoxic potential of both *p*-cresol conjugates is not clear.

Therefore, this study aimed to elucidate the interaction between pCS and pCG and the renal efflux transporters MRP4 and BCRP. Moreover, the human renal proximal tubule cell line (ciPTEC) was used to investigate the potential contribution of both *p*-cresol metabolites to CKD progression.

MATERIALS AND METHODS

Ethics statement

The ethical committee of the Radboud University Nijmegen Medical Centre on research involving human subjects approved this study, and written informed consent was obtained from each patient and each healthy volunteer.

Chemicals

All chemicals were obtained from Sigma (Zwijndrecht, the Netherlands) unless stated otherwise. Both pCS and pCG were kindly provided by Dr. Vanholder (University Hospital Ghent, Belgium). pCS was synthesized as a potassium salt as described previously [97]. pCG was produced from glucuronyl-trichloroacetimidate and *p*-cresol using the method previously described by Van der Eycken *et al.* [154]. Since pCS and pCG were obtained as a potassium and an ammonium salt, respectively, KCl and NH4Cl solutions were used as controls. [3',5',7'-^{3}H(*n*)]-methotrexate disodium salt ([^{3}H]-MTX) was purchased from Moravek (Brea, USA) and [6',7'-^{3}H(*n*)]-estrone-sulfate ammonium salt ([^{3}H]-E1S) was obtained from Perkin Elmer (Groningen, the Netherlands).

High-performance liquid chromatography (HPLC)

Blood samples were obtained from 4 patients with chronic renal failure (CRF) during regular check-up, 4 patients with end-stage renal disease (ESRD) before hemodialysis and 4 healthy controls. Clinical characteristics of study subjects are listed in Table 1. None of the subjects had been fasting at the time of blood sampling. Blood was collected in an EDTA Vacutainer and was immediately centrifuged at 3,000 x g for 10 min. Subsequently, plasma was collected and stored at -20°C. Before chromatography an aliquot of plasma was diluted in H_2O (1:1) and deproteinized with perchloric acid (PCA, final concentration 3.3% (v/v)). Next, samples were centrifuged at 12,000 x g for 3 min and 50 µl of the supernatant was injected into the HPLC-system (Spectra-Physics Analytical, Spectrasystem SCM400). For the detection of pCS and pCG, chromatography was performed on a C18

Table 1 Characteristics of study subjects

	CRF	ESRD	Control
Number	4	4	4
Age (years)	51 ± 6	57 ± 10	40 ± 12
Women (%)	0	25	50
Ureum (mmol/l)	22 ± 13	20 ± 6	ND
Creatinine (µmol/l)	211 ± 38	709 ± 105	ND
eGFR (ml/min/1.73 m^2) [a]	30 ± 5	7 ± 1	ND
Dialysis strategy	NA	3 HD, 1 CAPD	NA

Values are shown as mean ± SD. CRF, chronic renal failure; ESRD, end-stage renal disease; ND, not determined; NA, not applicable; HD, hemodialysis; CAPD, continuous ambulatory peritoneal dialysis.
[a]eGFR was calculated using the Modification of Diet in Renal Disease (MDRD) equation.

HPLC column (GraceSmart RP 18 5u 150 x 4.6 mm) with eluent A (95% (v/v) 50 mM KH_2PO_4 (pH 3.0) and 5% (v/v) acetonitrile) and eluent B (50 mM KH_2PO_4 (pH 3.0), methanol and acetonitrile in a 1:1:1 ratio) using the following gradient: 0-15 min, 100-20% eluent A; 15-16 min, 20-100% eluent A; 16-21 min, 100% eluent A. The flow rate was 1 ml/min and the *p*-cresol conjugates were detected at a wavelength of 220 nm. Standards of the compounds were also run in order to quantify the amount of metabolites found in the samples. Acquired data were processed with PC1000 software (Spectrasystem).

Transduction of Human Embryonic Kidney cells and membrane vesicle preparation

Human embryonic kidney (HEK293; purchased at American Type Culture Collection, Manassas, VA) cells were cultured in Dulbecco's modified Eagle's medium (Invitrogen life sciences, Breda, the Netherlands) containing 10% (v/v) fetal calf serum (MP Biomedicals, Uden, the Netherlands) at 37°C in a 5% (v/v) CO_2 atmosphere. To functionally overexpress MRP4 and BCRP, HEK293 cells were transduced with baculoviruses of human MRP4, BCRP or enhanced yellow fluorescent protein (eYFP; as a negative control), generated via the Bac-to-Bac system (Invitrogen) as previously described [132]. Subsequently, cell membranes were isolated and resuspended in isotonic buffer (10 mM Tris-HEPES and 250 mM sucrose, pH 7.4, adjusted with HEPES). Membrane vesicles were prepared via ultrafiltration as described previously [132]. Afterwards, vesicles were frozen in liquid nitrogen and stored at -80 °C until use. The orientation of the membrane vesicles was not determined, since ATP-dependent uptake occurs only in inside-out vesicles.

Membrane vesicle transport inhibition assay

A rapid filtration technique, well-established in our laboratory [89,132,150,155], was used to study the uptake of [^{3}H]-MTX and [^{3}H]-E1S into MRP4 or BCRP membrane vesicles. In short, 25 µl of TS buffer containing 4 mM ATP, 10 mM $MgCl_2$ and radiolabeled substrate was added to 5 µl of the membrane vesicles (1.5 mg/ml). The transport assay was performed in the absence or presence of various concentrations of pCS or pCG to evaluate the inhibitory effects of these compounds on MRP4-mediated [^{3}H]-MTX uptake and BCRP-mediated [^{3}H]-E1S uptake. Transport was started by incubating the mixture at 37 ºC for 1 min (BCRP) or 10 min (MRP4), time points at which substrate uptake was previously shown to be linear [132,134]. Uptake was stopped by placing the samples on ice and the addition of 150 µl ice cold TS buffer. Subsequently, the samples were transferred to a 96 well filter plate (Millipore, Etten-leur, the Netherlands) pre-incubated with TS buffer and filtered using a Multiscreen HTS-Vacuum Manifold filtration device (Millipore). Afterwards, 2 ml of scintillation liquid was added to each filter and radioactivity was determined using liquid scintillation counting. As negative controls ATP was substituted for AMP and eYFP-membrane vesicles were used. Each experiment was performed in triplicates.

Proximal tubule cell culture

The ciPTEC line was generated as previously described by Wilmer *et al.* [98]. The cells were cultured in ciPTEC medium containing phenol red free DMEM/F12 medium (Gibco/Invitrogen, Breda, the Netherlands) supplemented with 10% (v/v) fetal calf serum (FCS; MP Biomedicals, Uden, the Netherlands), insulin (5 µg/ml), transferrin (5 µg/ml), selenium (5 ng/ml), hydrocortisone (36 ng/ml), epithelial growth factor (10 ng/ml), and tri-iodothyronine (40 pg/ml) at 33ºC in a 5% (v/v) CO_2 atmosphere. Propagation of cells was maintained by subculturing the cells at a dilution of 1:3 to 1:6 at 33°C. For experiments, cells were cultured at 33ºC to 40% confluency, followed by maturation for 7 days at 37ºC. Experiments were performed using cells between passages 30 and 40.

Flow cytometry

In this study, flow cytometry was used to study the expression of vimentin, a mesenchymal cell marker. ciPTEC were seeded at 40% confluence in 12-well plates and allowed to adhere over night at 33ºC followed by maturation for 7 days at 37ºC, before being treated for 48 hours with either pCS or pCG (0-2 mM). After incubation, cells were harvested using trypsin-EDTA and centrifuged at 600 x g during 5 min. Subsequently, supernatant was removed and the cell pellet was resuspended in 100 µL PBS containing 1 µL mouse-α-human Vimentin-PE (Abcam, Cambridge, UK) followed by 30 min incubation at RT. Samples were acquired with a BD FACSCalibur (Becton Dickinson, Breda, the Netherlands) using channel FL-2. Analysis was performed using Flow Jo software (TreeStar, Ashland, USA), gating on live cells.

Quantitative PCR array

To study gene expression, total RNA was isolated from human kidney homogenate, HK-2 cells or ciPTEC (exposed to pCS or pCG) using an RNeasy Mini kit (Qiagen, Venlo, the Netherlands) according to the manufacturers recommendations. Subsequently, cDNA was generated using the Omniscript RT-kit (Qiagen) according to the manufacturers recommendations. Following cDNA-synthesis, quantitative PCR was performed using a CFX96 Real-Time PCR detection system (Bio-rad, Veenendaal, the Netherlands). GAPDH was used as housekeeping gene, and relative expression levels were calculated as percentage as compared with GAPDH (100%) or as fold change, calculated using the $2^{-\Delta\Delta CT}$ method. The primer-probe sets were obtained from Applied Biosystems (GAPDH, hs99999905_m1; OAT1, hs00537914_m1; OAT3, hs00188599_m1; OATP4C1, hs00698884_m1; Bcl-2, hs00608023_m1; Snail, hs00195591_m1; BCRP, hs00184979_m1; MRP4, hs00195260_m1; KIM-1, hs03054855_g1; Vanin-1, hs01546812_m1)

Kinetic analysis and statistics

Statistics were performed using GraphPad Prism 5.02 via one-way analysis of variance (ANOVA) followed by Bonferroni's or Dunnett's Multiple Comparison Test. Differences between groups were considered to be statistically significant when $p < 0.05$.

RESULTS AND DISCUSSION

Accumulation of pCS and pCG and changes in p-cresol metabolism in CKD patients

Figure 1A-B illustrates that mean pCS levels markedly increased from 20 µM in healthy controls to 107 µM in non-dialysis CRF patients and to 161 µM in dialysis patients. Moreover, the concentration of pCG increased from 0.3 µM (control) to 3 µM (CRF) and 46 µM (ESRD). Interestingly, the paradigm of *p*-cresol being one of the most important uremic toxins was an artifact resulting from strong acidification of plasma samples for deproteinization resulting in hydrolysis of both pCS and pCG [5]. In the current study, PCA extraction was used as a method for protein removal, still the pCS levels determined here are similar to the concentrations reported by several groups using different deproteinization methods including methanol extraction, enzymatic degradation or heating [6; 8; 22; 23]. Reports on pCG concentrations in CKD patients are scarce and considerably diverse, the results presented here corroborate the findings by Meert *et al.*, suggesting that pCG levels are much higher than previously reported [23]. Taken together, our results indicate that acidification can be successfully used as a deproteinization method when measuring plasma levels of pCS and pCG; yet one has to take into account that the *p*-cresol conjugates are prone to hydrolysis.

It is widely known that drug disposition is altered in CKD patients [24; 25], including the kinetics of drugs solely cleared via phase II metabolism [26-28]. Enzymes belonging to this class catalyze conjugation reactions such as glucuronidation, acetylation and sulfation [50]. Recently, using ciPTEC, our group demonstrated that uremic toxins can diminish renal UDP-glucuronosyltransferase functionality, probably through interference with mitochondrial succinate dehydrogenase activity and by reducing the reserve capacity of the energy-generating oxidative phosphorylation system [13]. Moreover, Simard *et al.*, reported that exposure of rat hepatocytes to uremic serum resulted in a decreased expression of N-acetyltransferase (NAT)1 and NAT2 [29]. Expression of both enzymes was also lower in the liver of CRF rats, which was accompanied by a reduction in NAT2-mediated acetylation of *p*-aminobenzoic acid [29]. However, little is known about sulfotransferase (SULT) expression and functionality in patients with renal failure. In the current study, HPLC revealed that the *p*-cresol metabolite fraction shifted from sulfation to glucuronidation with a pCG percentage of 2% in CRF patients and 22% in ESRD patients (Figure 1C). These findings provide the first evidence that SULT-mediated *p*-cresol metabolism is saturated or reduced in dialysis patients. Of interest, Sugimura *et al.* reported that SULT1C2 gene expression was decreased in an acquired polycystic kidney disease model in rats [30]. Still, the link between CKD and SULTs requires further investigation and may contribute to our understanding of the pathophysiology of CKD.

Basolateral transport of p-cresyl sulfate

Our results demonstrated that pCS and pCG are retained during CKD and it is known that active tubular transport is a necessity for the clearance of protein-bound uremic toxins [17]. Therefore, we aimed to identify the proximal tubular pumps involved in the renal handling of pCS and pCG. Recently, Miyamoto *et al.,* described a role for organic anion transporters (OATs) in the uptake of pCS using rat renal cortical slices and a human proximal tubule cell model, *viz.* HK-2 cells [31]. In their study, uptake of pCS in both model systems could be inhibited by several OAT inhibitors including probenecid and *p*-aminohippuric acid. As described by the authors, specificity of pCS transport was investigated using well-known substrates for OATs at a concentration of 1 or 10 mM in renal slices or HK-2 cells, respectively. As these concentrations are much higher compared to their inhibitory potencies reported [32], it could be argued that the affinity of pCS for OATs is very low in both models. Moreover, such concentrations are hardly soluble in an aqueous solution at physiological pH and highly influence cell viability [33].

In our opinion, it is more likely that HK-2 cells have only little or no expression at all of OATs. Functional transport by OATs is generally studied using heterologous expression in cultured cells or *Xenopus leavis* oocytes [32]. These systems are used because there are no stable cell lines known to date that highly express functional endogenous OATs and, to our knowledge, no publications are available for functional OAT transport in HK-2 cells. Moreover, functional expression of OATs in primary human proximal tubule cells can only

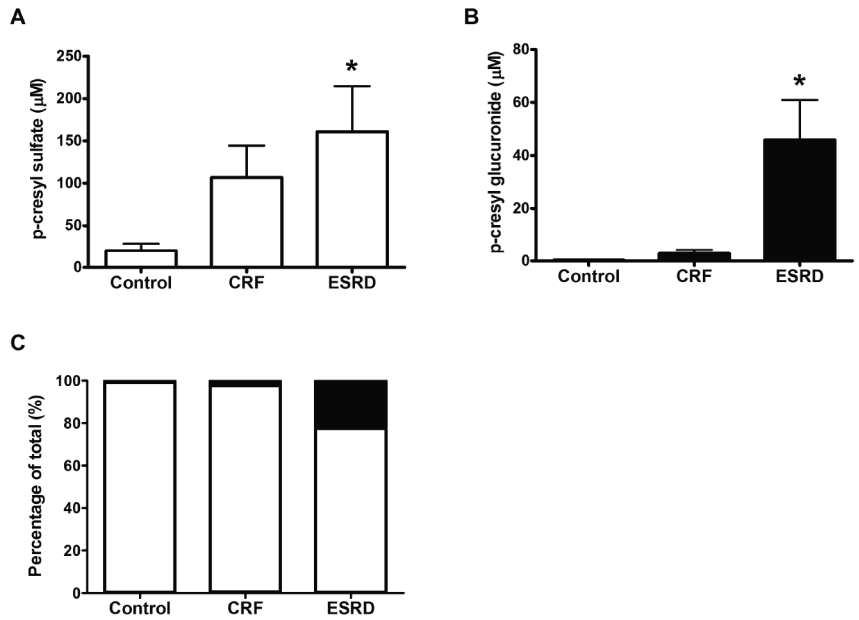

Figure 1 Accumulation of p-cresol metabolites during CKD.

HPLC was used to measure the total plasma concentrations of **(A)** pCS and **(B)** pCG. Plasma samples were obtained from healthy volunteers (n=4) and patients with CRF (n=4) or ESRD (n=4). Standards of the compounds were also analyzed in order to quantify the amount of toxins found in the samples. Acquired HPLC data were processed with PC1000 software (Spectrasystem). **(C)** Percentage of pCS and pCS. Statistical analysis was performed via one-way ANOVA followed by the Dunnett's Multiple Comparison Test for each toxin. Results are presented as mean ± SEM. * indicates $p < 0.05$ compared to control.

be sustained for a limited time in culture [34]. In the study from Miyamoto *et al.,* protein expression of OATs was solely demonstrated by an unconvincing Western blot. Previously, it has been reported that OATs can become non-functional upon culturing due to internalization [32]. These findings indicate that, although protein expression seems to be present, multiple assays are required to demonstrate functionality of transporters.

How can the uptake of pCS as observed by Miyamoto *et al.* be explained? Another kidney-specific basolateral transporter demonstrated to be involved in the removal of uremic toxins is the organic anion transporting polypeptide 4C1 (OATP4C1) [35; 36]. Note that the lack of inhibition by digoxin, as demonstrated by Miyamoto *et al.*, is not conclusive for the involvement of this transporter [36]. Using quantitative PCR, we indeed demonstrated the expression of OATP4C1 in human kidney homogenates and HK-2 cells with a 6-fold and

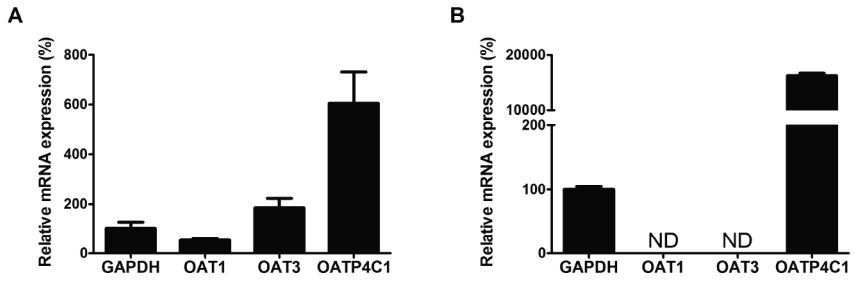

Figure 2 Expression of basolateral transporters.

Total mRNA was isolated from **(A)** human kidney homogenate or **(B)** HK-2 cells. Afterwards, cDNA was synthesized and transporter gene expression was studied using qPCR. Relative expression was calculated using the household gene GAPDH (100%). Bars represent mean ± SEM of one experiment. ND, not detected.

163-fold increased relative expression, respectively (Figure 2; GAPDH 100%), whereas gene expression levels of OAT1 and OAT3 were undetectable in the cell line (Figure 2B). These findings were recently confirmed in a study by Jenkinson *et al,* demonstrating that HK-2 cells indeed express OATP4C1 and lack OAT1 and OAT3 expression, as compared with human renal cortex samples [37]. In addition, they stated that HK-2 cells are a limited model of transporter expression and activity in the proximal tubule [37].
Taken together, the low affinity of pCS as demonstrated together with the absence of OATs in the HK-2 model suggest that the mechanism of pCS excretion in the kidney is more complicated than postulated by Miyamoto *et al.*, and the possible contribution of OATP4C1 warrants further investigation.

Apical transporters involved in pCS and pCG clearance

Two pumps that likely contribute to the urinary excretion of the *p*-cresol metabolites are multidrug resistance protein 4 (MRP4) and breast cancer resistance protein (BCRP). Both pumps are transmembrane proteins belonging to the superfamily of ATP-binding cassette (ABC) transporters. They are expressed in several tissues with a barrier function, including liver, intestine, brain and kidney, and both transporters are known to transport a wide variety of drugs and endogenous compounds against steep concentration gradients [18; 38]. Previously, we reported that several uremic toxins, such as kynurenic acid, hippuric acid and indoxyl sulfate, inhibited substrate-specific transport by MRP4 and BCRP at clinically relevant concentrations [17]. Since pCS and pCG share structural characteristics with the previously studied uremic solutes, we hypothesized that both pumps are also involved in the transport of pCS and pCG into the proximal tubule lumen. Using membrane vesicles isolated from MRP4- or BCRP-overexpressing human embryonic kidney cells it

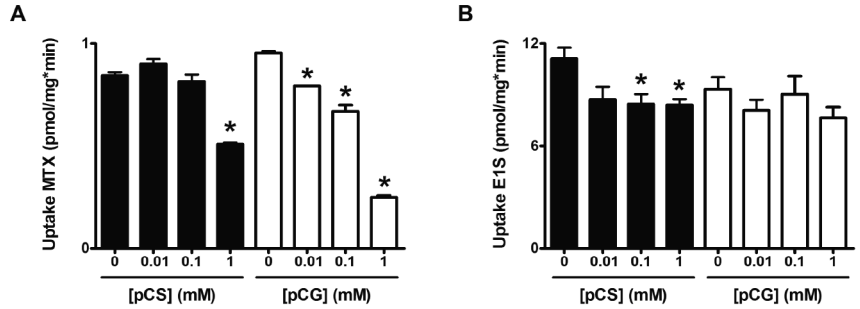

Figure 3 Uremic toxins inhibit MRP4- and BCRP-mediated transport.

A rapid filtration technique was used to study **(A)** MRP4-mediated [^{3}H]-MTX uptake or **(B)** BCRP-mediated [^{3}H]-E1S uptake into membrane vesicles in the presence of various concentrations of *p*-cresol metabolites. Radioactivity was determined using liquid scintillation counting. Statistical analysis was performed via one-way ANOVA followed by the Dunnett's Multiple Comparison Test for each toxin. Results are presented as mean ± SEM of one representative experiment performed in triplicate. * indicates $p < 0.05$ compared to control.

was demonstrated that, at the highest concentration (1 mM), pCS inhibited MRP4-mediated [^{3}H]-MTX uptake with 40% and BCRP-mediated [^{3}H]-E1S uptake with 25% (Figure 3A-B). In contrast, Figure 3A showed that pCG solely reduces [^{3}H]-MTX uptake by MRP4, concentration-dependently, with a 18% reduction in transport at 1 µM and a reduction of 75% at 1 mM. These results suggest that MRP4 and BCRP might contribute to the renal handling of *p*-cresol metabolites.

Induction of phenotypical changes by pCS and pCG

As described above, the toxicity of pCS is widely investigated and the metabolite is linked to the development of cardiovascular disease in CKD patients. In contrast, little is known about the biological activity of pCG. One of the first reports on the toxic effects of pCG demonstrated that the solute itself did not influence oxidative burst activity in multiple leukocyte subtypes [8]. Nonetheless, pCG did potentiate the pro-inflammatory effect of pCS [8]. Furthermore, pCS is often studied in conjunction with indoxyl sulfate, a protein-bound uremic toxin derived from tryptophan, and it was recently reported by Kim *et al.* that this solute induces epithelial-to-mesenchymal transition (EMT) in proximal tubular cells [39]. Therefore, the nephrotoxicity of both *p*-cresol conjugates was investigated, with an emphasis on EMT. Figure 4A shows that pCG concentration-dependently increased the expression of the mesenchymal marker vimentin and a 1.4-fold induction was observed at the highest concentration. Moreover, it is known that transitioning epithelial cells are resistant to apoptosis [40], indeed pCG induced expression

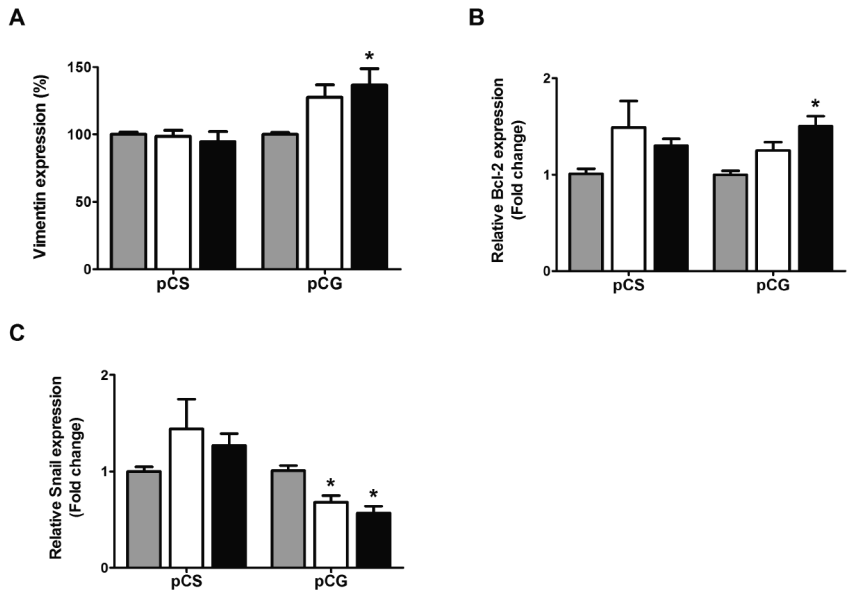

Figure 4 Induction of EMT by pCS and pCG in ciPTEC.
Cells were exposed for 48 h to salt control solution (grey bar), 1 mM (white bars) or 2 mM (black bars) of pCS or pCG. **(A)** Following treatment, cells were harvested and stained with mouse-α-human Vimentin-PE. Quantification of staining was done with a BD FACSCalibur flow cytometer using channel FL-2, and analyzed with FlowJo software, gating on live cells. Statistical analysis was performed via one-way ANOVA followed by the Dunnett's Multiple Comparison Test for each toxin. Results are presented as mean ± SEM of four independent experiments performed in duplicate. * indicates $p < 0.05$ compared with control. **(B-C)** Following treatment, ciPTEC were harvested and total mRNA was isolated. Afterwards, cDNA was synthesized and **(B)** Bcl-2 and **(C)** Snail expression was studied using qPCR. GAPDH was used as housekeeping gene and relative expression levels were calculated using the $2^{-\Delta\Delta CT}$ method. Statistical analysis was performed via one-way ANOVA followed by the Bonferonni's Multiple Comparison Test for each toxin. Values are shown as mean ± SEM of three independent experiments performed in triplicate. * indicates $p < 0.05$ compared to control.

of the anti-apoptotic gene Bcl-2, as demonstrated in Figure 4B. The process of EMT is regulated by several transcription factors, including Slug, Twist and Snail. As depicted in Figure 4C, Snail gene expression was significantly down-regulated following pCG exposure. In contrast to our findings, up-regulation of vimentin is normally secondary to increased mRNA levels of Snail. However, Berzal *et al.*, demonstrated in HK-2 cells, that during cyclosporine A-induced EMT, Snail gene expression decreased while protein expression increased due to a reduced rate of protein degradation [41]. Thus, our results indicate that pCG can induce EMT in ciPTEC, thereby possibly augmenting CKD development.

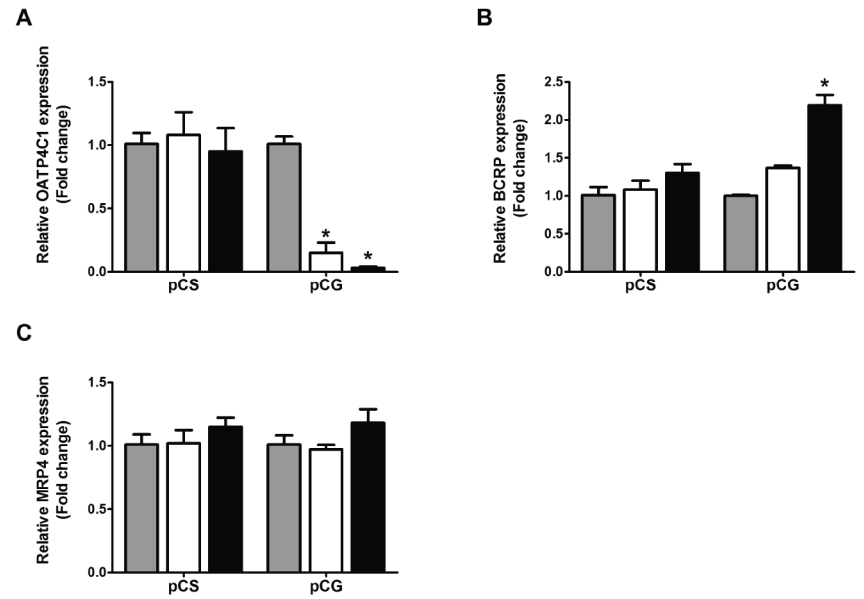

Figure 5 Impact of pCS and pCG on expression of apical transporters.
Cells were exposed for 48 h to salt control solution (grey bar), 1 mM (white bars) or 2 mM (black bars) of pCS or pCG. Following treatment, ciPTEC were harvested and total mRNA was isolated. Afterwards, cDNA was synthesized and **(A)** OATP4C1, **(B)** BCRP and **(C)** MRP4 expression was studied using qPCR. GAPDH was used as housekeeping gene and relative expression levels were calculated using the $2^{-\Delta\Delta CT}$ method. Statistical analysis was performed via one-way ANOVA followed by the Bonferonni's Multiple Comparison Test for each toxin. Values are shown as mean ± SEM of minimally two independent experiments performed in triplicate. * indicates $p < 0.05$ compared to control.

Since pCG exposure resulted in a loss of proximal tubular characteristics, gene expression of key transporters was studied in more detail. Following treatment with pCG, OATP4C1 expression was significantly reduced, whereas expression of BCRP increased more than 2-fold (Figure 5A-B). In addition, no changes in MRP4 mRNA levels were observed, as demonstrated in Figure 5C. Together with the observed induction of EMT, these results suggest that pCG exposure causes cell stress.
Next, it was investigated whether pCS and pCG induced cell injury by determining the mRNA levels of two early markers of tubular damage, namely kidney injury molecule-1 (KIM-1) and vanin-1 [42; 43]. Figure 6A shows that exposure of ciPTEc to pCG caused a significant, concentration-dependent, reduction in KIM-1 expression; while pCS did not change expression levels. Moreover, vanin-1 mRNA levels remained unchanged following treatment with either pCS or pCG (Figure 6B). This suggests, that both solutes did not induce tubular damage.

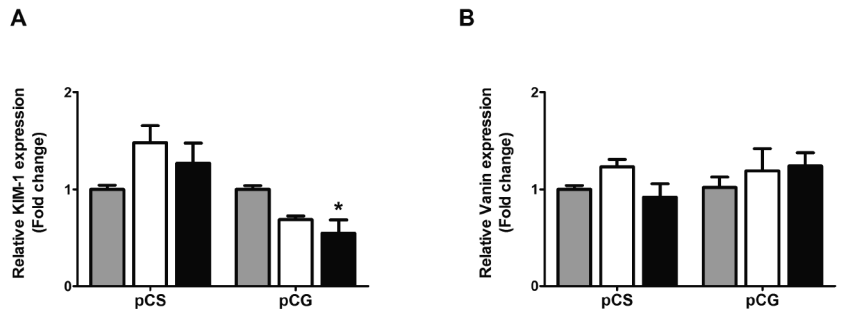

Figure 6 pCS and pCG do not induce proximal tubular damage.

Cells were exposed for 48 h to salt control solution (grey bar), 1 mM (white bars) or 2 mM (black bars) of pCS or pCG. Following treatment, ciPTEC were harvested and total mRNA was isolated. Afterwards, cDNA was synthesized and **(A)** KIM-1 and **(B)** vanin-1 expression was studied using qPCR. GAPDH was used as housekeeping gene and relative expression levels were calculated using the $2^{-\Delta\Delta CT}$ method. Statistical analysis was performed via one-way ANOVA followed by the Bonferonni's Multiple Comparison Test for each toxin. Values are shown as mean ± SEM of minimally two independent experiments performed in triplicate. * indicates $p < 0.05$ compared to control.

In contrast to the marked impact of pCG on ciPTEC phenotype, *e.g.* increased vimentin expression and altered expression of in- and efflux transporters, no changes were observed following exposure to pCS (Figure 4 and 5). Which is in stark disparity with previous results obtained in leukocytes [8]. This suggests, that the toxicity of both *p*-cresol metabolites is cell type-specific. Moreover, a drawback of the present study is that the pCS and pCG concentrations used do not reflect the clinical situation. Still, we are the first to demonstrate, to the best of our knowledge, that pCG might promote CKD progression by inducing phenotypical changes in human proximal tubule cells.

In conclusion, in this study we report the retention of pCS and pCG in CKD patients and we provide the first evidence for the involvement of MRP4 and BCRP in the physiological renal clearance of both solutes. Moreover, our results demonstrated that pCS does not exert nephrotoxic effects, whereas pCG induced cell stress and EMT in ciTPEC. These findings offer novel insights on the divers contribution of both *p*-cresol conjugates in CKD pathophysiology.

ACKNOWLEDGEMENTS

This work was supported by the Dutch Kidney Foundation (grant number IK08.03; www.nierstichting.nl). M.J.G. Wilmer was supported by a grant from the Dutch government to the Netherlands Institute for Regenerative Medicine (NIRM, grant No. FES0908; www.nirm.nl) and J.G. Hoenderop was supported by an EURYI award from the European Science Foundation.

5

Hyperuricemia influences tryptophan metabolism via inhibition of Multidrug Resistance Protein 4 (MRP4) and Breast Cancer Resistance Protein (BCRP)

Anita C.A. Dankers*, Henricus A.M. Mutsaers*, Henry B.P.M. Dijkman, Lambertus P. van den Heuvel, Joost G. Hoenderop, Fred C.G.J. Sweep, Frans G.M. Russel and Rosalinde Masereeuw

Biochimica et Biophysica Acta (BBA) - Molecular Basis of Disease, Volume: 1832, Issue: 10, Page: 1715-1722, 2013

ABSTRACT

Hyperuricemia is related to a variety of pathologies, including chronic kidney disease (CKD). However, the pathophysiological mechanisms underlying disease development are not yet fully elucidated. Here, we studied the effect of hyperuricemia on tryptophan metabolism and the potential role herein of two important uric acid efflux transporters, multidrug resistance protein 4 (MRP4) and breast cancer resistance protein (BCRP). Hyperuricemia was induced in mice by treatment with the uricase inhibitor oxonic acid, confirmed by the presence of urate crystals in the urine of treated animals. A transport assay, using membrane vesicles of cells overexpressing the transporters, revealed that uric acid inhibited substrate-specific transport by BCRP at clinically relevant concentrations (calculated IC_{50} value: 365 ± 13 μM), as was previously reported for MRP4. Moreover, we identified kynurenic acid as a novel substrate for MRP4 and BCRP. This finding was corroborated by increased plasma levels of kynurenic acid observed in $Mrp4^{-/-}$ (107 ± 19 nM; p = 0.145) and $Bcrp^{-/-}$ mice (133 ± 10 nM; p = 0.0007) compared to wild type animals (71 ± 11 nM). Hyperuricemia was associated with >1.5 fold increase in plasma kynurenine levels in all strains. Moreover, hyperuricemia led to elevated plasma kynurenic acid levels (128 ± 13 nM, p = 0.005) in wild type mice but did not further increase kynurenic acid levels in knockout mice. Based on our results, we postulate that elevated uric acid levels hamper MRP4 and BCRP functioning, thereby promoting the retention of other potentially toxic substrates, including kynurenic acid, which could contribute to the development of CKD.

INTRODUCTION

Uric acid is a weak organic acid and the end-product of purine nucleotides degradation in humans. One of the enzymes involved in this process is xanthine oxidoreductase, which enables the oxidation of hypoxanthine to xanthine and can further catalyze the oxidation of xanthine to uric acid. During this reaction, reactive oxygen species are generated as by-product [156,157]. Therefore, uric acid is recognized as a marker for oxidative stress. However, the molecule itself has antioxidant properties and can act as a free radical scavenger and chelator of transitional metal ions which are converted into poorly reactive forms [158]. Hyperuricemia, *i.e.* elevated plasma uric acid levels (≥ 360 μM) [159], is related to a variety of pathologies, including gout, cardiovascular disease and chronic kidney disease (CKD). Gout is the most common form of inflammatory arthritis caused by sodium uric acid crystal precipitation, which is followed by phagocytosis of the crystals by neutrophils and macrophages and activation of acute inflammation and tissue injury [160]. Epidemiological studies show that prevalence and incidence are still increasing [161,162]. Formation of uric acid crystals is also the cause of nephrolithiasis, *i.e.* kidney stones, which is significantly more common among patients diagnosed with metabolic syndrome, obesity and type 2 diabetes [163]. Hyperuricemia also correlates with the development and progression of cardiovascular diseases [164-166], potentially via interfering with nitric oxide function. In animal models, it has been shown that mild hyperuricemia contributes to the development of hypertension as a result of endothelial dysfunction and reduction of nitric oxide levels [165,167,168]. Recently, hyperuricemia has received attention as a possible risk factor for CKD [159,169], which affects approximately 10% of the adult population in developed countries [5]. Hyperuricemia has been associated with a hazard ratio of 2.1 and 1.3 for men and women for developing CKD [159], respectively. Several mechanisms were proposed via which uric acid could contribute to the development of CKD, including uric acid-induced glomerular hypertrophy and endothelial dysfunction [159,170]. However, the pathophysiological mechanism has as of yet not been fully elucidated.

In healthy individuals, two-thirds of uric acid is excreted by the kidney and one-third by the intestine due to breakdown of urate by gut bacteria. Purine ingestion, endogenous synthesis of purines from nonpurine precursors and reutilization of preformed purine compounds are the sources of uric acid production, a process that, under steady-state conditions, is in balance with the uric acid disposal [171,172]. Hyperuricemia can develop due to overproduction or a diminished excretion of uric acid. Maintaining uric acid homeostasis is highly dependent on kidney function and regulated by a number of transporters, including the urate transporter 1 (URAT1; *SLC22A12*) - responsible for up to 99% of uric acid reabsorption after glomerular filtration - the facilitated glucose transporter (solute carrier family 2 member 9 (*SLC2A9*) [173], several organic anion transporters including OAT1 (*SLC22A6*) and OAT3 (*SLC22A8*) [160], and the ATP-dependent urate efflux

transporters multidrug resistance protein 4 (MRP4; *ABCC4*) [87] and breast cancer resistance protein (BCRP; *ABCG2*) [88,130,174].

As uric acid is one of the important factors in a variety of pathologies, tight regulation of this metabolite is of key importance. The vital role of transporters in uric acid homeostasis can clearly be observed in patients suffering from hyperuricemia due to single nucleotide polymorphisms (SNPs) that render the transporters inactive, such as the common SNP *C421A* encoding the Q141K mutation of BCRP [88,130,175] and several genetic variants for *SLC2A9* [173]. Next to genetic factors, high plasma levels of uric acid might also result in a reduced transporter activity [87]. Since these transporters are also involved in the excretion of a wide variety of other compounds, changes in transport efficacy could result in metabolic disturbances. This hypothesis is corroborated by two recent studies showing that high uric acid levels in patients with acute gout were associated with altered tryptophan concentrations in plasma and urine [176,177]. Therefore, the aim of our study was to investigate the effect of hyperuricemia on tryptophan metabolism and the potential role herein of two important uric acid efflux transporters, MRP4 and BCRP. Both transporters are expressed in the apical membrane of renal proximal tubule cells, amongst other tissues, and are involved in the urinary excretion of a multitude of endogenous compounds and drugs [84]. Using Mrp4$^{-/-}$ and Bcrp$^{-/-}$ mice, we show that hyperuricemia is associated with the accumulation of tryptophan and associated metabolites, most likely due to transporter dysfunction.

MATERIAL AND METHODS

Transduction of Human Embryonic Kidney cells and preparation of membrane vesicles

Overexpression of MRP4 and BCRP in human embryonic kidney cells (HEK293; American Type Culture Collection, Manassas, VA) was established using baculoviruses, which were produced using the Bac-to-Bac and the Gateway system (Invitrogen, The Netherlands), as described previously [132,150]. As a control, the enhanced yellow fluorescent protein (eYFP) was introduced as mock protein into the baculovirus expression system. Crude membranes of HEK293-MRP4, -BCRP and -mock cells were isolated, resuspended in TS buffer (10 mM Tris-HEPES and 250 mM sucrose, pH 7.4) and membrane vesicles were prepared according to a previously described method [132] by means of ultracentrifugation. Crude membrane vesicles were dispensed in aliquots, snap frozen in liquid nitrogen, and stored at -80 °C until further use.

Membrane vesicle inhibition and uptake assays

The effects of uric acid and oxonic acid on MRP4 and/or BCRP activity were assessed by a well-established assay in our laboratory [89,132,150,155]. In brief, a reaction mix consisting of TS buffer supplemented with 4 mM ATP/AMP, 10 mM $MgCl_2$ and 250 nM [^{3}H]-methotrexate (MTX; for MRP4) or [^{3}H]-estrone sulphate (E_1S; for BCRP) at pH 7.4 was added to 7.5 µg of membrane vesicles (based on total protein content). After incubation at 37 °C to enable ATP-dependent uptake, the reaction was stopped by placing the samples on ice and by addition of ice-cold TS buffer. Reaction mix was removed and the vesicles were washed by means of a rapid filtration technique using filter plates (Millipore, Etten-Leur, The Netherlands). Scintillation fluid was added to the filters and the amount of radioactivity was determined using a scintillation counter (Tri-Carb® 2900TR; Perkin Elmer, Waltham, MA, USA). Reference samples were measured to calculate the amount of transported MTX and E_1S. ATP-dependent transport was calculated by subtracting values measured in the presence of AMP from those measured in the presence of ATP. Net transporter-mediated substrate uptake was calculated by subtracting ATP-dependent uptake in HEK293-mock vesicles from that of HEK293-transporter vesicles.

Uptake of kynurenic acid into MRP4-overexpressing membrane vesicles was established using the same assay. Vesicles were incubated with 0.1 mM kynurenic acid in the presence of AMP or ATP. After the described washing step, kynurenic acid was determined by LC-MS/MS.

Oxonic acid-mediated induction of hyperuricemia in mice

All experiments were approved by the local Animal Welfare Committee of the Radboud University Nijmegen Medical Centre (RU-DEC 2012-018), in accordance with the directive for animal experiments (2010/63/EU) of the European Parliament. The effects of hyperuricemia *in vivo* were examined in wild type (WT) Friend leukemia virus B (FVB) mice as well as Mrp4$^{-/-}$ and Bcrp$^{-/-}$ mice (both FVB background). The WT FVB and Bcrp$^{-/-}$ mice were kindly provided by Dr. A. Schinkel (Netherlands Cancer Institute, Amsterdam, The Netherlands) and the Mrp4$^{-/-}$ mice by Dr. J. Schuetz (St. Jude Children's Research Hospital, Memphis, TN, USA) and Dr. P. Borst (Netherlands Cancer Institute, Amsterdam, The Netherlands), all animals were bred and housed at the Central Animal Laboratory of the RUNMC. The animals (N=9) received the uricase inhibitor oxonic acid (2% w/v; pH 7) via their drinking water, *ad libitum*, to induce hyperuricemia [178]. The animals were individually caged and housed under controlled conditions. Parallel control groups were also individually caged and received normal tap water at equal pH. After 14 days, mice were placed individually in metabolic cages (Techniplast, Germany GmbH) to collect 24 h urine samples, with access to water (with or without oxonic acid 2% w/v) and pulverized standard chow *ad libitum*. Next, blood was collected from the orbital sinus in lithium-heparin tubes via a terminal procedure performed under isoflurane anesthesia and centrifuged for 15 min at 3,000 x g to obtain plasma. Animals were sacrificed by cervical dislocation. Isolated kidneys, plasma and urine were immediately snap frozen in liquid nitrogen and stored at -80 °C until further analysis. Biochemical parameters were determined by routine clinical chemistry.

Energy-dispersive X-ray (EDX) microanalysis

Transmission electron microscopy and EDX were performed for identification of the ultrastructure and composition of the insoluble crystals found in the urine samples of oxonic acid-treated mice. Urine samples were spotted onto copper grids (100 mesh) coated with a support film, air dried, negative stained with uranyl acetate and examined using a Jeol 1200 EX II. For EDX measurements, the grids were examined using a Jeol 1200/ STEM in combination with a Thermo Noran microanalysis six system. Accelerated voltage of 60 KeV was used for X-ray microanalysis. X-ray spectra for element distribution were acquired. In each sample, 3-5 measuring points were selected.

RNA isolation and quantitative PCR

Effects of hyperuricemia on kidney injury were evaluated by determining mRNA expression levels of early renal injury markers kidney injury molecule-1 (Kim-1) and neutrophil gelatinase-associated lipocalin (Ngal) in kidneys of treated and control mice. Frozen kidneys were homogenized using a Mikro-dismembrator U (Sartorius B. Braun Biotech Int., Melsungen, Germany). Subsequently, total RNA was isolated using a NucleoSpin® RNA II kit (Macherey-Nagel, Düren, Germany) according to manufacturer's instructions. Immediately, a reverse transcriptase reaction was performed with 250 ng RNA using random primers (Invitrogen, Breda, The Netherlands) and an Omniscript® RT kit (Qiagen, Hilden, Germany), following manufacturer's recommendations. Synthesized cDNA was used for quantitative PCR, performed in a StepOnePlus™ Real-Time PCR system by means of the TaqMan® protocol (Applied Biosystems, Warrington, UK). *Kim-1* and *Ngal* mRNA concentrations were normalized to the mRNA concentration of the housekeeping gene *glyceraldehyde-3-phosphate dehydrogenase (Gapdh).* The primer-probe sets were obtained from Applied Biosystems (*Gapdh*; Mm999999915_g1, *Kim-1*; havcr1 Mm00506686_m1, *Ngal*; lcn2 Mm01324470_m1).

Tryptophan, kynurenine and kynurenic acid measurements by LC-MS/MS

After the vesicle uptake experiments, kynurenic acid was extracted from the filters in 3.3% perchloric acid. Plasma samples were diluted in H_2O (1:1) prior to LC-MS/MS measurements and deproteinized with perchloric acid (final concentration 3.3%). Samples were centrifuged at 12,000 x g for 3 min. Clear supernatant was injected into the LC-MS/MS system that consisted of an Accela HPLC system (Thermo scientific, Breda, the Netherlands) equipped with a C18 HPLC column (VisionHT C18 B 10062 mm, 1.5 mm; Grace). Tryptophan, kynurenine and kynurenic acid were measured in the same run. Deuterated kynurenic acid was added as an internal standard for quantification. Measurements were performed as published earlier [89].

Kinetic analysis and statistics

Statistics were performed using GraphPad Prism 5.02 via one-way analysis of variance (ANOVA) followed by the Dunnett's Multiple Comparison Test to study differences between all groups as well as an unpaired Student's *t*-test to study the impact of oxonic acid treatment within each strain. Differences between groups were considered to be statistically significant when $p < 0.05$. GraphPad Prism was also used to perform non-linear regression analysis.

RESULTS

Oxonic acid induces hyperuricemia

To study the impact of hyperuricemia on murine physiology, wild type (WT), $Mrp4^{-/-}$ and $Bcrp^{-/-}$ mice were treated with the uricase inhibitor oxonic acid as described before [178]. Two weeks of oxonic acid treatment did neither affect overall weight of the mice, nor plasma levels of urea, sodium and calcium (Table 1). Interestingly, water intake was strongly increased after oxonic acid treatment in all strains investigated, with an increase up to four times that of controls in Bcrp-deficient mice. This was accompanied by a two-fold increase in urine flow in treated WT animals; whereas no significant changes were observed in knockout animals. Yet baseline urine flow of $Bcrp^{-/-}$ mice tended to be increased as compared to WT animals.

Following oxonic acid treatment, the urine collected from all animals was turbid due to presence of crystals (Figure 1A-D). Energy-dispersive X-ray microanalysis (EDX) revealed that the major constituents of the urinary crystals were sodium, potassium, phosphorus and calcium; the copper signals arose from the sample grid used in the analysis (Figure 1E). Two types of crystals could be distinguished: first, crystals that showed an archetypical peak pattern corresponding to uric acid crystals, which consisted primarily of sodium, calcium and phosphorus (Figure 1F). Second, crystals that mainly contained calcium and potassium (Figure 1G), which was likely due to the treatment with oxonic acid potassium salt. These data are in accordance with the development of hyperuricemia in oxonic acid-treated mice.

Uric acid inhibits BCRP activity

Plasma urate levels are controlled by an interplay of transporters expressed in the kidney proximal tubules. MRP4 and BCRP have been associated with active urinary urate efflux, and MRP4 was also sensitive to inhibition by urate [87]. We determined the inhibitory properties of uric acid on BCRP activity using membrane vesicles prepared from BCRP-overexpressing HEK293 cells. Uric acid dose-dependently inhibited BCRP-mediated uptake of the substrate E_1S (Figure 2A) with a calculated half maximal inhibitory concentration (IC_{50}) value of 365 ± 13 µM. Complete inhibition of BCRP activity was found at the highest uric acid concentration used (*i.e.* 1 mM). These findings indicate that uric acid can reduce transport activity of two important efflux pumps at concentrations demonstrated in patients with hyperuricemia (≥ 360 µM).

Table 1 General characteristics and serum and urine biochemistry of experimental groups

	WT	WT + oxonic acid	Mrp4$^{-/-}$	Mrp4$^{-/-}$ + oxonic acid	Bcrp$^{-/-}$	Brcp$^{-/-}$ + oxonic acid
General characteristics						
Weight d.0 (g)	22.4 ± 0.8	25.3 ± 1.1	23.4 ± 1.4	25.0 ± 1.5	23.8 ± 1.1	25.7 ± 1.0
Weight d.14 (g)	24.6 ± 1.0	24.9 ± 1.2	23.5 ± 0.9	24.6 ± 0.9	24.5 ± 0.7	24.6 ± 0.6
Water intake (ml/24h)	1.6 ± 0.4	5.5 ± 0.8***	2.9 ± 0.6	5.5 ± 1.0*	2.1 ± 0.7	8.5 ± 0.5***
Urine flow (ml/24h)	0.3 ± 0.1	0.6 ± 0.1*	0.3 ± 0.1	0.7 ± 0.3	0.7 ± 0.2	0.7 ± 0.1
Plasma						
Urea (mM)	12.5 ± 0.8	11.8 ± 0.7	11.4 ± 0.4	10.5 ± 0.5	12.5 ± 0.5	11.7 ± 0.6
Sodium (mM)	149.7 ± 1.1	151.1 ± 1.4	147.6 ± 1.8	151.7 ± 0.8	149.4 ± 0.9	148.0 ± 1.0
Calcium (mM)	2.3 ± 0.02	2.4 ± 0.03	2.2 ± 0.02	2.3 ± 0.02	2.3 ± 0.01	2.3 ± 0.02
Urine						
Creatinine (µmol/24h)	1.4 ± 0.6	1.6 ± 0.2	1.1 ± 0.2	1.5 ± 0.3	2.4 ± 0.8	1.3 ± 0.3
Sodium (µmol/24h)	139.7 ± 63.1	126.3 ± 14.1	93.4 ± 17.4	150.8 ± 42.7	196.0 ± 49.2	138.8 ± 21.4

Individually caged mice were treated with oxonic acid via their drinking water for 14 days. Mice were weighed before and after treatment period. Water intake, urine flow and urine content were determined after a 24h-period in metabolic cages at day 14. Plasma was collected at day 14. Data represent means ± SEM of 9 mice per group. *indicates $p < 0.05$ and *** indicates $p < 0.001$ compared to untreated mice from the same strain using a Student's *t*-test. Differences between the strains were not significant (one-way ANOVA).

MRP4-mediated transport of kynurenic acid

There is some evidence linking hyperuricemia to changes in tryptophan levels [176]. In addition, we recently reported that kynurenic acid, a tryptophan derivative, can interact with MRP4 and BCRP [89], and we identified kynurenic acid as a BCRP substrate (Dankers *et al.*, submitted for publication). Here, we investigated whether kynurenic acid is also a substrate for MRP4. Figure 2B shows that the ATP-dependent uptake of kynurenic acid in MRP4-overexpressing vesicles is 7-fold higher as compared to controls with an average rate of 21.6 pmol/mg*min^{-1}. Furthermore, Figure 2B demonstrates that non-specific, AMP-dependent, uptake is very low. These results indicate that kynurenic acid is indeed transported by MRP4.

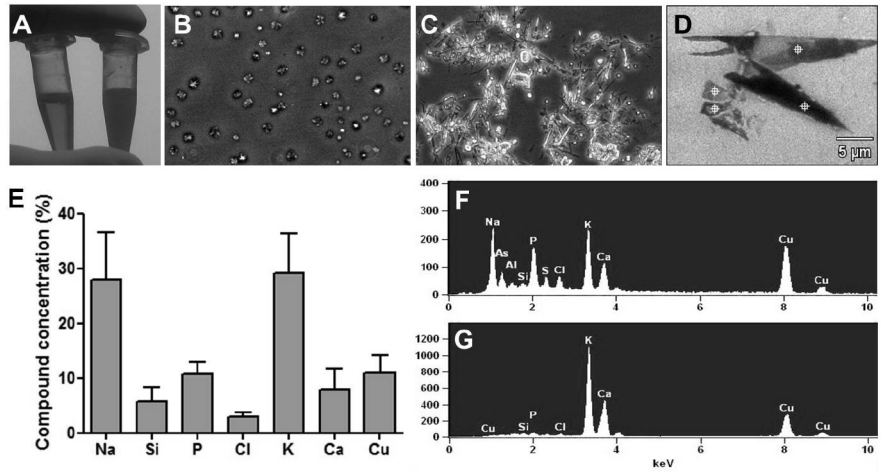

Figure 1 Analysis of urine samples of WT, Mrp4$^{-/-}$ and Bcrp$^{-/-}$ mice after 14 days of treatment with oxonic acid via their drinking water.

A representative sample of clear urine of an untreated animal **(A, left and B)** and turbid, crystal-filled urine of an oxonic acid-treated animal **(A, right and C)** is shown by a photograph and micrographs (magnification 10x). The contents of the insoluble crystals were determined by energy dispersive X-ray microanalysis (EDX). In each sample, 3-5 measuring points were selected **(D)**. The components of all urinary crystals of three oxonic acid-treated WT mice were depicted as mean + SEM of twelve measurements **(E)**. Mainly two types of crystals were found. A typical EDX spectrum of urate crystals, containing sodium, calcium and phosphorus, is depicted in panel **(F)**, while panel **(G)** represents an EDX spectrum of oxonic acid crystals consisting of calcium and potassium.

Retention of tryptophan and its metabolites during hyperuricemia

As uric acid can inhibit MRP4 and BCRP-mediated transport and kynurenic acid is a substrate for both pumps, we determined the effects of hyperuricemia on tryptophan metabolism and the role of the efflux pumps herein. Plasma tryptophan levels were similar in all untreated groups, but oxonic acid treatment led to increased tryptophan levels in Mrp4$^{-/-}$ mice (125 µM) as compared to untreated animals (93 µM; Figure 3). Baseline plasma levels of the intermediate tryptophan metabolite, kynurenine, were similar in knockout animals as compared to WT animals. And oxonic acid treatment led to a >1.5 fold increase in kynurenine plasma levels in all three strains, without differences between strains. In contrast, baseline plasma kynurenic acid levels of knockout mice were elevated compared to WT mice, which was significant for Bcrp$^{-/-}$ mice. Hyperuricemia did not further increase plasma kynurenic acid levels in knockout mice, but led to significantly elevated levels in WT animals to the levels of untreated knockout mice. Furthermore, IDO activity, represented by the ratio between tryptophan and kynurenine, was similar in untreated

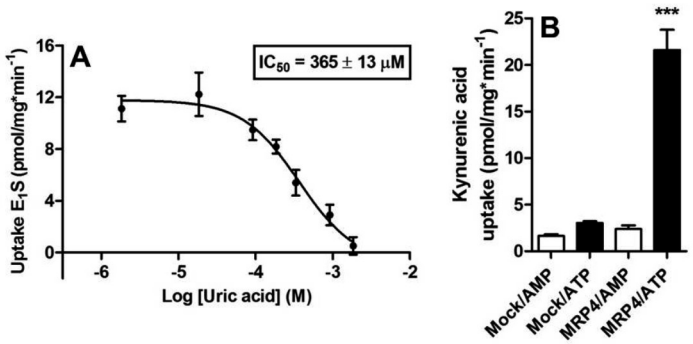

Figure 2 Concentration-dependent inhibition of net BCRP-mediated [^{3}H]-estrone sulphate (E1S) uptake by uric acid and MRP4-mediated kynurenic acid uptake into membrane vesicles.

(A) Membrane vesicles were incubated with 250 nM E_1S and increasing concentrations of uric acid in the presence of AMP or ATP, for 60 sec at 37 ºC. Net BCRP-mediated E_1S uptake was calculated by subtraction of corresponding mock values. Curve fitting was performed by non-linear regression analysis using GraphPad Prism software (version 5.02, GraphPad Software Inc., San Diego, CA, USA). Graph represents means ± SEM of three independent experiments. **(B)** Kynurenic acid uptake was assessed by LC-MS/MS analysis after incubating membrane vesicles with 0.1 mM kynurenic acid in the presence of AMP or ATP, for five min at 37 ºC. Bars represent means + SEM of three independent experiments. *** indicates $p < 0.001$ compared to other bars by one-way ANOVA followed by Dunnett's post hoc test.

strains, but significantly increased after oxonic acid treatment in Bcrp$^{-/-}$ mice (0.5 vs 0.7). Thus, hyperuricemia clearly affects tryptophan metabolism.

Oxonic acid does not influence MRP4 and BCRP activity

To exclude the possibility that oxonic acid itself inhibited the efflux pumps resulting in metabolite retention, we investigated the effect of oxonic acid on MRP4 and BCRP transport activity. Membrane vesicle uptake studies revealed that oxonic acid itself did not affect MRP4-mediated MTX uptake and BCRP-mediated E_1S uptake with more than 15% in a concentration range of 1 µM to 1000 µM (Figure 4).

Hyperuricemia induces expression of the early kidney injury marker Ngal

Finally, we studied whether hyperuricemia and changes in tryptophan metabolism coincided with an amelioration of kidney function. Renal damage was evaluated by assessing mRNA expression of the early renal injury markers Kim-1 and Ngal in kidneys of treated and control mice. As shown in Figure 5A, Kim-1 was not differentially expressed in oxonic acid-treated mice compared to untreated mice. In contrast, renal Ngal expression

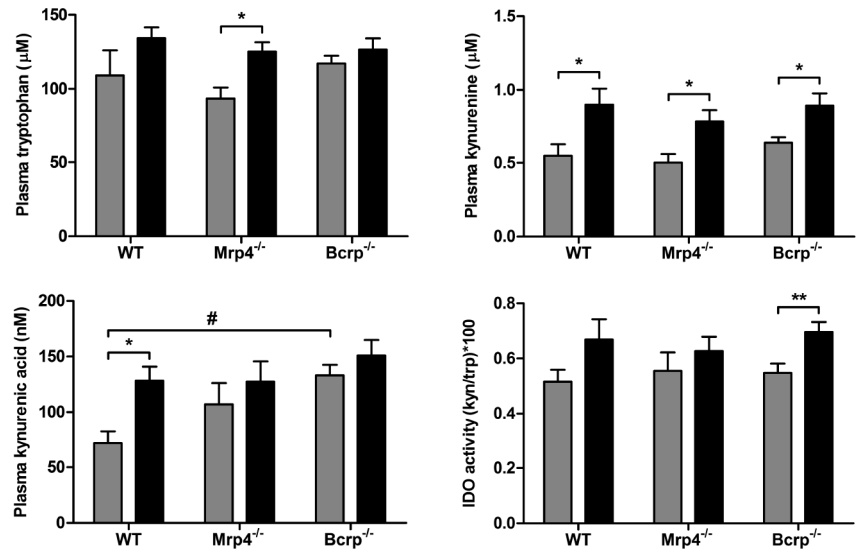

Figure 3 Plasma tryptophan metabolism in WT, Mrp4$^{-/-}$ en Bcrp$^{-/-}$ mice.

Plasma tryptophan, kynurenine and kynurenic acid levels and IDO activity of untreated (grey) and oxonic acid-treated (black) WT, Mrp4$^{-/-}$ en Bcrp$^{-/-}$ mice after 14 days of treatment via drinking water, determined by LC-MS/MS analysis. IDO activity is expressed as the ratio between kynurenine and tryptophan * 100. Bars represent means + SEM of 9 mice per group. Statistical analysis was performed using both one-way ANOVA followed by the Dunnett's Multiple Comparison Test and an unpaired Student's *t*-test. * indicates $p < 0.05$ and ** indicates $p < 0.01$ by Student's *t*-test and # indicates $p < 0.001$ by one-way ANOVA.

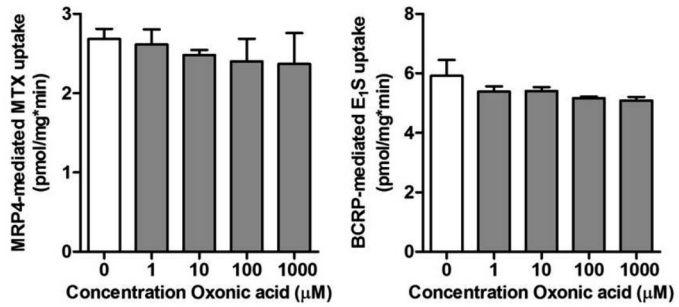

Figure 4 Oxonic acid does not interfere with MRP4-mediated MTX uptake and BCRP-mediated E1S uptake.

Membrane vesicles were incubated with 250 nM [^{3}H]-MTX or [^{3}H]-E_1S and indicated concentrations of oxonic acid for 5 min at 37 °C in the presence of AMP or ATP. AMP values were subtracted from ATP values. Net transporter-mediated uptake was expressed as means + SEM of triplicate measurements in a representative experiment. Results were analyzed by one-way ANOVA followed by Dunnett's post hoc test.

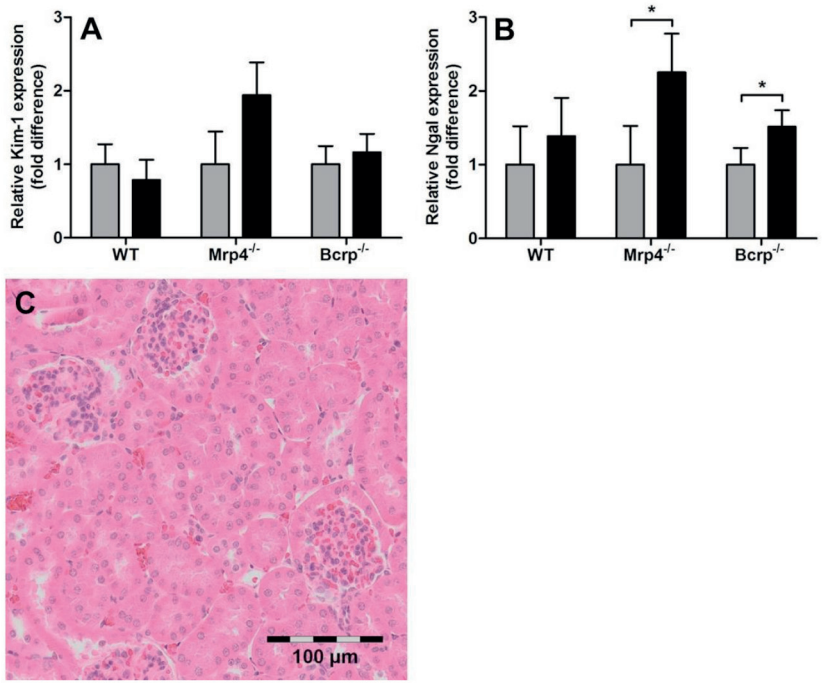

Figure 5 Expression of kidney injury markers and histology after oxonic acid treatment.

Relative mRNA expression levels of kidney injury markers **(A)** Kim-1 and **(B)** Ngal in kidney tissue of untreated (grey) and oxonic acid-treated (black) mice obtained by qPCR. Animals were exposed to oxonic acid via their drinking water for 14 days. Cycle threshold (Ct) values were normalized for the endogenous reference gene *Gapdh* and expressed as mean fold difference from untreated animals + SEM (N=9). * indicates $p < 0.05$ by Student's *t*-test. Both genes were not differentially expressed in untreated animals of the different strains. **(C)** representative micrograph of a oxonic acid-treated WT mice and shows that no kidney damage was observed in oxonic acid-treated mice (HE staining), which was comparable in treated knockout mice.

(Figure 5B) was increased after oxonic acid-induced hyperuricemia. These increases were significant for both knockout strains, and in Mrp4$^{-/-}$ mice expression levels rose up to 2.3 times that of untreated mice. With regard to kidney function, no significant effect was observed on creatinine and sodium excretion (Table 1), suggesting the absence of overt kidney damage which was confirmed by histology. Light microscopic evaluation of HE-stained kidney slices (Figure 5C) revealed intact brush borders and absence of casts or destroyed tubules in exposed animals. Taken together, these results indicate that two weeks of oxonic acid-induced hyperuricemia reveals, at most, early signs of kidney damage.

DISCUSSION

This study reports for the first time that hyperuricemia is associated with disturbances in tryptophan metabolism, most likely due to uric acid-induced dysfunction of the renal efflux pumps MRP4 and BCRP. High levels of uric acid are associated with an increased risk for the development of various diseases and the common mode of action is the formation of crystals (*e.g.* gout and nephrolithiasis) or by negatively influencing the endothelium (*e.g.* hypertension). Here, we hypothesized that hyperuricemia could also contribute to disease development in an indirect manner by promoting the retention of other potentially toxic metabolites. Our results revealed that oxonic acid-induced hyperuricemia resulted in elevated plasma levels of tryptophan, kynurenine and kynurenic acid *in vivo*. The findings are in agreement with two recent studies by Liu *et al.* [176,177], who reported that plasma levels of tryptophan were increased in patients with acute gout while their urinary concentrations were decreased. Hence, there appears to be a link between hyperuricemia and disturbances in tryptophan metabolism.

The efflux transporters MRP4 and BCRP are important in regulating uric acid levels, but also essential for the clearance of many exogenous and endogenous waste products. Recently, we demonstrated that kynurenic acid could interact with MRP4 and BCRP activity in the membrane vesicle transport assay, suggesting that the metabolite is a possible substrate for both transporters [89]. Using the same assay, we have shown that kynurenic acid is indeed transported by BCRP (Dankers *et al.*, submitted for publication) and here we report that kynurenic acid is also a substrate for MRP4. These findings are in agreement with the observed increase in plasma kynurenic acid levels in Mrp4$^{-/-}$ and Bcrp$^{-/-}$ mice. Therefore, MRP4 and BCRP could be potential novel therapeutic targets for the regulation of kynurenic acid levels in a variety of diseases.

Kynurenic acid is a widely studied antagonist of the *N*-methyl-D-aspartate-receptor and the α7-nicotinic acetylcholine receptors, and elevated levels of kynurenic acid are related to several neurological disorders [179]. Another target of kynurenic acid is the orphan G-protein-coupled receptor GPR35, of which kynurenic acid is one of the most potent endogenous agonists currently known. The receptor is highly expressed in the intestine and in several immune cells, including monocytes and T cells. Kynurenic acid also alters the release of multiple growth factors such as nerve growth factor and fibroblast growth factor-1 [55]. Thus, perturbations in kynurenic acid levels can result in marked effects on receptor activation and changes in growth factors. With regard to pathophysiological effects, classic experiments have demonstrated that kynurenic acid inhibited pro-insulin synthesis in isolated rat pancreatic islets and increased the release of insulin in rats, suggesting a role in diabetes [180,181]. Furthermore, in CKD patients, kynurenic acid accumulates [89] and increased levels correlate positively to multiple markers of endothelial dysfunction, namely von Willebrand factor, thrombomodulin and soluble adhesion molecules (sICAM-1, sVCAM-1) [182,183]. In addition, kynurenic acid is suggested to be an

important early mediator of leukocyte recruitment [184]. Moreover, kynurenic acid reduces glucuronidation activity of UDP-glucuronosyltransferases, as shown in proximal tubule cells, thereby affecting the metabolic capacity of the kidney [100]. Hence, elevated levels of kynurenic acid induced by hyperuricemia, as observed in our study, might play a pivotal role in the pathophysiological effects currently attributed to uric acid.

Our results further demonstrated that kynurenine levels were similar in untreated WT and knockout animals, suggesting that the levels of this metabolite are not influenced by MRP4 and BCRP activity. Following induction of hyperuricemia, kynurenine levels were markedly increased in all groups. The observed increase might be due to a reduced activity of a uric acid transporter other than MRP4 and BCRP, elevated tryptophan levels, as seen in Mrp4$^{-/-}$ mice, and/or increased activity of indoleamine 2,3-dioxygenase (IDO), as observed in Bcrp$^{-/-}$ mice. Interestingly, IDO is involved in immune regulation and enzyme activity is higher during chronic inflammation and in CKD patients [185]. The exact interaction between hyperuricemia and IDO requires further investigation. For a long time, kynurenine was regarded as an intermediate of tryptophan metabolism with little biological activity. Yet Opitz *et al.* [186] recently demonstrated that this metabolite is a ligand for the aryl hydrocarbon receptor (AHR) and can promote tumor cell survival and suppress antitumor immune responses. The AHR signaling pathway is involved in a myriad of cellular processes, including embryogenesis, inflammation and phase I and phase II metabolism. Fascinatingly, another tryptophan metabolite, indoxyl sulfate, is also reported to activate the AHR in primary human hepatocytes and human umbilical vein endothelial cells [187,188]. Thus, by disturbing tryptophan metabolism, hyperuricemia could indirectly be involved in AHR activation and subsequent pathologies.

Several polymorphisms in transporter genes are associated with elevated serum uric acid levels. For instance, Woodward *et al.* [88], described that the common single nucleotide polymorphism (SNP) rs2231142 encoding the Q141K mutation of BCRP caused hyperuricemia-based gout. Also in a Japanese population, Q141K was shown to be a common dysfunctional form of BCRP causing gout [130]. Another transporter recently implicated in uric acid metabolism is SLC2A9. Using *Xenopus* oocytes, Vitart *et al.* [173] demonstrated that SLC2A9-mediated uptake of uric acid was sevenfold higher in SLC2A9-expressing oocytes compared to URAT1-expressing oocytes. These findings have been confirmed by others [165,189]. Moreover, multiple genome-wide association studies reported a relationship between uric acid levels and SNPs in several transporters including SLC17A3, SLC22A11 and SLC22A12 [174,190,191]. Taken together, when studying the link between uric acid and disease progression it is important to take into consideration the presence of possible polymorphisms in transporter genes as well as changes in metabolite levels of transporter-specific substrates.

Two weeks of hyperuricemia induced early signs of kidney damage, as observed by an increased mRNA expression of Ngal in knockout animals. In contrast, no signs of renal damage were seen in WT animals. These findings suggest that knockout animals were more prone to the development of renal failure. Since, kynurenic acid levels were already elevated in Mrp4$^{-/-}$ and Bcrp$^{-/-}$ animals before the induction of hyperuricemia, one could argue that other tryptophan metabolites are responsible for induction of Ngal observed in knockout mice. To better understand the effect of hyperuricemia on the development of CKD, future studies should include longer treatment periods (> 2 wk) and also determine the levels of other intermediates and end-products of tryptophan metabolism.

In conclusion, our results showed that uric acid dose-dependently inhibited BCRP activity and inhibition occurred at physiologically relevant levels as was reported previously for MRP4 [87]. Moreover, we demonstrated that Mrp4- and Bcrp-deficiency as well as hyperuricemia are associated with alterations in tryptophan metabolism and the retention of kynurenine and kynurenic acid, two metabolites with a broad array of biological activities. Therefore, we postulate that elevated uric acid levels hamper MRP4 and BCRP functioning, thereby promoting the retention of other potentially toxic substrates, including KynA, which could contribute to the development of CKD. These finding underline the complex relation between hyperuricemia and linked pathologies, which should be taken into account when interpreting results obtained using *in vivo* hyperuricemia models.

ACKNOWLEDGEMENTS

This work was funded by the Dutch Kidney Foundation (grant number IK08.03) and J.G. Hoenderop was supported by an EURYI award from the European Science Foundation. The authors want to thank V. Verweij for her help regarding the animal experiment, A.E.M. Seegers for his technical assistance and P.H.H. van den Broek for the LC-MS/MS measurements.

6

Uremic toxins inhibit renal metabolic capacity through interference with glucuronidation and mitochondrial respiration

Henricus A.M. Mutsaers, Martijn J.G. Wilmer, Dorien Reijnders, Jitske Jansen, Petra H.H. van den Broek, Marleen Forkink, Eva Schepers, Griet Glorieux, Raymond Vanholder, Lambertus P. van den Heuvel, Joost G. Hoenderop and Rosalinde Masereeuw

Biochimica et Biophysica Acta (BBA) - Molecular Basis of Disease, Volume: 1832, Issue: 1, Page: 142-150, 2013

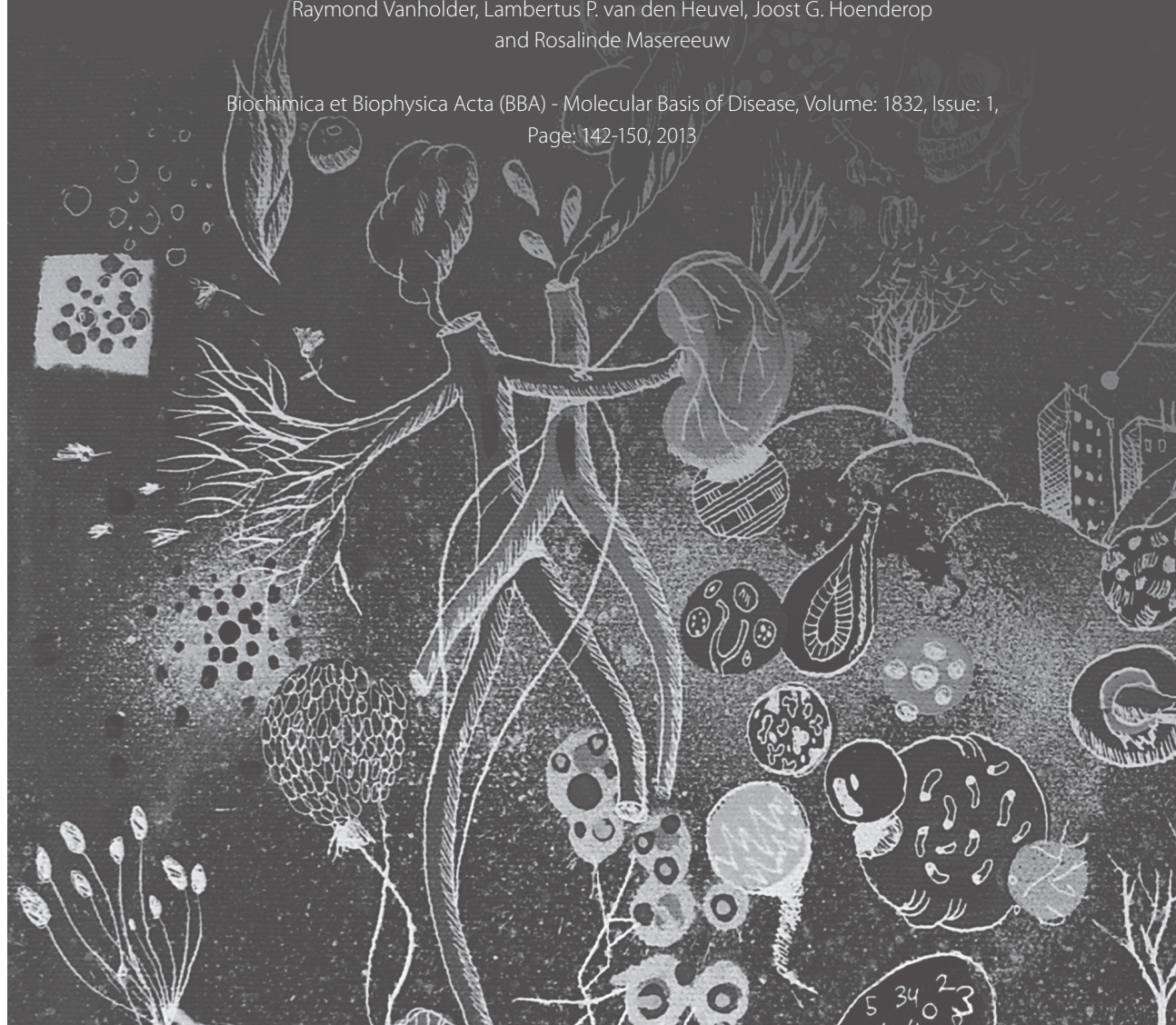

ABSTRACT

During chronic kidney disease (CKD), drug metabolism is affected leading to changes in drug disposition. Furthermore, there is a progressive accumulation of uremic retention solutes due to impaired renal clearance. Here, we investigated whether uremic toxins can influence the metabolic functionality of human conditionally immortalized renal proximal tubule epithelial cells (ciPTEC) with the focus on UDP-glucuronosyltransferases (UGTs) and mitochondrial activity. Our results showed that ciPTEC express a wide variety of metabolic enzymes, including UGTs. These enzymes were functionally active as demonstrated by the glucuronidation of 7-hydroxycoumarin (7-OHC; K_m of 12 ± 2 μM and a V_{max} of 76 ± 3 pmol/min/mg) and p-cresol (K_m of 33 ± 13 μM and a V_{max} of 266 ± 25 pmol/min/mg). Furthermore, a wide variety of uremic toxins, including indole-3-acetic acid, indoxyl sulfate, phenylacetic acid and kynurenic acid, reduced 7-OHC glucuronidation with more than 30% as compared with controls ($p < 0.05$), whereas UGT1A and UGT2B protein expressions remained unaltered. In addition, our results showed that several uremic toxins inhibited mitochondrial succinate dehydrogenase (*i.e.* complex II) activity with more than 20% as compared with controls ($p < 0.05$). Moreover, indole-3-acetic acid decreased the reserve capacity of the electron transport system with 18% ($p < 0.03$). In conclusion, this study shows that multiple uremic toxins inhibit UGT activity and mitochondrial activity in ciPTEC, thereby affecting the metabolic capacity of the kidney during CKD. This may have a significant impact on drug and uremic retention solute disposition in CKD patients.

INTRODUCTION

Renal function is an important aspect in drug clearance and it is widely known that drug disposition is altered in patients with chronic kidney disease (CKD) [49,192,193]. These changes in pharmacokinetics are partially due to a decreased glomerular filtration and tubular secretion. Another hallmark of CKD is the accumulation of potentially toxic solutes that are normally excreted via the urine. These uremic toxins can cause a multitude of pathologies, including renal fibrosis, anemia, bone disorders and cardio-vascular disease [135,194]. Currently, more than 110 uremic toxins are known, divided into three distinct classes based on their physico-chemical properties: the small water-soluble compounds, the middle molecules and the protein-bound solutes [23,135]. The latter group of retention solutes are actively secreted by the healthy kidney and are difficult to eliminate using current dialysis strategies [195]. Since protein-bound uremic toxins accumulate during renal failure it could be argued that these compounds affect drug metabolism in CKD patients by interacting with renal enzymes. Many drugs commonly used in the clinic are metabolized by phase II enzymes, which catalyze conjugation reactions, including sulfation, acetylation and glucuronidation [196]. Several studies demonstrated that the pharmacokinetics of drugs solely cleared via phase II metabolism is changed in CKD patients. For instance, a decreased glucuronidation of metoclopramide, chloramphenicol, p-aminobenzoic acid, zidovudine and morphine have been reported in patients with chronic renal failure (CRF) [48,197-201]. Moreover, the acetylation of isoniazid is reduced in CKD patients [202]. However, little information is available about the mechanism underlying the observed decrease in phase II metabolism during renal failure.

UDP-glucuronosyltransferases (UGT) are an important class of phase II enzymes that catalyze the conjugation of glucuronic acid to many xenobiotics, environmental pollutants and endogenous compounds [203,204]. Next to drugs, uremic retention solutes are also prone to glucuronidation, and at least two glucuronides have been identified in uremic biological fluids, p-cresyl glucuronide and indoxyl glucuronide [43,52,53]. UGTs are expressed in several organs including the liver, gastro-intestinal tract and kidney, and to date 19 human UGT proteins have been identified [205,206]. Due to the relative abundance of the essential cofactor UDP-glucuronic acid (UDPGA), glucuronidation is the most prevalent conjugation reaction and under normal metabolic conditions, the supply of UDPGA is not rate-limiting for this process [50]. Yet, during excessive glycogenesis or under altered redox conditions, UGT activity is impaired [50,207]. After the liver, UGT activity is highest in the kidney, emphasizing the pivotal role of this organ in facilitating xenobiotic clearance via glucuronidation [196,208]. Previously, Yu *et al.* demonstrated that UGT expression and activity were down-regulated in the liver and kidney of 5/6 nephrectomized rats. However, this effect was also observed in control pair-fed rats and was possibly due to a decreased food intake [209]. Thus, the repercussions of CKD on UGTs remain to be elucidated.

In the present study, conditionally immortalized human renal proximal tubule epithelial cells (ciPTEC) were used to investigate the impact of multiple uremic toxins on renal UGT activity. Our results show that ciPTEC express a broad array of drug metabolism enzymes, similar to human kidney. Furthermore, UGT proteins were functionally active in ciPTEC, as demonstrated by 7-hydroxycoumarin (7-OHC) and p-cresol glucuronidation. Uremic toxins inhibited the glucuronidation of 7-OHC without affecting UGT1A and UGT2B protein expression, indicating a reduction in enzyme activity. Moreover, exposure of ciPTEC to uremic toxins caused a reduction in mitochondrial succinate dehydrogenase activity and in the maximum capacity of the oxidative phosphorylation (OXPHOS) system, which could explain the observed inhibitory effect of uremic toxins on glucuronide formation. These results present a novel pathway via which uremic retention solutes affect the metabolic capacity of the kidney and are likely involved in altering drug metabolism by glucuronidation in CKD patients.

MATERIALS AND METHODS

Chemicals

All chemicals were obtained from Sigma (Zwijndrecht, the Netherlands) unless stated otherwise. Stock solutions of uremic toxins were prepared as described by Cohen *et al.*, [131] and were stored at -20ºC. Both p-cresyl sulfate and phenyl sulfate were synthesized as a potassium salt as described previously [97]. P-cresyl glucuronide was produced from glucuronyl-trichloroacetimidate and *p*-cresol using the method previously described by Van der Eycken *et al.* [154].

Cell culture

The ciPTEC line was generated as previously described by Wilmer *et al.* [98]. The cells were cultured in ciPTEC medium containing phenol red free DMEM/F12 medium (Gibco/Invitrogen, Breda, the Netherlands) supplemented with 10% (v/v) fetal calf serum (FCS; MP Biomedicals, Uden, the Netherlands), insulin (5 µg/ml), transferrin (5 µg/ml), selenium (5 ng/ml), hydrocortisone (36 ng/ml), epithelial growth factor (10 ng/ml), and tri-iodothyronine (40 pg/ml) at 33ºC in a 5% (v/v) CO_2 atmosphere. Propagation of cells was maintained by subculturing the cells at a dilution of 1:3 to 1:6 at 33°C. For experiments, cells were cultured at 33ºC to 40% confluency, followed by maturation for 7 days at 37ºC. Experiments were performed on the cells between passages 30 and 40.

Quantitative PCR array

To study the gene expression of drug metabolism enzymes, ciPTEC were cultured and differentiated cells (7 days at 37ºC) were harvested. Total RNA was isolated using an RNeasy Mini kit (Qiagen, Venlo, the Netherlands) according to the manufacturers recommendations. Subsequently, cDNA was generated using the Omniscript RT-kit (Qiagen) according to the manufacturers recommendations. Following cDNA-synthesis, RT^2 Profiler PCR arrays (drug metabolism: phase I and phase II enzymes; Qiagen) were performed according to the manufacturers recommendations, using a CFX96 Real-Time PCR detection system (Bio-rad, Veenendaal, the Netherlands). Quantification of gene expression was performed using the CFX96 system software (Bio-rad) and the web-based PCR array data analysis software (Qiagen). GAPDH was used as housekeeping gene, and relative expression levels were calculated as percentage as compared with GAPDH (100%).

Western blotting

To study the protein expression of UGT1A and UGT2B, ciPTEC were cultured and exposed to 0–2 mM of different uremic toxins for 48 h. After treatment, cells were harvested using RIPA buffer containing 1% (v/v) Igepal CA630, 0.5% (v/v) Nadeoxycholate, 0.1% (w/v) SDS, 0.01% (w/v) phenylmethane sulphonylfluoride, 3% (v/v) aprotinin and 1 mM Na-orthovanadate. Total protein (50 µg) was separated via SDS/PAGE using 10% (w/v) gels and blotted onto nitrocellulose membranes using the iBlot dry blotting system (Invitrogen). Afterwards, the membrane was blocked using Odyssey Blocking Buffer, (1:1 diluted with PBS; LI-COR Biosciences, Lincoln, NE, USA) during 1 h at RT. The membrane was then incubated overnight at 4ºC with rabbit polyclonal UGT1A or UGT2B antibody (1:200; both Santa Cruz Biotechnology, Inc., Santa Cruz, CA, USA). Mouse monoclonal β-actin antibody (1:10,000; Sigma) was simultaneously incubated to serve as a protein loading control. Antibodies were diluted in Odyssey Blocking Buffer containing 0.1% (v/v) Tween-20. Afterwards, the membrane was thoroughly washed three times during 10 min with PBS containing 0.1% (v/v) Tween-20. The secondary antibodies, goat-α-mouse Alexa Fluor 680 (1:20,000; Invitrogen) and goat-α-rabbit IRDye 800 (1:20,000; Rockland, Gilbertsville, PA, USA), were incubated for 1 h at RT in Odyssey Blocking Buffer containing 0.1% (v/v) Tween-20 and 0.01% (w/v) SDS. The membrane was thoroughly washed, as described above, and then scanned using the Odyssey Infrared Imaging System (LI-COR Biotechnology). Intensity of the protein bands was quantified using the Odyssey Application software version 2.1.

Confocal microscopy

Cellular localization of UGT1A and UGT2B proteins was investigated using confocal microscopy. ciPTEC were seeded on 12-well Corning Costar Transwell Permeable Supports (type 3460, Corning Costar, NY, USA). Before seeding, the supports were coated with 50 µg/ml collagen type IV for 2 h at 37ºC. Subsequently, supports were washed with HBSS buffer (Gibco) and cells were seeded at a density of 1.33 x 10^5 cells/cm^2. Following maturation, as described above, cells were washed with wash solution (4% (v/v) FCS in HBSS) and fixed for 5 min with 2% (w/v) paraformaldehyde in HBSS. Next, cells were permeabilized for 10 min in HBSS with 0.3% (v/v) Triton and aspecific epitopes were blocked for 30 min with blocking buffer (2% (v/v) FCS, 0.5% (w/v) bovine serum albumin

and 0.1% (v/v) Tween-20 in HBSS). Subsequently, the cells were incubated overnight at 4°C with rabbit polyclonal UGT1A or UGT2B antibody (1:50 in blocking buffer, Santa Cruz Biotechnology) using dynamic conditions. Afterwards, cells were incubated for 30 min with the secondary antibody goat-α-rabbit Alexa568 (1:200, Molecular Probes, Invitrogen). Subsequently, ciPTEC were incubated for 1 h with a mouse monoclonal antibody against the tight junction protein ZO-1 (1:50 in blocking buffer, Invitrogen, CA, USA). Next, the cells were simultaneously incubated for 30 min with goat-α-mouse Alexa488 (1:200, Molecular Probes, Invitrogen) and DAPI nucleic acid stain (300 nM, Molecular Probes, Invitrogen). The slides were then mounted using Fluorescent Mounting Medium (DakoCytomation, Dako Netherlands b.v., Heverlee, Belgium). Between all incubation steps the cells were washed with wash solution. Fluorescence was examined using the Olympus FV1000 Confocal Laser Scanning Microscope (Olympus, UK) and images were captured using the Olympus software FV10-ASW version 1.7.

High-performance liquid chromatography (HPLC)

HPLC was used to measure UGT activity via the glucuronidation of 7-hydroxycoumarin (7-OCH), as described previously, [99] and p-cresol. To determine enzyme kinetics, ciPTEC were exposed to 7-OCH or p-cresol dissolved in HBSS at 37°C and 4°C (as negative control) using different concentrations (0–500 µM) and different incubation times (0–5 h). When used, β-glucuronidase from *Helix Pomatia* was added 1 h prior to incubation with 7-OHC (50 µM for 3 h). In addition, UGT activity was also determined following exposure to uremic toxins for 48 h. Following treatment, ciPTEC were incubated with 10 µM 7-OCH for 3 h at 37°C. Before chromatography an aliquot of culture medium was collected and centrifuged at 12,000xg for 3 min and 50 µl of the supernatant was injected into the HPLC-system (Spectra-Physics Analytical, Spectrasystem SCM400). To measure 7-OCH and 7-OCH glucuronide (7-OCHG) the HPLC was equipped with a C18 HPLC column (GraceSmart RP 18 5u 150 x 4.6 mm; Grace, Breda, the Netherlands). Separation was performed at a flow rate of 1 ml/min with eluent A (95% (v/v) H_2O, 5% (v/v) methanol and 0.2% (v/v) acetic acid) and eluent B (50% (v/v) H_2O, 49% (v/v) acetonitrile and 1% (v/v) tetrahydrofuran) under the following gradient conditions: 0-3 min, 80-50% eluent A; 3-8 min, 50% eluent A; 8-9 min, 50-80% eluent A; 9-14 min, 80% eluent A. The compounds were detected at a wavelength of 316/382 nm. For the detection of p-cresyl sulfate and p-cresyl glucuronide, chromatography was performed on a C18 HPLC column (GraceSmart RP 18 5u 150 x 4.6 mm) with eluent A (95% (v/v) 50 mM KH_2PO_4 (pH 3.0) and 5% (v/v) acetonitrile) and eluent B (50 mM KH_2PO_4 (pH 3.0), methanol and acetonitrile in a 1:1:1 ratio) using the following gradient: 0-15 min, 100-20% eluent A; 15-16 min, 20-100% eluent A; 16-21 min, 100% eluent A. The flow rate was 1 ml/min and the p-cresol metabolites were detected at a wavelength of 220 nm. Standards of the compounds were also run in order to quantify the amount of metabolites found in the samples. Acquired data were processed with PC1000 software (Spectrasystem).

3-[4,5-dimethylthiazol-2-yl]-2,5-diphenyl tetrazolium bromide (MTT) assay

Mitochondrial succinate dehydrogenase activity was assessed using the MTT assay. ciPTEC were cultured in a 96 well culture plate and exposed to 1 mM or 2 mM of uremic toxins for 48 h. Next, medium was removed and 20 µl preheated (37°C) MTT-solution (5 mg 3-[4,5-dimethylthiazol-2-yl]-2,5-diphenyl tetrazolium bromide/ml ciPTEC medium) was added and incubated for 4 h at 37°C. Afterwards, MTT-solution was removed, followed by the addition of 200 µl DMSO to dissolve produced formazan crystals. The extinction of the solution was measured at 570 nm using a Benchmark Plus Microplate Spectrophotometer (Bio-rad).

Flow cytometry

In this study, flow cytometry was used to study ciPTEC morphology and viability. Cells were cultured in 12-well culture plates and treated for 48 h with 2 mM of uremic toxins. After incubation, cells were harvested using trypsin-EDTA and centrifuged at 600xg during 5 min. Subsequently, supernatant was removed and the cell pellet was resuspended in 100 µl PBS containing 4% (w/v) paraformaldehyde and 0.1% (v/v) saponin followed by 10 min incubation on ice. Subsequently, samples were centrifuged (600xg for 5 min) and resuspended in 100 µl PBS. Samples were acquired on a BD FACSCalibur (Becton Dickinson, Breda, the Netherlands). Analysis was performed using Flow Jo software (TreeStar, Ashland, USA), gating on live cells.

High-resolution respirometry

Cells were cultured in T25 culture flasks and treated for 48 h with 2 mM indole-3-acetic acid. Subsequently, cells were harvested using trypsin-EDTA and centrifuged at 1500xg during 5 min. Afterwards, the supernatant was removed and the cell pellet was resuspended in ciPTEC medium to obtain a suspension of approximately 1 x 10^6 cells/ml. Two milliliters of the cell suspension was used to measure cellular oxygen consumption. Oxygen consumption was measured at 37°C using polarographic oxygen sensors in a two-chamber Oxygraph (Oroboros Instruments, Innsbruck, Austria) using an established protocol [210]. The cells were allowed to respire at basal level for at least 10 min until the flux was stable, representing routine respiration (R). Next, leak respiration (L) was determined by addition of the specific mitochondrial ATP synthase inhibitor oligomycin A (omy; 2.5 µM). Then, maximal ETS capacity (E) was quantified using increasing concentrations of the mitochondrial uncoupler p-trifluoromethoxy carbonyl cyanide phenyl hydrazone (FCCP; 2.5 µM maximal concentration). Finally, non-mitochondrial respiration (ROX) was assessed by adding a maximal (0.5 µM) concentration of the specific mitochondrial complex I inhibitor rotenone (ROT) followed by the Complex III inhibitor antimycin A (AA; 2.5 µM).

Kinetic analysis and statistics

Statistics were performed using GraphPad Prism 5.02 via one-way analysis of variance (ANOVA) followed by Dunnett's Multiple Comparison Test or an unpaired t test. Differences

between groups were considered to be statistically significant when $p < 0.05$. The software was also used to perform linear and nonlinear regression analysis (Michaelis-Menten) and correlation analysis (Spearman).

RESULTS

Selection of uremic toxins

In our study, 13 uremic solutes were selected containing one water-soluble solute (oxalate, Ox) and 12 protein-bound solutes. The latter group contained 4 tryptophan metabolites (indoxyl sulfate, IS; indole-3-acetic acid, I3A; kynurenic acid, KA; and quinolinic acid, QA), six phenols (phenylacetic acid, PHA; phenyl glucuronide, PHG; phenyl sulfate, PHS; p-cresol, pC; p-cresyl sulfate, pCS; and p-cresyl glucuronide, pCG), one hippurate (hippuric acid, HA) and one polyamine (putrescine, Pu). Moreover, a mix of several uremic toxins (Mix) was used, consisting of putrescine, oxalate, indoxyl sulfate and p-toluenesulfonic acid, a previously described phenolic model compound (1:1:1:1) [89]. This specific mix was chosen because it contained different classes of solutes, of which the stock solutions were all prepared in the same solvent (*e.g.* milli-Q).

Expression and activity of UGT in ciPTEC

Extrahepatic glucuronidation occurs mainly in the kidney and UGT expression and activity were demonstrated in both human and rat primary proximal tubule cells [196,211,212]. We used a recently established human renal proximal tubule cell line, [98,101] in which phase I and phase II drug metabolism enzyme expression levels were studied, with an emphasis on the class of UGT enzymes. A complete overview of the drug metabolism enzyme gene expression in ciPTEC is provided in Figure S1. This figure clearly demonstrates that ciPTEC express a broad range of drug metabolism enzymes, including cytochrome p450 (CYP), sulfotransferase (SULT) and glutathione S-transferase (GST) enzymes, next to members of the UGT family. Figure 1A shows that the gene expression of 18 UGTs was detected in ciPTEC of which UGT1A1, 1A9, 2B7, 2B10 and 2B28 were most abundantly expressed compared with GAPDH, with a relative expression of 11%, 2143%, 16%, 145% and 9%, respectively. Furthermore, using Western blotting UGT1A and 2B family members were detected in ciPTEC, with the predicted molecular weight of the enzymes (approximately 68 kD; Figure 1B-C). Protein expression of the enzymes was also demonstrated in human kidney lysates, whereas their expression was absent in human embryonic kidney (HEK293) cells. Glucuronide formation occurs in the cytosol, and confocal microscopy demonstrated that both UGT1A and 2B enzymes exhibit cytosolic localization in ciTPEC (Figure 1D-E). Moreover, expression of tight junction protein 1 (ZO-1) revealed that ciPTEC form tight monolayers and that the cells maintain their epithelial characteristics during culturing.

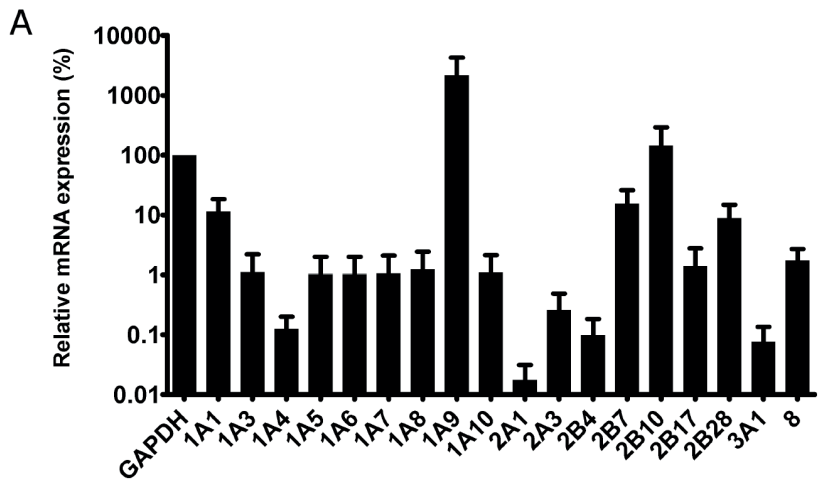

Figure 1 Expression of UGTs in ciPTEC.

(A) Differentiated ciPTEC were harvested and total mRNA was isolated. Afterwards, cDNA was synthesized and UGT gene expression was studied using a qPCR array. Relative expression was calculated using the household gene GAPDH (100%). Bars represent mean ± SEM of two experiments. **(B-C)** UGT1A and UGT2B protein expression was studied by Western blotting. Proteins were separated via SDS/PAGE and blotted onto nitrocellulose membranes. Lysates of HEK293 cells were used as a negative control and homogenates from human kidney (HuKid) were used as positive control. Both UGT1A and UGT2B were detected at 68 kD.

Figure 1 Continued.

(D-E) Confocal microscopy was used to study intracellular localization of UGTs in ciPTEC. Following maturation, cells were fixed and permeabilized and subsequently stained using an antibody against UGT1A or UGT2B and ZO-1. Detection was performed using Alexa568 for UGTs (red) and Alexa488 for ZO-1 (green) labeled secondary antibodies. Nucleus was stained with DAPI (blue). **(B-E)** Representative images of two independent experiments.

To determine whether the UGTs were enzymatically active, a glucuronidation assay was performed using 7-OHC as a substrate. A concentration-dependent formation of 7-OHC glucuronide was observed (Figure 2A), and curve fitting revealed an apparent K_m of 12 ± 2 μM and a V_{max} of 76 ± 3 pmol/min/mg. Glucuronidation was demonstrated to be linear up to 5 h (Figure 2B). Furthermore, as depicted in Figure 2A and 2B, 7-OHC metabolism was completely absent at 4ºC, indicating enzyme-dependent conjugation. Glucuronidation of 50 μM 7-OHC was concentration-dependently inhibited by β-glucuronidase with an approximate IC_{50} value of 50 U/ml, as demonstrated in Figure 2C.

Uremic toxins decrease UGT activity

Next, it was investigated whether exposure of ciPTEC to uremic toxins could influence 7-OHC glucuronidation. Figure 3 shows that a myriad of uremic toxins belonging to three different physico-chemical classes, *viz.* tryptophan metabolites, phenols and water-soluble compounds, concentration-dependently inhibited the glucuronidation of 7-OHC. Kynurenic acid, indole-3-acetic acid, phenylacetic acid and a mixture of uremic toxins most potently inhibited UGT activity (Figure 3A-C). At the highest concentration, these toxins decreased glucuronide formation by 52%, 44%, 36% and 50%, respectively. In addition, at the same concentration, indoxyl sulfate, phenyl sulfate, oxalate, putrescine and hippuric acid inhibited the formation of 7-OHCG by 32%, 30%, 16%, 18% and 32%, respectively. In contrast, quinolinic acid and phenyl glucuronide did not affect 7-OHC metabolism.

A decline in enzyme activity is often secondary to a decrease in protein expression, therefore, the impact of uremic toxins on UGT expression was examined. Exposure of ciPTEC to none of the different toxins reduced UGT1A and UGT2B protein expression with more than 15%, with both tested concentrations, compared to control. A representative sample of toxins is shown in Figure 4, and the other toxins in Figure S2.

P-cresol metabolism and impact on glucuronidation

To further investigate the mode of inhibition, ciPTEC were exposed to p-cresol, which can be metabolized to both p-cresyl sulfate and p-cresyl glucuronide [30]. Figure 5A shows that p-cresol is indeed conjugated to glucuronic acid in ciPTEC and a concentration-dependent formation of p-cresyl glucuronide is demonstrated with a calculated K_m of 33 ± 13 μM and a V_{max} of 266 ± 25 pmol/min/mg. In contrast, ciPTEC did not metabolize p-cresol to p-cresyl sulfate (data not shown), despite the expression of multiple sulfo-

transferases, the enzymes that catalyze sulfation reactions (Figure S1). Furthermore, HPLC revealed that p-cresol inhibited 7-OHCG formation by 72% (Figure 5B). Yet, both p-cresol metabolites also inhibited UGT activity with approximately 20%.

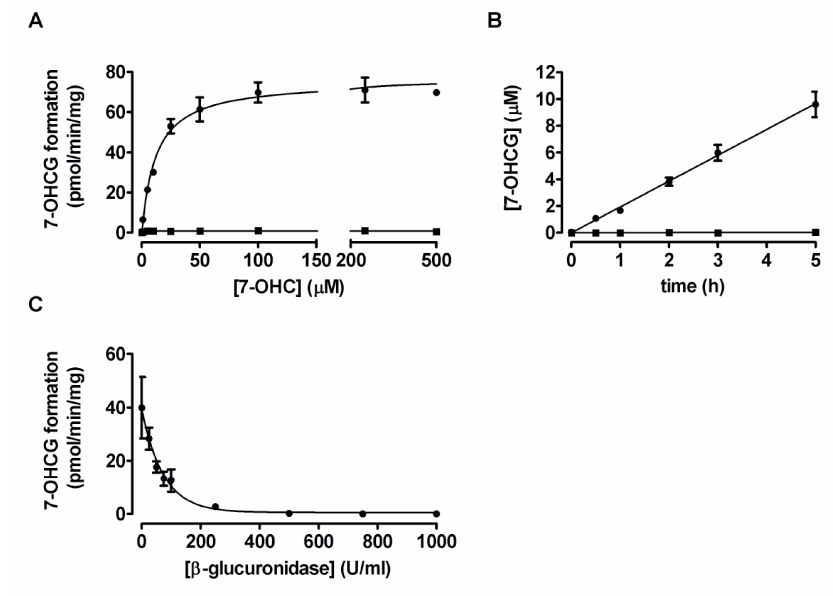

Figure 2 UGTs are functionally active.

HPLC was used to study UGT activity via 7-OHC glucuronidation. Cells were incubated with 7-OHC (0–500 μM) for 0–5 h at 37ºC (●) or 4ºC (negative control; ■). To further demonstrate specificity of the HPLC method, cells were incubated with 50 μM 7-OHC for 3 h in the presence of β-glucuronidase (0–1000 U/ml). **(A)** Concentration-dependent formation of 7-OHCG. **(B)** Time curve of 7-OHC glucuronidation. **(C)** β-glucuronidase inhibits glucuronide formation. Standards of 7-OHCG were also analyzed in order to quantify the amount of glucuronide found in the samples. Acquired HPLC data were processed with PC1000 software (Spectrasystem). Nonlinear and linear regression analyses were performed using Graphpad Prism 5.02. Results are presented as mean ± SEM of three independent experiments performed in triplicate.

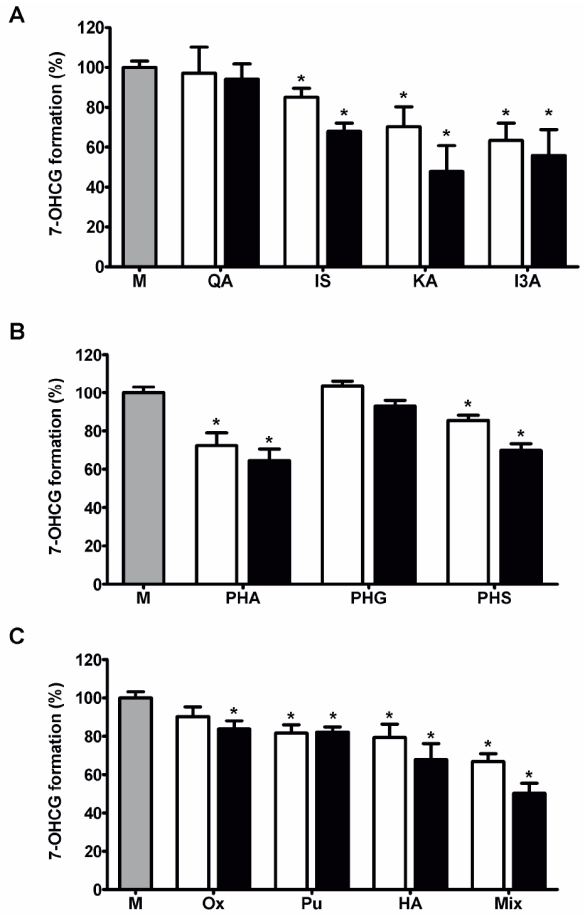

Figure 3 Uremic toxins inhibit 7-OHC glucuronidation.

Impact of uremic toxin exposure on 7-OHC glucuronidation was studied using HPLC. Cells were exposed for 48 h to ciPTEC medium (gray bar), 1 mM (white bars) or 2 mM (black bars) of several uremic toxins belonging to three different physico-chemical classes: **(A)** tryptophan metabolites, **(B)** phenols and **(C)** water-soluble compounds. Following treatment, ciPTEC were incubated for 3 h with 10 µM 7-OHC. Afterwards, an aliquot of culture medium was collected and injected into the HPLC-system. Standards of 7-OHCG were also analyzed in order to quantify the amount of glucuronide found in the samples. Acquired HPLC data were processed with PC1000 software (Spectrasystem). Statistical analysis was performed via one-way ANOVA followed by Dunnett's Multiple Comparison Test for each toxin. Results are presented as mean ± SEM of three experiments performed in duplicate or triplicate. * indicates $p < 0.05$ compared with control. HA, hippuric acid; I3A, indole-3-acetic acid; IS, indoxyl sulfate; KA, kynurenic acid; M, medium; Mix, uremic toxin mix; Ox, oxalate; PHG, phenyl glucuronide; PHS, phenyl sulfate; PHA, phenylacetic acid; Pu, putrescine; QA, quinolinic acid.

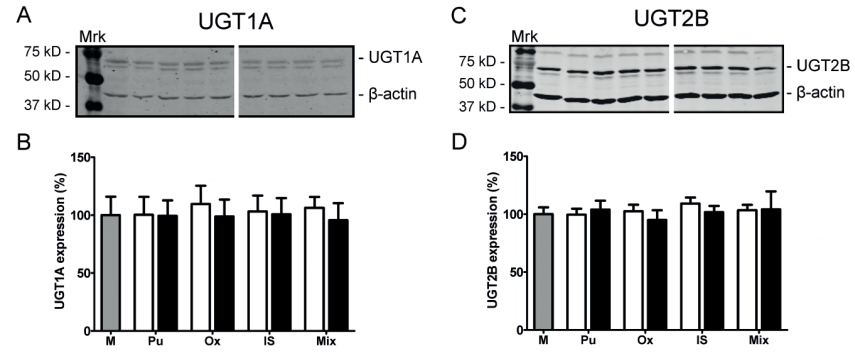

Figure 4 UGT1A and UGT2B protein expression is not affected by uremic toxins.

UGT1A and UGT2B protein expression was studied via Western blot. Cells were exposed for 48 h to ciPTEC medium (gray bar), 1 mM (white bars) or 2 mM (black bars) of several uremic toxins. **(A/C)** Afterwards cells were lysed and proteins were separated via SDS/PAGE and blotted onto nitrocellulose membranes. Both UGT1A and UGT2B were detected at 68 kD. **(B/D)** Fluorescence of the specific protein bands was determined using the Odyssey Infrared Imaging System. Bars represent mean ± SEM of the UGT band intensities corrected for β-actin from 3 independent experiments. IS, indoxyl sulfate; M, medium; Mix, uremic toxin mix; Ox, oxalate; Pu, putrescine.

Uremic toxins inhibit mitochondrial metabolism

Reduction of MTT is mainly dependent on mitochondrial succinate dehydrogenase activity [213]. Our results indicate that the majority of the toxins tested (*e.g.* putrescine, oxalate, indoxyl sulfate) did not significantly decrease MTT reduction with more than 15% compared to control (Figure S3). Yet, p-cresol, p-cresyl sulfate and p-cresyl glucuronide significantly reduced mitochondrial succinate dehydrogenase activity with 28%, 21% and 14%, respectively (Figure 6A). In addition, the toxins that most potently inhibited UGT activity (*i.e.* indole-3-acetic acid, phenylacetic acid and a mixture of uremic toxins) also significantly decreased MTT reduction at the highest concentration by 28%, 26% and 33%, respectively. Moreover, we observed a significant correlation between the two parameters studied, with a calculated Spearman r of 0.69 ($p < 0.005$; Figure 6B). Since the MTT assay is often used to study cell viability, we aimed to confirm that the observed correlation was not due to the induction of cell death by uremic toxins. Flow cytometry revealed that exposure of ciPTEC to the solutes that had the most pronounced impact on cellular and mitochondrial metabolism did not affect cell morphology nor the percentage of living cells as compared with untreated cells (Figure S4).

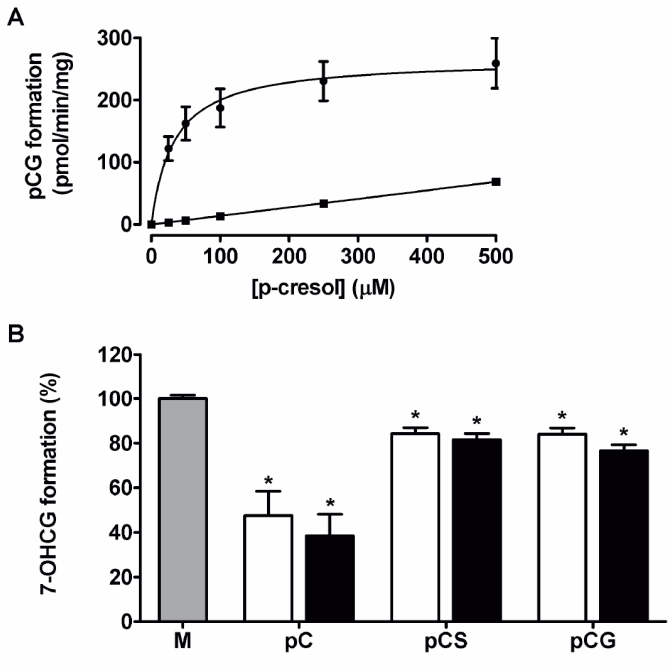

Figure 5 P-cresol glucuronidation and impact on UGT activity by cresols.

(A) HPLC was used to study p-cresol glucuronidation. Cells were incubated with p-cresol (0–500 μM) for 1 h at 37ºC (●) or 4ºC (negative control; ■). **(B)** Cells were exposed for 48 h to ciPTEC medium (gray bar), 1 mM (white bars) or 2 mM (black bars) of p-cresol or the metabolites. Following treatment, ciPTEC were incubated for 3 h with 10 μM 7-OHC. After incubation with p-cresol or 7-OHC, an aliquot of culture medium was collected and injected into the HPLC-system. Standards of the compounds were also analyzed in order to quantify the amount of metabolites found in the samples. Acquired HPLC data were processed with PC1000 software (Spectrasystem). Nonlinear analysis was performed using Graphpad Prism 5.02 and statistical analysis was performed via one-way ANOVA followed by Dunnett's Multiple Comparison Test for each toxin. Results are presented as mean ± SEM of three independent experiments performed in duplicate or triplicate. * indicates $p < 0.05$ compared with control. M, medium; pC, p-cresol; pCG, p-cresyl glucuronide; pCS, p-cresyl sulfate.

Inhibition of mitochondrial respiration by indole-3-acetic acid

Mitochondrial succinate dehydrogenase plays an essential role in the electron transfer chain and the tricarboxylic acid cycle (*i.e.* citric acid cycle) [214]. Therefore, we investigated the impact of indole-3-acetic acid on the OXPHOS system, since this solute had the most profound effect on both 7-OHC glucuronidation and MTT reduction. High-resolution respirometry revealed that basal mitochondrial respiration (R; ROUTINE), electron transport

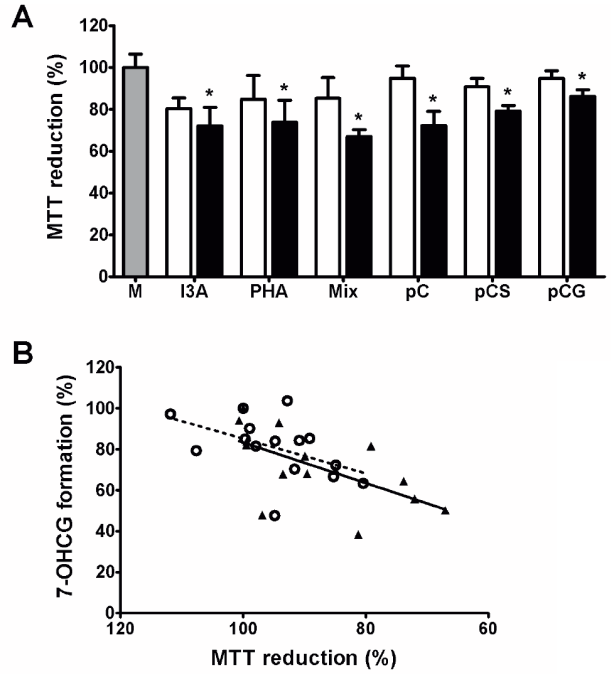

Figure 6 Inhibitory effect of uremic toxins on MTT reduction.

(A) The MTT assay was used to study the impact of uremic toxins on mitochondrial metabolism. Cells were exposed for 48 h to ciPTEC medium (gray bar), 1 mM (white bars) or 2 mM (black bars) of several uremic toxins. Afterwards, cells were incubated for 4 h with MTT-medium at 37ºC. Subsequently, produced formazan crystals were dissolved in DMSO and extinction was measured at 570 nm. Statistical analysis was performed via one-way ANOVA followed by Dunnett's Multiple Comparison Test for each toxin. Results are presented as mean ± SEM of three independent experiments performed in triplicate. * indicates $p < 0.05$ compared with control. I3A, indole-3-acetic acid; M, medium; Mix, uremic toxin mix; pC, p-cresol; pCG, p-cresyl glucuronide; pCS, p-cresyl sulfate; PHA, phenylacetic acid. **(B)** Correlation between UGT activity and MTT reduction. Cells were exposed for 48 h to 1 mM (○) or 2 mM (▲) of several uremic toxins and 7-OHC glucuronidation and MTT reduction were investigated. Nonparametric Spearman correlation analysis revealed a significant association between the reduction in glucuronidation and mitochondrial dehydrogenase activity when ciPTEC were treated with 2 mM of uremic toxins ($r = 0.69$; $p < 0.005$). Following exposure to 1 mM of uremic toxins, no significant correlation was observed ($r = 0.48$; $p = 0.07$).

that was not coupled to ATP production (L; LEAK) and non-mitochondrial respiration (ROX; residual oxygen consumption) was not compromised by indole-3-acetic acid (Figure 7A-B), further supporting the impression that uremic toxins did not induce cell

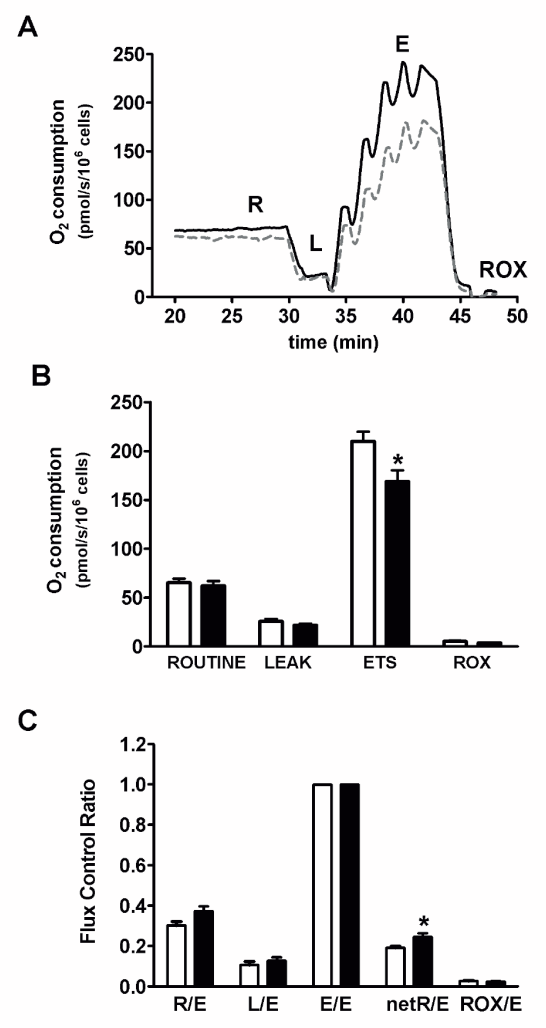

Figure 7 Reduction in mitochondrial respiration by indole-3-acetic acid.

High-resolution respirometry was used to measure mitochondrial oxygen consumption. Cells were treated for 48 h with ciPTEC medium (white bar) or 2 mM indole-3-acetic acid (black bar) and oxygen consumption was measured at 37ºC using polarographic oxygen sensors in an Oxygraph. **(A)** Online high-resolution respirometry traces of mitochondrial respiration in a representative experiment with control (solid line) and indole-3-acetic acid (dashed line) treated cells. Titrations: ROUTINE (R) respiration (intact cells), omy (LEAK respiration; L), FCCP (ETS capacity; E), Rot and AA (ROX). **(B)** Quantification of cellular respiration. **(C)** Quantification of cellular respiration corrected for electron transport system capacity. Statistical analysis was performed via an unpaired t test. Results are presented as mean ± SEM of three experiments performed in duplicate. * indicates $p < 0.05$ compared with control.

death in ciPTEC. In contrast, the maximum capacity of the electron transport system (E; ETS) was reduced from 221 ± 21 pmol/s·10^6 cells in untreated cells to 182 ± 17 pmol/s·10^6 cells in ciPTEC exposed to indole-3-acetic acid, indicating that treatment caused a reduction in the reserve capacity for energy production. Figure 7C shows that exposure of the cells to indole-3-acetic acid resulted in a significantly increased netRoutine/ETS ratio, with a 1.3 fold change. This signifies that a higher proportion of the maximum capacity of the OXPHOS system is activated to drive ATP synthesis, and implies that ciPTEC exposed to uremic toxins have a limited ability to supply energy for other cellular processes, such as enzymatic activity.

DISCUSSION

This study reports for the first time that multiple uremic toxins directly inhibit the function of an important class of phase II drug metabolism enzymes, namely UGTs, in human renal proximal tubule cells. Our results showed that uremic toxin-induced UGT inhibition was independent of an effect on protein expression, and inhibition seemed to occur in both a competitive (*e.g.* p-cresol) and non-competitive fashion (*e.g.* p-cresyl sulfate). It is likely that most uremic solutes act as non-competitive inhibitors of UGT activity, since the majority of these compounds are end-products of endogenous metabolism.

To further unravel the mode of inhibition, mitochondrial respiration was studied and the results indicated that indole-3-acetic acid reduced the reserve capacity of the electron transport system. This finding provides more insight into the mechanism by which uremic toxins possibly inhibit UGT activity. As stated before, glucuronide formation is dependent on the availability of UDPGA, the donor of the glucuronide moiety [50]. UDPGA is formed from UDP-glucose by UDP-glucose dehydrogenase using nicotinamide adenine dinucleotide (NAD^+), a coenzyme that plays an important role in energy metabolism [215]. In the mitochondria, enzymes of the citric acid cycle reduce NAD^+ to NADH. Subsequently, NADH is oxidized by complex I of the electron transport chain during OXPHOS-mediated ATP production, resulting in the conversion of NADH to NAD^+ [215]. Therefore, we postulate that a reduction in the activity of the mitochondrial electron transport chain induced by uremic toxins, as demonstrated in this study, caused a drop in NAD^+ levels and, consequently, led to depletion of UDPGA, thereby decreasing UGT-mediated metabolism. *De novo* synthesis of NAD^+ in mammals is dependent on tryptophan metabolism via the kynurenine pathway [215]. Dietary tryptophan is converted to kynurenine by tryptophan 2,3-dioxygenase and indoleamine 2,3-dioxygenase, which are both considered the rate-limiting steps in this pathway [55,215]. Kynurenine can, subsequently, be metabolized to kynurenic acid by kynurenine aminotransferase or, via several other enzymatic steps, to quinolinic acid [55]. The latter metabolite is used by quinolinic acid phosphoribosyl transferase to form NAD^+. Interestingly, it is known that plasma tryptophan levels are

significantly diminished in CKD patients [90]. Furthermore, Fukuwatari *et al.* reported that NAD (NAD^+ + NADH) concentrations were decreased in the liver, kidney and blood of rats with adenine-induced renal failure [216]. Thus, it is likely that UDPGA levels are reduced in patients with CKD due to altered tryptophan metabolism, resulting in a reduced UGT activity. To our knowledge, this is the first report to demonstrate the influence of uremic toxins on mitochondrial metabolism and respiration in human proximal tubule cells. Previously, Owada *et al.* demonstrated that indoxyl sulfate stimulated renal mitochondrial superoxide production in rats [217]. Dzurik *et al.* described that hippuric acid reduced ammonia production by P-dependent mitochondrial glutaminase in kidney homogenates of acidified rats [218]. Furthermore, using isolated rat liver mitochondria, Kitagawa revealed that p-cresol inhibited state 3 respiration without affecting oxidative phosphorylation [219]. Yet, p-cresol is no longer regarded as a uremic toxin, [30] and it remains to be elucidated whether its major metabolite, p-cresyl sulfate, has a similar impact on mitochondrial respiration. Additionally, Riegel *et al.* reported that treatment of hepatocytes with ultrafiltrates of patients treated with high-flux membrane dialyzer significantly diminished MTT reduction [220]. However, the effect correlated with an increased LDH release, a marker of cell injury, and the decrease in metabolic activity might have been due to hepatotoxicity. These findings, together with our current results, suggest that uremic toxins might directly influence mitochondrial activity in different organs.

The uremic toxin concentrations used in this study do not always reflect the plasma levels determined in CKD patients, for instance the highest concentration reported for kynurenic acid is 50 μM, whereas the maximal uremic concentration for hippuric acid and phenylacetic acid are 2.6 and 7.7 mM, respectively [21,136]. An overview of the maximal uremic concentrations of the solutes used in the present study are provided in Table S1, and for a detailed description of uremic toxin concentrations the interested reader is referred to reviews by the European Uremic Toxin Work Group [21,22].

Since UGTs are located in the cytosol, enzyme activity depends on the intracellular levels of substrates rather than substrate concentrations in the blood. Uptake of uremic toxins in renal proximal tubules is fairly well characterized and shown to be dependent on a wide variety of transport proteins. Both organic anion transporter (OAT) 1 and OAT3, as well as organic anion transporting polypeptide 4C1, play an important role in the tubular uptake of uremic toxins [60,64,72,221]. In addition, it has been demonstrated that the multi-ligand receptor megalin is involved in the endocytotic uptake of a specific group of uremic toxins, *i.e.* advanced glycation end products [222]. Previously, Masereeuw *et al.* demonstrated that methyl hippuric acids accumulate in the isolated perfused rat kidney during secretory transport [137,138]. They reported that 2-methyl hippuric acid levels were 175-times higher in renal tissue compared to the perfusate and 4-methyl hippuric acid concentrations were even 600-times higher. Thus, it is likely that intracellular uremic toxin concentrations are much higher than total plasma concentrations. Therefore, it is complicated to extrapolate our findings to the clinical situation.

The present study demonstrates that UGT1A1, 1A9, 2B7 and 2B28 are highly expressed in ciPTEC, which corroborates previous reports on proximal tubule cells [205,211]. Lash *et al.* described that primary human proximal tubule cells (PTEC) express UGT1A1, 1A6 and 2B7 on protein level [211]. Furthermore, they postulated that UGT2B7 is the major UGT isoform present in PTEC cells. In the study from Ohno and coworkers, gene expression was demonstrated for UGT1A5, 1A6, 1A7, 1A9, 2B4, 2B7 and 2B17 in human kidney tissue, and they reported that UGT1A9 and 2B7 were most abundantly expressed [205]. Next to members of the UGT family, ciPTEC were currently demonstrated to have RNA expression of phase I enzymes, such as CYP3A4, CYP4A11, CYP2D6, that have previously been detected in primary PTEC by Lash *et al.* [211]. Additionally, the phase II enzymes GSTA4, GSTP, GSTT and SULT1A3 were demonstrated in our current study, as well as in primary PTEC. Taken together, ciPTEC have a similar phase I and phase II enzyme expression profile compared with primary PTEC, indicating that this cell line is a suitable model to study extrahepatic drug metabolism. Together with the endogenous expression of renal influx and efflux drug transporters, previously described by our group, [98] these data demonstrate that human ciPTEC is a unique tool to study renal pharmacokinetics.

The majority of studies investigating the effect of renal failure on drug metabolism focused on CYP enzymes. For instance, Leblond *et al.* demonstrated that during CKD, both hepatic protein and gene expression of CYP2C11, CYP3A1 and CYP3A2 decreased in rats, which correlated with a decreased metabolism of aminopyrine and erythromycin [223,224]. The same group also showed that 48 h exposure of HK-2 cells to serum from uremic rats decreased the protein expression of CYP3A1, suggesting a role for uremic toxins in this process [225]. Moreover, using rat liver microsomes, Sun *et al.* described that indoxyl sulfate and 3-carboxy-4-methyl-5-propyl-2-furanpropanoic acid (CMPF) directly inhibited CYP3A-mediated metabolism of erythromycin [226]. With regard to phase II drug metabolism, Simard *et al.* demonstrated that N-acetyl-transferase (NAT)1 and NAT2 expression decreased in the liver of CRF rats accompanied by a decrease in NAT2-mediated N-acetylation of p-aminobenzoic acid [197]. Furthermore, expression of both NAT1 and NAT2 decreased in rat hepatocytes following exposure to uremic serum, possibly via the action of parathyroid hormone, a known uremic toxin [197]. Taken together, there is a clear impact of uremic solutes on both phase I and phase II drug metabolism. Hepatic and renal transporters play an important role in xenobiotic handling. Previously, our group described that several uremic toxins, including hippuric acid and indoxyl sulfate, inhibited transport by two important renal efflux transporters, namely breast cancer resistance protein and multidrug resistance protein 4 [89]. Huang *et al.* showed that uremic plasma, obtained from rats with CRF, inhibited p-glycoprotein-mediated transport [142]. Moreover, it is demonstrated that CMPF and hippuric acid inhibited the uptake by the renal uptake transporter OAT3 [64]. The impact of uremic toxins on the functionality of multiple transporters in those reports, and the inhibition of enzyme activity described in this study, indicate that the altered drug disposition observed in CKD patients can be attributed, at least in part, to uremic retention solutes.

In the present study, renal glucuronidation was solely studied *in vitro* using the ciPTEC model, which could differ from *in vivo* metabolism. Generally, UGT activity is studied using microsomes isolated from the organ of interest; however, by using a complete cell model instead of microsomes, we were able to unravel the possible mechanism via which uremic toxins indirectly influence UGT functionality. Moreover, it is known that there are species differences in renal glucuronidation [227], which did not hamper our study since ciPTEC are of human origin. Another possible drawback of the present study is that we studied renal metabolism, while during CKD, xenobiotics are metabolized mainly in the liver and intestine. However, it is known that both renal and non-renal clearance are affected in CKD patients [48], therefore we postulate that our results uncovered a general mechanism via which uremic toxins can diminish both renal and non-renal UGT activity, irrespective of the tissue-specific UGT expression profiles [205].

A main feature of CKD is the dysfunction of multiple organs and alterations in xenobiotic elimination pathways, however, the pathophysiological mechanism underlying these changes are not fully elucidated. In this study we demonstrated that a wide variety of uremic toxins, belonging to several physico-chemical classes, inhibited renal glucuronidation, most likely by reducing the reserve capacity of the energy-generating OXPHOS system. Our results provide additional insight into the widespread toxic effect of uremic solutes and depict a novel pathway via which uremic toxins impede renal metabolic function and may have a clinically significant impact on drug disposition in patients with CKD.

ACKNOWLEDGEMENTS

This work was funded by the Dutch Kidney Foundation (grant number IK08.03). M.J.G. Wilmer was supported by a grant from the Dutch government to the Netherlands Institute for Regenerative Medicine (NIRM, grant No. FES0908) and J. Jansen received funding from the BioMedical Materials institute (Project P3.01 BioKid), co-funded by the Dutch Ministry of Economic Affairs, Agriculture and Innovation. J.G. Hoenderop was supported by an EURYI award from the European Science Foundation. The authors would like to thank A. Bilos for excellent technical support regarding the HPLC measurements. In addition, we thank A.E.M. Seegers for assisting in the experimental work.

Supplementary data

Supporting information is available online at www.journals.elsevier.com/bba-molecular-basis-of-disease.

7

General Discussion

In part published as:
The kidney and uremic toxin removal: glomerulus or tubule?

Rosalinde Masereeuw, Henricus A.M. Mutsaers, Takafumi Toyohara, Takaaki Abe, Sachin Jhawar, Douglas H. Sweet and Jerome Lowenstein

Seminars in Nephrology, Volume: 34, Issue: 2, Page: 191-208, 2014

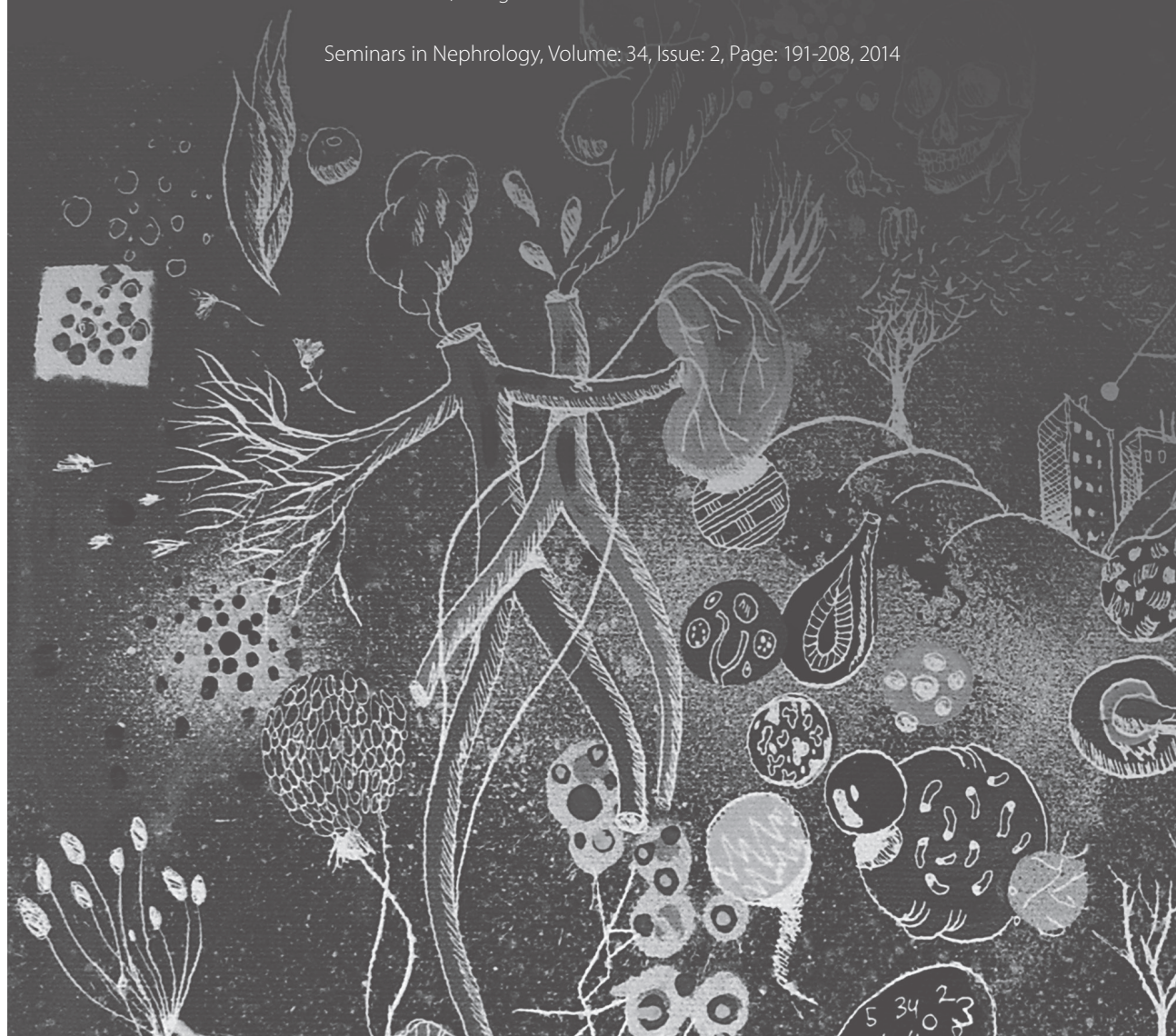

The kidney is essential for the clearance of diverse xenobiotics and endogenous metabolic waste products from the systemic circulation [18]. To facilitate this process, the kidney is equipped with filter units, the glomeruli, and a broad array of transport proteins located in the tubular system, that work in concert to remove waste and potential harmful elements from the body [18]. Mitigation of physiological functioning of the kidney, as is the case in patients with chronic kidney disease (CKD), will result in the retention of solutes that are normally excreted into the urine by the healthy kidney [21]. These uremic retention solutes elicit a myriad of toxic effects and may contribute to renal disease progression and the development of comorbidities associated with CKD, including cardio-vascular disease [135,194]. In this thesis, we strived to gain more insight into the broad expanse of solutes retained in CKD patients during different stages of the disease, as well as the nephrotoxic effect of a multitude of both known and hitherto unknown uremic retention solutes.

Methods to determine uremic solute levels

Over the years many uremic toxins have been studied using targeted analytical approaches including enzyme-linked immunosorbent assay (ELISA) and high-performance liquid chromatography (HPLC) [21]. Recently, there has been a surge in the number of compounds identified as uremic solutes due to the widespread use of untargeted techniques such as metabolomics and proteomic profiling [22,90,95,96,122]. Targeted techniques solely measure defined compounds, whereas untargeted approaches provide a comprehensive overview of all the metabolites in a biological sample without prior identification. In this thesis, both targeted techniques, *i.e.* HPLC and liquid chromatography-tandem mass spectrometry (LC-MS/MS; **Chapters 3-5**) and ^{1}H-nuclear magnetic resonance (NMR) spectroscopy (**Chapter 2**), an untargeted approach, were applied to study the accumulation of uremic solutes in different stages of CKD. Using these analytical techniques we have successfully investigated to which extent uremic solutes accumulated in non-dialysis CKD patients in addition to patients treated with either hemodialysis or continuous ambulatory peritoneal dialysis. However, precise determination of uremic solute concentrations is cumbersome and fraught with technical difficulties due to the physico-chemical characteristics of these compounds, including binding to plasma proteins. Therefore, it is essential to have a clear understanding of the pros and cons of each analytical approach before setting out to study the uremic metabolome. ^{1}H-NMR spectroscopy makes use of the magnetic properties of hydrogen atoms present in molecules to obtain information regarding the chemical properties, including structure, of organic compounds. For a detailed description of NMR spectroscopy the interested reader is referred to the NMR handbook by Engelke *et al.* [228] (freely available from www.bodyfluidnmr.nl). As stated above, NMR is an untargeted approach, indicating that advance knowledge of the metabolic status is not required, and the technique is used to obtain an overview of the metabolome of individuals. This makes NMR an extremely valuable tool in finding novel uremic solutes and potential CKD biomarkers. Moreover,

every metabolite has a specific fingerprint, *i.e.* NMR spectrum, allowing for precise identification of solutes. The identity of metabolites can be gleaned from previously recorded spectra or authentic compounds used as reference standard. However, NMR has a limited sensitivity with detection limits in the micromolar range. In addition, quantification of metabolite concentrations is based upon an internal standard that is added to the sample before spectroscopy, in our case trimethylsilyl-2,2,3,3-tetradeuteropropionic acid (TSP), therefore, NMR is semi-quantitative. For this thesis, both HPLC and LC-MS/MS were used as targeted approaches, even though LC-MS/MS may also be used for untargeted metabolomic studies. For targeted analysis of metabolites, prior knowledge regarding the compound of interest is a prerequisite and before each measurement the instruments need to be prepped to allow for proper detection and quantification of specific metabolites. During chromatography, constituents of a mixture are separated - and in the case of HPLC, identified - based on chemical properties such as size and charge. For this purpose, there are many variables that can be adjusted, including the mobile phase (*i.e.* eluent), separation column and detector (*e.g.* UV or fluorescence), to cater to the needs of each compound of interest. However, separation of highly similar molecules remains difficult and as a result HPLC is less specific with regard to metabolite identification. This limitation can be overcome by the addition of mass spectrometry. During LC-MS/MS analysis, metabolites are identified using both the mass-to-charge ratio (*m/z*) and compound fragmentation, *i.e.* selected reaction monitoring (SRM) transitions, making LC-MS/MS very precise. In addition, for both HPLC and LC-MS/MS, quantification is performed using a calibration curve and both techniques have detection limits in the nano- or picomolar range. Yet, detection limits can vary widely, depending on which metabolite is studied. Taken together, there is a broad assortment of analytical tools that can be used to identify and quantify uremic solutes and each technique has its own merits, therefore, it is key to select the appropriate technique fitting to the avenue of research. An overview of the assets and drawbacks of the analytical techniques used for this thesis are provided in Tabel 1.

Classification of uremic solutes

Uremic retention solutes are a heterogeneous group of molecules that, at present, are divided into three groups based on their physico-chemical properties affecting their elimination pattern during dialysis or other extracorporeal removal strategies [23]. The currently defined classes encompass (1) small water-soluble compounds (≤500 Da) that readily pass dialysis membranes; (2) middle molecules (>500 Da) for which filtration is limited due to their size; and (3) protein-bound solutes, which are very difficult to clear using current dialysis modalities. Interestingly, many uremic solutes arise from similar sources and an alternative classification has been proposed based on the source of origin, namely, endogenous metabolism (*e.g.* asymmetric dimethylarginine), microbial metabolism (*e.g. p*-cresyl sulfate) and exogenous intake (*e.g.* oxalate) [93]. This classification

Table 1 Characteristics of analytical tools used to detect uremic solutes in body fluids

	Proton NMR	HPLC	LC-MS/MS
Approach	Untargeted	Targeted	Targeted*
Detection limit	Micromolar	Nanomolar	Picomolar
Identification	Chemical shift (++)	Chromatogram (+)	*m/z*, SRM transition (++)
Quantification	TSP reference	Calibration curve	Calibration curve

*LC-MS/MS can also be used for untargeted studies.
Specificity (*i.e.* correct metabolite identification) + ambiguous, ++ unequivocal.
m/z, mass-to-charge ratio; SRM, selected reaction monitoring;
TSP, trimethylsilyl-2,2,3,3-tetradeuteropropionic acid.

provides information about potential therapeutic targets other than dialysis. The uremic solutes scrutinized in **Chapters 2-4** mostly fit in the origin-based categories described above. Yet, using NMR-spectroscopy the previously unknown uremic solute 2-hydroxy-isobutyric acid (2-HIBA; **Chapter 2**) was identified, which defies classification in the currently defined groups. 2-HIBA is constitutively present in human urine and serum [113,114], and it is the major urinary metabolite in humans following exposure to the gasoline additives methyl *tert*-butyl ether and ethyl *tert*-butyl ether [115,116]. Inhalation is the major route of exposure to both oxygenates and is highest in industrialized countries. Although it is widely accepted that there is a link between occupational exposure to toxic molecules, including heavy metals and industrial solvents [229], and the development of kidney disease, little information is available regarding exposure to common air pollutants, such as exhaust fumes, and CKD. Recently, Qin *et al.* reported that inhalation exposure to a mixture of gasoline, dimethylbenzene and formaldehyde induced severe proximal tubular damage in rats [230]. Furthermore, it was demonstrated in rats that diesel exhaust particles enhanced cisplatin-induced acute renal failure [231]. Thus, inhaled substances may have a deleterious effect on the kidney and it is interesting to speculate that the air that we breathe is also a potential source of uremic toxins. Therefore, we would like to postulate that, next to the three previously described origin-based categories of uremic solutes, there is a fourth class namely compounds originating from air pollutants and, to the best of our knowledge, 2-HIBA is the first described uremic solute belonging to this group.

On the origin of uremic solutes (Eat Me, Drink Me)

Many of the well-studied uremic toxins originate from the diet and are generated in the colon due to putrefaction, *i.e.* protein fermentation, by intestinal bacteria including *Escherichia Coli* and anaerobes from the genera *Lactobacillus, Enterobacter* and *Clostridium*

[93,232]. Breakdown of tyrosine and phenylalanine results in the formation of phenylacetic acid, phenol and *p*-cresol, which is subsequently metabolized into *p*-cresyl sulfate and *p*-cresyl glucuronide [30,93]. On the other hand, bacterial metabolism of tryptophan results in the formation of indole, which can give rise to a myriad of indolic uremic solutes, including indoxyl sulfate and indole-3-acetic acid [93,125]. To glean information about the interplay between dietary protein and uremic solutes, we examined the impact of a high protein diet on the plasma concentration of a variety of uremic toxins. To this end, wild type (WT) Friend leukemia virus B (FVB) mice were provided either a control (21% crude protein; n = 10) diet or a high protein (HP; 45% crude protein; n = 10) diet for 21 days. Mice fed the HP diet showed significantly higher plasma levels of the phenol-derived metabolites phenylacetic acid (1.9 ± 0.3 μM), phenyl sulfate (3.9 ± 0.8 μM), phenyl glucuronide (0.20 ± 0.05 μM), *p*-cresyl glucuronide (1.6 ± 0.3 μM) and hippuric acid (0.10 ± 0.01 μM) compared to mice provided with control diet (1.1 ± 0.1 μM, 1.4 ± 0.3 μM, 0.03 ± 0.007 μM, 0.7 ± 0.1 μM and 0.040 ± 0.008 μM, respectively; Figure 1A). In addition, a reduction in tryptophan concentration (HP: 93 ± 11 μM vs. Control: 127 ± 5 μM; Figure 1B) was observed as well as an 1.2 fold increase in indoleamine 2,3-dioxygenase (IDO) activity (p = 0.0389; Figure 1C). Furthermore, in mice fed the HP diet, indoxyl sulfate levels significantly increased from 3.6 ± 0.7 μM (Control) to 7 ± 2 μM. In contrast, *p*-cresyl sulfate and kynurenic acid levels remained unaltered, and kynurenine and indole-3-acetic acid concentrations diminished. Taken together, a HP diet alters the metabolic status of mice consonant with changes observed in CKD patients [90,233]. In addition, mice on the HP diet developed significant polyuria (HP: 0.8 ± 0.2 mL/18 h vs. control: 0.30 ± 0.04 mL/18 h; Figure 1C), implying the presence of renal failure [234]. Therefore, it is important to manage the levels of dietary protein intake in CKD patients, since high protein intake will augment uremic toxin levels, whereas a restriction in dietary protein might cause protein-energy wasting [235]. One can see that dietary management, hampering colonic uptake and/or formation of uremic solutes and even engineering new food products might be extremely valuable tools to combat uremic illness.

Efflux transporters involved in uremic toxin clearance

Next to reducing uptake and formation of uremic solutes, CKD treatment can gain ground by understanding and harnessing the capacity of efflux transporter to clear uremic solutes from the circulation. As delineated in **Chapter 1**, renal proximal tubule cells are well outfitted with a multitude of specialized transporters each mainly dealing with a specific set of substrates (*e.g.* anions or cations). In the last decades, small steps have been made in unraveling the contribution of uptake transporters in the extrusion of uremic solutes, whereas the identity of efflux transporters tasked with uremic solute clearance remained a mystery... until now. In **Chapters 3-4**, we observed that several uremic solutes, *e.g.* indoxyl sulfate, hippuric acid and *p*-cresyl sulfate, inhibited transport mediated by the apically expressed transporters MRP4 and BCRP. And for most toxins, the calculated Ki

values were below the reported maximal plasma concentrations, indicating that the tested uremic solutes impede kidney excretory function and can promote uremic toxin accumulation which may subsequently contribute to the progression of CKD. However, these studies did not confirm whether the toxins are also substrates for MRP4 and BCRP. In a follow-up study, using membrane vesicles isolated from HEK293 overexpressing either MRP4 or BCRP, we demonstrated that kynurenic acid is indeed actively transported by both pumps (**Chapter 5** and Dankers *et al.* unpublished data). Moreover, as described in **Chapter 5**, LC-MS/MS analysis revealed that kynurenic acid levels are significantly elevated in the plasma of Mrp4 and Bcrp knockout mice, correlating loss of efflux transporter function with decreased uremic solute elimination. These findings provide essential information regarding the processes of renal uremic toxin handling, which might aid in developing novel therapeutic approaches to limit cellular toxicity and possibly mitigate CKD progression.

Intracellular fate of uremic solutes

Following transport across the plasma membrane, there are a multitude of intracellular targets that uremic solutes can affect to elicit biochemical and toxic responses, including the aryl hydrocarbon receptor (AhR), mitochondria and metabolizing enzymes. The AhR is a major transcription factor belonging to the superfamily of basic helix-loop-helix DNA binding proteins [236]. The inactive form is present in the cytosol as a multiprotein complex with the chaperones heat shock protein (Hsp)90, p23 and hepatitis B virus X-associated protein 2 (XAP2). Upon ligand binding, the AhR translocates to the nucleus where it forms a complex with AhR nuclear translocator (ARNT) which then binds to dioxin-responsive elements resulting in gene transcription. To this date, most of the known AhR-ligands are exogenous chemicals such as the environmental pollutant 2,3,7,8-tetrachlorodibenzo-*p*-dioxin (TCDD), yet, an increasing number of endogenous metabolites have recently been identified as AhR agonists, including bilirubin [237,238]. Interestingly, several of these compounds are also well-known uremic retention solutes. At present, kynurenine, kynurenic acid, indole-3-acetic acid and indoxyl sulfate – all indolic products of tryptophan metabolism – have been demonstrated to bind to the AhR or induce the expression of AhR response genes, such as CYP1A1 [186-188,239-241]. Moreover, as depicted in Table 2, all four metabolites activate the AhR at concentrations either similar to the highest maximal plasma concentrations (C_{max}) determined in dialysis patients (e.g indole-3-acetic acid) or at levels decisively lower than the C_{max}, for instance indoxyl sulfate. As of yet, the clinical implications of AhR activation in the setting of CKD development and progression remain unclear, however, it has been postulated that uremic solutes might evoke 'dioxin-like' toxicity [240] leading to suppression of immune responses, induction of carcinogenesis and accelerating tumor growth, and promoting atherosclerosis [240,242-244].

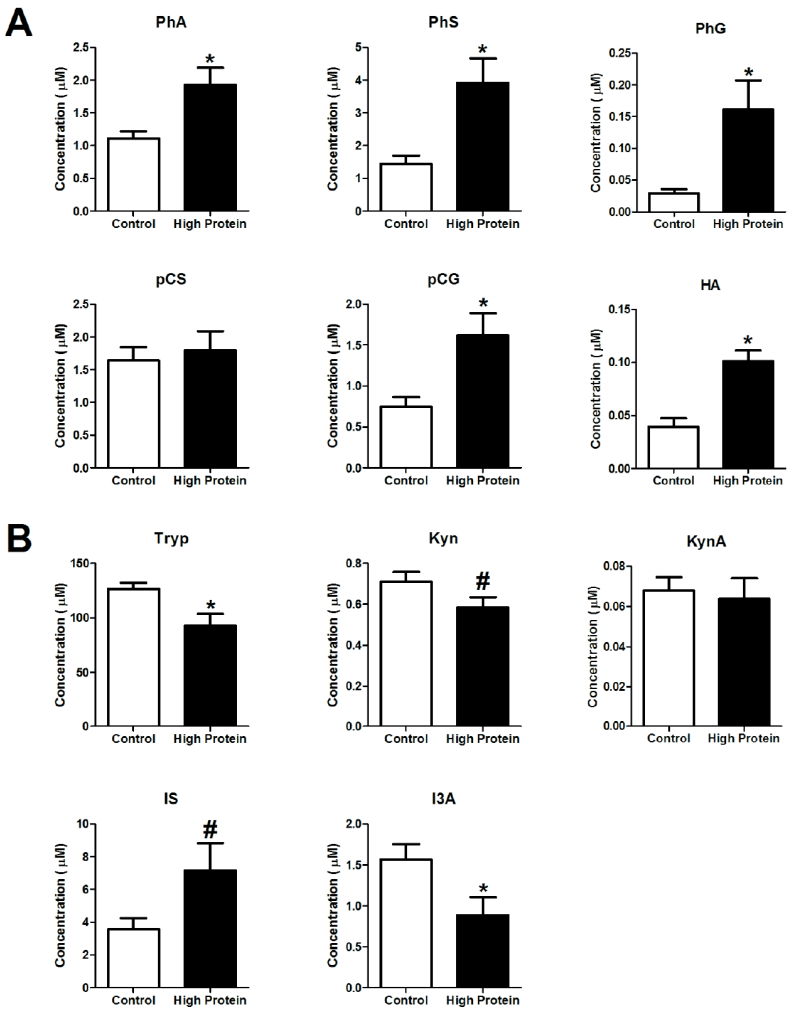

Figure 1 General characteristic and serum biochemistry of experimental groups.

Mice were fed either control diet (white bars) or high protein diet (black bars) for 21 days. Plasma was collected at day 22 and, using LC-MS/MS, uremic toxin levels from different classes were determined: **(A)** phenolic compounds and **(B)** tryptophan and metabolites. **(C)** Urine flow was determined after a 18 h-period in metabolic cages at day 22. Statistical analysis was performed via an unpaired t test. Bars represent mean ± SEM of 10 mice per group. * indicates $p < 0.05$ compared to control (two-tailed), # indicates $p < 0.05$ compared to control (one-tailed). HA, hippuric acid; I3A, indole-3-acetic acid; IDO, indoleamine 2,3-dioxygenase; IS, indoxyl sulfate; Kyn, kynurenine; KynA, kynurenic acid; pCG, p-cresyl glucuronide; pCS, p-cresyl sulfate; PhA, phenylacetic acid; PhS, phenyl sulfate; PhG, phenyl glucuronide; Tryp, tryptophan.

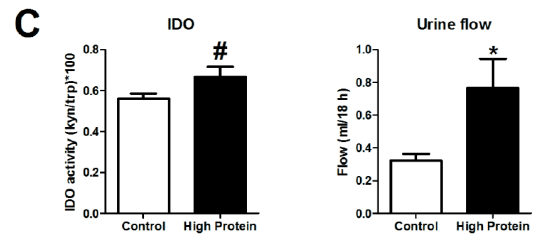

Figure 1 Continued.

It is well-documented that several uremic toxins can induce apoptosis in a variety of cell types, such as smooth muscle cells, neutrophils and proximal tubule cells [153,245-247]. However, only a few studies report a direct effect of uremic solutes on cell metabolism, including mitochondrial functioning. Mitochondria are best known for the production of ATP, the main source of cellular energy, via the oxidative phosphorylation (OXPHOS) system [248]. Next to their role in providing energy, mitochondria are also involved in other important cellular processes including ion homeostasis, production of reactive oxygen species and apoptosis [249-251]. As reported in **Chapter 6** a myriad of uremic solutes decreased mitochondrial complex II (*i.e.* succinate dehydrogenase) activity in ciPTEC as shown by the MTT-assay. Especially, indole-3-acetic acid had a pronounced negative impact on MTT reduction, and high-resolution respirometry revealed that this solute diminished the maximum capacity of the electron transport system, signifying a reduction in the reserve capacity of the OXPHOS system (**Chapter 6**). In addition, Owada and coworkers demonstrated that indoxyl sulfate increases the production of superoxide and hydroxyl radicals in rat kidney mitochondria [217], and Dzurik *et al.*, reported that hippuric acid reduces ammonia production by P-dependent mitochondrial glutaminase in kidney homogenates from rats, thereby shifting ammonia production from mitochondria to the lumen of proximal tubules [218]. Also, a reduced functioning of hepatic mitochondria following exposure to dialysate and *p*-cresol have been reported previously [219,220]. These findings indicate that uremic toxins can cause mitochondrial dysfunction which is detrimental to normal cellular functioning.

CKD is characterized by changes in drug disposition partially due to a reduction in glomerular filtration and active tubular secretion of xenobiotics, as well as mediated by a direct effect of uremic toxins on the expression level and activity of drug metabolism enzymes [48,49]. Most studies on the interaction between CKD and drug metabolism have focused on hepatic CYP expression and activity. Leblond *et al*, reported a reduction in CYP2C11, 3A1 and 3A2 expression, both on gene and protein level, in CRF rats which associated with a reduction in erythromycin and aminopyrine metabolism [223,224]. Also

in CKD patients mitigation of CYP-mediated drug metabolism is demonstrated [252,253], including changes in bupropion, alprazolam and fexofenadine pharmacokinetics [254-256]. Moreover, it has been demonstrated both *in vitro* and *in vivo* that hemodialysis improves functional expression of hepatic CYP3A4 [257,258], implicating a role for uremic toxins in altering drug metabolism in CKD patients. This notion is supported by the study from Sun *et* al., showing that indoxyl sulfate and CMPF reduced erythromycin metabolism by CYP3A in rat liver microsomes [226]. In addition, CYP-mediated losartan metabolism can be inhibited by indoxyl sulfate, as demonstrated in human liver microsomes [259]. Furthermore, protein expression of CYP1A decreased in proximal tubule (*i.e.* HK-2) cells treated with serum from CRF rats, whereas CYP3A expression was unaffected [225]. With regard to phase II metabolism, it is shown that the pharmacokinetics of multiple drugs that are completely dependent on phase II enzymes for their clearance are changed in patients with CKD. For instance, acetylation of isoniazid is decreased as well as the glucuronidation of morphine, *p*-aminobenzoic acid and metoclopramide [198,200-202]. Only a few studies investigated the direct effect of uremic toxins on phase II enzymes. Using primary rat hepatocytes, Simard *et al.*, demonstrated that exposure of the cells to clinical relevant concentrations of parathyroid hormone results in a reduced gene and protein expression of N-acetyltransferase 2 [197]. Moreover, they observed a diminished N-acetylation of *p*-aminobenzoic acid in 5/6-nephrectomized rats [197]. In addition, we reported in **Chapter 6** that over ten different uremic toxins, including indoxyl sulfate, kynurenic acid and phenylacetic acid, diminished UDP-glucuronosyltransferase activity in ciPTEC, as demonstrated by a reduction in glucuronidation of 7-hydroxycoumarin.

Renal fibrosis is an integral process in the development and progression of CKD [260]. Moreover, it is a key event contributing to renal graft failure. The pathophysiological mechanism underlying renal fibrosis remains unclear and in recent years epithelial-to-mesenchymal transition (EMT) has emerged as a leading, yet highly debated, hypothesis for the origin of collagenous matrix-producing myofibroblasts which contribute to organ fibrosis [261,262]. EMT is a biologic process well known in embryogenesis. During early development, the epiblast gives rise to the primary mesenchyme via EMT which in turn further develops into secondary epithelia, this type of EMT is classified as type 1[263]. Type 3 EMT is involved in carcinogenesis, more specifically in the acquisition of an invasive phenotype by cancer cells [263]. The transition of adult epithelial cells to fibroblasts following injury is called type 2 EMT, which is postulated to be involved in the development of tissue fibrosis [263]. Although the role of EMT in fibrogenesis is controversial, markers that demonstrate the loss of epithelial cell characteristics in the kidney, *viz.* increased expression of vimentin and the translocation of β-catenin into the cytoplasm, could be used to study nephrotoxicity. Of note, vimentin was reported to be a good marker of proximal tubule damage in rats [264]. Moreover, indoxyl sulfate is reported to be capable of inducing EMT in renal cell models from different species, such as murine PKSV-PRs, rat NRK-52E cells and human HK-2 cells [41,153,265]. These findings are in line with the results

Table 2 Uremic solutes that activate the aryl hydrocarbon receptor

Name	Chemical structure	AhR activation	C_{max} (μM)	References
Kynurenine	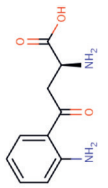	36.6 μM (EC_{50}, DRE–luciferase activity)[B] 12.3 μM (EC_{50}, EROD assay)[D] 4 μM (K_d, Radioligand binding assay)	5	[186]
Kynurenic acid	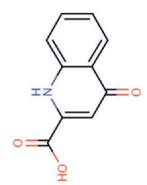	104 nM (EC_{25}, DRE–luciferase activity)[B]	50	[239]
Indoxyl sulfate	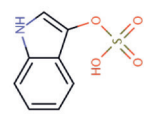	1 mM (Microarray)[A] 500 μM (CYP1A1 gene expression)[C] 100 nM (CYP1A1 gene expression) 12.1 nM (EC_{50}, DRE–luciferase activity)[B]	940	[240] [188] [241] [187]
Indole-3-acetic acid	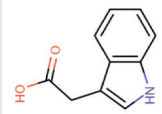	50 μM (Microarray)[A]	52	[240]

Maximal uremic concentrations (C_{max}) were obtained from www.uremic-toxing.org and chemical structures were obtained from the Human Metabolome Database (www.hmdb.ca). Experiments were performed in the presence of either [A]2% (v/v), [B]8% (v/v), [C]10% (v/v) or [D]20% (v/v) Fetal Bovine Serum.

described in **Chapters 2 and 4**, showing that the uremic solutes $DMSO_2$, 2-HIBA and *p*-cresyl glucuronide increased vimentin expression and altered functionality of ciPTEC, suggesting a phenotypic transition. EMT can also be induced via an indirect pathway involving the induction of endoplasmic reticulum (ER) stress [266]. Several known nephrotoxicants have been demonstrated to induce ER stress, including cadmium, cisplatin and cyclosporine A [267]. More interestingly, it is also reported that indoxyl sulfate can induce ER stress [268]. Thus, there is some evidence that uremic retention solutes initiate or directly contribute to renal fibrosis by means of EMT and ER stress. And the implementation of new experimental models, such as precision-cut tissue slices [269], will hopefully aid in unraveling the pathophysiological mechanism of CKD-associated renal fibrosis. Taken together, it is clear that uremic solutes can affect diverse intracellular targets and (patho) physiological processes thereby hampering cellular functioning, illustrating the complex nature of uremic toxicity.

Use of uremic solute levels as biomarkers for CKD

The glomerular filtration rate (GFR) is regarded as the best indicator for kidney function and is widely used to classify renal failure, however, direct measurement of this index is difficult to achieve [270,271]. Therefore, serum creatinine (SCr) is generally used as an estimate for GFR. Unfortunately, changes in SCr are insensitive to detect injury, since a relative large amount of injury can occur without affecting GFR, especially in patients with a renal reserve or during unilateral renal dysfunction [270,271]. Furthermore, GFR can drop with 50% before SCr levels increase [270,271]. The limitations of SCr as a marker for kidney failure is further supported by the fact that SCr concentrations do not only depend on GFR, but also on tubular secretion and systemic production of creatinine, which is for instance affected by muscle wasting [270]. Thus, SCr is subjected to high interindividual variability and is not suitable for early and site-specific detection of kidney injury. Reasoning from the notion that (1) CKD is synonymous with uremic retention solutes and (2) a number of studies, including the research described in **Chapters 2-4**, have demonstrated that plasma levels of multiple uremic toxins, *e.g.* indole-3-acetic acid, hippuric acid and indoxyl sulfate, are significantly elevated in non-dialysis CKD patients [96,272], we investigated in a preliminary study whether uremic toxins levels may predict the rate of eGFR decrease in CKD patients. To this end, we determined baseline concentrations of several uremic toxins, using HPLC and LC-MS/MS, in serum samples of patients that participated in the MASTERPLAN trial [273]. Cases were rapid progressors, *i.e.* patients with decline of eGFR > -4.5 ml/min/1.73m^2/year, and as controls we selected patients with a lower rate of progression matched for baseline eGFR. In total, 27 cases and 65 controls were included, of whom 43 were slow progressors (decline 4.5 to 1.0 ml/min/1.73m^2/year) and 22 stable patients (decline < 1 ml/min/1.73m^2/year). Mean age in the selected patients was 59 ± 13 years and 67% was male. Most patients had moderate CKD with a mean eGFR of 37 ± 12 ml/min/1.73m^2 and received blood pressure lowering drugs (96%), and ACE inhibitors and/or angiotensin II receptor blockers (82%). Rapid progressors were more likely to be male, younger and have polycystic kidney disease; had higher blood pressure and proteinuria, and lower serum albumin and bicarbonate levels. Correlations between uremic toxin concentration and eGFR ranged between -0.58 to 0.07. Uremic toxins correlated poorly with other known risk factors. None of the uremic toxins were significantly associated to eGFR decline in neither univariate nor multivariate linear regression analysis. Figure 2 shows regression coefficients and 95% confidence intervals for the association between uremic toxins and the rate of eGFR decline adjusted for baseline eGFR, proteinuria, blood pressure, age and gender. In conclusion, baseline serum uremic toxin concentrations are not associated with eGFR decline in CKD patients (van den Brand *et al.*, unpublished data). Taken together, uremic toxins could possibly be useful biomarkers to detect tubular (and possibly glomerular) damage, however, they seem to be poor predictors of disease progression. Nevertheless, more research is needed to elucidate their full biomarker potential.

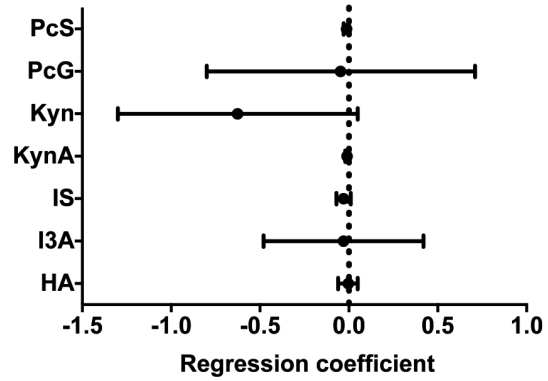

Figure 2 Absence of an association between baseline uremic toxin levels and eGFR decrease.

A multiple adjusted linear regression analysis between uremic toxin concentration and change in eGFR was created. The model included baseline eGFR, proteinuria, blood pressure, age and gender. Dots represent regression coefficient (*i.e.* eGFR decline per unit of the solute) with the 95% confidence interval. HA, hippuric acid; I3A, indole-3-acetic acid; IS, indoxyl sulfate; Kyn, kynurenine; KynA, kynurenic acid; pCG, p-cresyl glucuronide; pCS, p-cresyl sulfate.

Future perspectives

The findings described in this thesis have expanded our knowledge on the number of solutes retained in patients with a reduced kidney function. Furthermore, we have demonstrated the important role that the efflux transporters MRP4 and BCRP play in the

renal handling of uremic solutes, and we demonstrated that inactivity of these ABC-transporters directly results in accumulation of several potential toxic metabolites. In addition, the nephrotoxic actions of multiple uremic retention solutes were elucidated using a unique proximal tubular cell model, identifying diverse targets affected by these compounds, including mitochondria, drug metabolism enzymes and transporters. Since dialysis is inapt in removing uremic solutes from the circulation, harnessing the ability of transporters to clear these metabolites might prove to be the long coveted therapeutic modality needed to improve clinical outcomes for CKD patients. Recently, Toyohara and coworkers demonstrated that statins could be used to increase the expression of OATP4C1 and improve renal uremic toxin clearance [60]. However, 'therapeutic manipulation' of transporters, while intriguing, should be approached with caution. It is conceivable that upregulation of uptake transporter expression might ensue improved uremic toxin clearance. Yet, it could also result in increased renal proximal tubule cell death from toxic exposure. Therefore, it is key to simultaneously target both basolateral and apically expressed transporters in order to maintain the perfect, and delicate, balance between cellular uptake and efflux. An alternative might be employing "living dialysis membranes" consisting of bioreactors containing stem cell derived, and possibly patient specific, transporter-expressing cells to better mimic normal renal function and improve therapy efficacy. In our lab, first steps have been undertaken to realize a bio-artificial kidney (BioKid) device using a unique and stable proximal tubule cell model, *i.e.* ciPTEC. This cell line has been established from cells exfoliated in the urine from a healthy volunteer. ciPTEC have been demonstrated to maintain proximal tubular characteristics, including expression of important in- and efflux transporters as well as megalin-mediated albumin uptake and sodium-dependent phosphate transport, over a prolonged period of cell culturing [98]. Moreover, ciPTEC can be used to study nephrotoxicity as shown by their sensitivity to gentamicin [101], and OCT-mediated organic cation transport [78]. Moreover, using a similar immortalization approach, our group was able to create ciPTEC from renal tissue (ciPTEC-T; Jansen *et al.*, unpublished data). This novel model showed an analogous expression and activity profile as compared to ciPTEC. Of note, ciPTEC-T appeared to have retained the ability to create their own extracellular matrix, illustrated by increased gene expression levels of collagen I and –IV α1. Unfortunately, both ciPTEC and ciPTEC-T lack the important influx transporters OAT1 and OAT3 on gene, protein and functional level. Clearly, there is still much ground for the transporter field to cover, but the very fact that BioKid concepts are being discussed and practically achievable [274], foreshadows some exciting times to come.

Progress can also be made in reducing the exogenous intake of uremic toxins as well as the diminishing the production of uremic solutes by the intestinal flora. Aronov *et al.* recently reported that in plasma of dialysis patients without a colon several uremic toxins were absent or present at lower concentrations compared to patients with a colon [92]. This finding underlines the notion that the gut is an important therapeutic target to

reduce uremic retention solute levels. AST-120, an oral charcoal adsorbent, has been demonstrated to reduce plasma levels of uremic solutes, including *p*-cresyl sufate, indoxyl sulfate and hippuric acid [275], and is suggested to reduce a number of comorbidities associated with CKD such as atherosclerosis [276-279]. However, the beneficial impact of AST-120 still needs to be studied in large clinical trials. Other potential suppressive therapies include dietary and probiotic treatments. Several small intervention studies (n<30) have demonstrated that preparations with lactic acid bacilli and *Bifidobacterium longum* reduce serum levels of indoxyl sulfate with 9-30% [93,280-282]. Yet, studies on the impact of probiotics on hard clinical end points (*e.g.* mortality) in CKD patients have not been performed to date.

Finally, there is much attention for the risk that CKD possess for cardiovascular mortality and morbidity [283], yet little effort is made to elucidate the kidney-brain axis [284]. Several known uremic toxins, *e.g.* kynurenic acid and quinolinic acid, have neuroactive properties and can modulate the activity of important receptors in the brain, including the α7-nicotinic-acetylcholine (α7nAch)- and the *N*-methyl-D-aspartate (NMDA) receptor. Recently, we demonstrated that kynurenic acid concentration-dependently increased glucose uptake by malignant neuroblastoma (N2a) cells, and we unveiled a link between BCRP and kynurenic acid transport with brain energy metabolism, indicating that the efflux pump is an interesting therapeutic target to modulate cerebral glucose and kynurenic acid levels (Dankers *et al.* unpublished data). This exciting observation warrants further investigation into uremic toxin-induced neuronal dysfunction as well as CKD-associated cognitive impairment and neuropathy.

The results within this thesis expanded the currently known universe of uremic solutes by implementing and improving both targeted and untargeted analytical techniques. Furthermore, a multitude of uremic solutes, irrespective of the source of origin, were demonstrated to negatively influence numerous physiological processes and phenotypic characteristics that define the healthy renal proximal tubule cell. Moreover, we shed a light on the essential role of efflux transporters in the renal extrusion of uremic solutes, laying the foundation for future studies aiming to utilize these pumps to suppress or halt CKD progression and associated pathologies.

8

Summary & Samenvatting

SUMMARY

A hallmark of chronic kidney disease (CKD) is the retention and subsequent accumulation of a myriad of chemically diverse metabolites that are normally cleared by the healthy kidney. These uremic retention solutes likely contribute to the complex pathophysiology that epitomizes uremic illness. In this thesis we strived to gain more insight on the multitude of uremic retention solutes along with the possible detrimental impact of these solutes on renal proximal tubule cells.

To obtain more knowledge about the multitude of uremic solutes retained during CKD we studied the metabolic status of non-dialysis stage 3-4 CKD patients using non-targeted ^{1}H-nuclear magnetic resonance (NMR) spectroscopy, following three distinct deproteinization strategies (*e.g.* ultrafiltration, protein precipitation via perchloric acid or via acetonitrile extraction). Our results demonstrated that both ultrafiltration and acetonitrile extraction are required as deproteinization methods to obtain a clear metabolome profile. Using this approach we revealed that a total of 14 metabolites accumulated in uremic plasma. Next to confirming the retention of several previously identified uremic toxins, including p-cresyl sulfate, two novel uremic retentions solutes were detected, namely dimethyl sulphone ($DMSO_2$) and 2-hydroxyisobutyric acid (2-HIBA). Furthermore, we showed that exposure of the human renal proximal tubule cell line (ciPTEC) to either $DMSO_2$ or 2-HIBA negatively impacted the epithelial characteristics of the cells, illustrated by an increased expression of the mesenchymal marker vimentin and a loss of glucuronidation activity, without affecting cell viability. These results indicate that NMR is a useful tool in the search for CKD biomarkers and revealed new solutes that may contribute to the progression of renal disease.

The renal proximal tubule is equipped with a multiplicity of transporters involved in the active clearance of endo- and xenobiotics, yet the contribution of this transport system to the secretion of uremic solutes is for a part still unknown. In chapter 3, we studied the interaction between several uremic toxins and two important efflux pumps present at the apical membrane of the proximal tubule, *namely* multidrug resistance protein 4 (MRP4) and breast cancer resistance protein (BCRP). Furthermore, the concentrations of various uremic toxins were determined in plasma of CKD patients, treated with dialysis, via high performance liquid chromatography and liquid chromatography/tandem mass spectrometry. Using membrane vesicles isolated from MRP4- or BCRP-overexpressing human embryonic kidney cells, we demonstrated that hippuric acid, indoxyl sulfate and kynurenic acid inhibited substrate specific uptake by both MRP4 and BCRP, whereas indole-3-acetic acid and phenylacetic acid only reduced transport mediated by MRP4. Moreover, the calculated inhibition constant (Ki) values, *i.e.* the concentration needed to inhibit 50% of the transport activity, are in general lower than the maximal plasma

concentrations of the tested toxins in CKD patients. These results depict that uremic toxins can impede kidney excretory function and subsequently contribute to the accumulation of uremic solutes.

Recently, the two *p*-cresol metabolites, *p*-cresyl sulfate (pCS) and *p*-cresyl glucuronide (pCG), have gained much attention from the scientific community as key uremic toxins, yet how they are handled by the kidney and their nephrotoxic potential remain unknown. In chapter 4, we demonstrated that pCS inhibited both MRP4- and BCRP-mediated transport, whereas pCG solely mitigated transport by MRP4. In addition, exposure of ciPTEC to pCG had a pronounced effect on ciPTEC physiology as illustrated by an increased expression of vimentin, Bcl-2 and BCRP, while the expression of the organic anion transporting polypeptide 4C1 decreased. Of note, pCS did neither influence the protein expression of vimentin nor the gene expression of the studied transporters. Moreover, the biomarkers kidney injury molecule-1 and vanin-1 revealed that both pCS and pCG did not induce tubular damage. These findings indicate that MRP4 and BCRP are likely involved in the renal excretion of both solutes and that the two *p*-cresol conjugates have a different impact on renal proximal tubule cells.

In chapter 5, we tried to unveil whether uremic retention solutes are solely a consequence of CKD or if they can instigate metabolite accumulation. Using the membrane vesicle transport assay, we revealed that the well-known uremic toxin, uric acid, inhibited BCRP-mediated transport at levels also reported in patients with hyperuricemia, as was previously shown for MRP4. In addition, we identified kynurenic acid as a novel substrate for MRP4 and BCRP. Moreover, using mouse models, we demonstrated that Mrp4- and Bcrp-deficiency as well as hyperuricemia, in the absence of renal failure, are associated with alterations in tryptophan metabolism and the retention of the widely biologically active compounds kynurenine and kynurenic acid. These results suggest that elevated uric acid levels impede MRP4 and BCRP functioning, thereby promoting the retention of other potentially harmful substrates, such as kynurenic acid. These findings underline the complex relation between hyperuricemia and its pathologies as well as hinting at the tantalizing notion that uremic solutes, by stimulating metabolite retention, might be one of the culprits in CKD development.

Next to the accumulation of uremic solutes, CKD is also characterized by altered drug metabolism, partially due to a decline in glomerular filtration and tubular secretion. However, the direct impact of uremic solutes on the activity of drug metabolism enzymes is largely unknown. In chapter 6, we describe the interaction between a multiplicity of uremic solutes with an important class of phase II enzymes, namely UDP-glucuronosyl-transferases (UGT), and the mitochondria. Our results demonstrated that a wide variety of uremic toxins, including indole-3-acetic acid, indoxyl sulfate, phenylacetic acid and kynurenic acid, reduced UGT activity, as demonstrated by a diminished glucuronidation of 7-hydroxycoumarin, without affecting UGT1A and UGT2B protein expression. In addition, several uremic toxins inhibited mitochondrial succinate dehydrogenase activity, and indole-3-acetic acid reduced the reserve capacity of the energy-generating oxidative phosphorylation system. These results present a novel pathway *via* which uremic retention solutes affect the metabolic capacity of the kidney and are likely involved in altering drug metabolism during CKD.

Taken together, the results delineated in this thesis have improved our knowledge of the uremic metabolome and the nephrotoxic effects of multiple uremic retention solutes. This body of work provides essential and new insights required to advance our understanding of CKD, and paves the way for future research plus deliver leads for novel therapies.

SAMENVATTING

Chronische nierinsufficiëntie (CKD) wordt gekenmerkt door een verminderde uitscheiding en dientengevolge stapeling van verscheidene metabolieten. Deze zogenoemde uremische toxines leveren hoogstwaarschijnlijk een belangrijke bijdrage aan het complexe ziektebeeld dat typerend is voor het uremisch syndroom. In dit proefschrift streefden wij ernaar om meer inzicht te verkrijgen in de grote verscheidenheid aan uremische toxines en de mogelijke schadelijke invloed van deze stoffen op de cellen van de proximale tubulus.

Om de stapeling van metabolieten tijdens chronische nierinsufficiëntie beter te begrijpen, hebben wij met behulp van proton-nucleair-magnetische resonantie (NMR; of H-1-kern-spinresonantie) spectroscopie de metabole status van stadium 3-4 chronische nierpatiënten bestudeerd. Hiervoor hebben we door middel van ultrafiltratie of door de toevoeging van perchloorzuur of acetonitril het plasma ontdaan van eiwitten. Onze resultaten wijzen uit dat zowel ultrafiltratie als acetonitrilextractie nodig zijn om een compleet metaboliet profiel te verkrijgen. Op deze wijze hebben wij aangetoond dat een totaal van 14 metabolieten stapelen gedurende uremie. Naast het detecteren van al bekende uremische toxines, zoals para-cresolsulfaat, hebben wij twee tot dan toe onbekende uremische toxines kunnen identificeren, te weten dimethylsulfon ($DMSO_2$) en 2-hydroxyisoboterzuur (2-HIBA). Bovendien hebben wij bewezen dat beide stoffen een negatieve invloed hadden op het fenotype en de functionaliteit van de humane proximale tubulus cellijn (ciPTEC), zonder celdood te induceren. Deze resultaten beschrijven dat NMR spectroscopie een zeer nuttige techniek is in de zoektocht naar nieuwe biomarkers van chronische nierinsufficiëntie alsmede in de ontdekking van nieuwe metabolieten die wellicht een bijdrage leveren aan het verslechteren van de nierfunctie.

De proximale tubuluscel van de nier is uitgerust met een breed scala aan transporteiwitten die zorgdragen voor de actieve uitscheiding van zowel lichaamseigen als lichaamsvreemde stoffen in de urine. Toch is het aandeel van de verschillende transporteiwitten in de klaring van uremische toxines nog voor een groot deel onbekend. In hoofdstuk 3 laten we zien dat verscheidene uremische toxines een interactie aangaan met twee belangrijke effluxpompen, MRP4 en BCRP, die normaliter aanwezig zijn op de apicale membraan van de proximale tubulus. Daarnaast hebben we de concentratie van een aantal uremische toxines bepaald in het plasma van dialysepatiënten door middel van vloeistofchromatografie onder hoge druk (HPLC) en een combinatie van vloeistofchromatografie en massaspectrometrie (LC-MS/MS). Door gebruik te maken van membraanvesikels, vervaardigd van cellen die MRP4 of BCRP tot overexpressie brachten, hebben we aangetoond dat hippuurzuur, indoxylsulfaat en kynureninezuur een remmend effect hebben op de activiteit van beide transporters. Daarentegen hadden indool-3-azijnzuur en fenylazijnzuur

alleen een remmende werking op de activiteit van MRP4. Bovendien zagen we dat het verslechteren van de transportfunctie al plaats vond bij concentraties van uremische toxines die te meten zijn in dialysepatiënten. Deze resultaten laten zien dat uremische toxines een direct effect hebben op de pompfunctie van MRP4 en BCRP die nodig is voor het ontgiften van bloed en zodoende een bijdrage kunnen leveren aan de progressieve, steeds ernstigere nierproblemen.

Recentelijk hebben de twee metabolieten van para-cresol, para-cresolsulfaat (pCS) en para-cresolglucuronide (pCG), als prominente spelers in het uremisch syndroom veel aandacht gekregen van de wetenschappelijke gemeenschap. Desondanks is er nog niet veel bekend over de normale renale klaring van beide stoffen en ook de nefrotoxiciteit van pCS en pCG is tot op heden grotendeels onbekend. In hoofdstuk 4 beschrijven we dat pCS de activiteit van MRP4 en BCRP remt, terwijl pCG alleen een remmend effect heeft op MRP4-gemedieerd transport. Daarnaast bleek uit onze experimenten dat pCG een negatief effect had op de epitheliale kenmerken van ciPTEC, aangetoond door een toename in de expressie van vimentine (een eiwit kenmerkend voor fibroblasten maar niet voor epitheliale cellen, zoals ciPTEC), Bcl-2 (een anti-apoptose gen) en de pomp BCRP, en een verminderde expressie van de basolaterale transporteur OATP4C1. Dit in tegenstelling tot pCS, welke geheel geen invloed had op deze karakteristieken van ciPTEC. Voorts werd ook duidelijk dat beide metabolieten van para-cresol geen directe schade veroorzaakten aan ciPTEC. Samengevat suggereren deze bevindingen dat MRP4 en BCRP hoogstwaarschijnlijk betrokken zijn bij de uitscheiding van pCS en pCG in de nier en dat beiden een verschillend effect hebben op het fenotype van proximale tubuluscellen.

In hoofdstuk 5, hebben we bestudeerd of uremische toxines slechts een product zijn van chronische nierinsufficiëntie of dat ze ook de accumulatie van metabolieten kunnen veroorzaken. Urinezuur, een afbraakproduct van purines, is een bekende uremische toxine maar de bloedspiegels van deze metaboliet zijn ook verhoogd in patiënten met hyperuricemie. Middels de eerder beschreven membraan vesikel transport test hebben we laten zien dat urinezuur de transportactiviteit van BCRP kan remmen. Dat gebeurt al bij concentraties die we ook waarnemen in patiënten met hyperuricemie. Hetzelfde is eerder al beschreven voor MRP4. Voorts maakten onze experimenten ook duidelijk dat kynureninezuur een substraat is voor zowel MRP4 als BCRP. Verder hebben we via muismodellen bewezen dat de afwezigheid van MRP4 of BCRP alsook hyperuricemie (in afwezigheid van nierschade) kan leiden tot veranderingen in tryptofaanmetabolisme en de accumulatie van kynurenine plus kynureninezuur. Deze bevindingen lijken erop te duiden dat verhoogde spiegels van urinezuur het functioneren van MRP4 en BCRP belemmert en zodoende de retentie van andere potentieel toxische stoffen, zoals bijvoorbeeld kynureninezuur, bevordert. Verder illustreren deze resultaten de complexe relatie tussen hyperuricemie en daarmee geassocieerde ziektebeelden, en ondersteunen

ze de hypothese dat uremische toxines mogelijk ook een bijdrage kunnen leveren aan het ontstaan van chronische nierinsufficiëntie.

Naast de stapeling van uremische toxines wordt chronische nierinsufficiëntie ook gekenmerkt door veranderingen in het metabolisme van medicijnen. Deels is dit te verklaren door een veranderde enzym expressie in de lever alsmede afname in glomerulaire filtratie en actieve tubulaire secretie. Maar het is goed voor te stellen dat uremische toxines ook een directe bijdrage kunnen leveren aan dit fenomeen, door de functionaliteit van enzymen, welke essentieel zijn voor afbraak van farmaca, te verstoren. Het onderzoek beschreven in hoofdstuk 6 geeft weer dat een veelvoud aan uremische toxines, waaronder indool-3-azijnzuur, indoxylsulfaat en kynureninezuur een remmend effect hebben op de activiteit van UDP-glucuronosyltransferases (UGT), een belangrijke groep van enzymen die fase II reacties, oftewel conjugatiereacties, katalyseren. Dit effect werd waargenomen zonder verandering in de UGT eiwitexpressie, hetgeen suggereert dat uremische toxines UGT activiteit op een indirecte manier beïnvloeden. Daarnaast hadden meerdere uremische toxines een negatief effect op de activiteit van mitochondriaal-succinaatdehydrogenase, en indool-3-azijnzuur verminderde de reservecapaciteit van de oxidatieve fosforylatie, essentiële onderdelen van de cellulaire energiehuishouding. Samengevat belichten deze resultaten een nieuwe wijze waarop uremische toxines het niermetabolisme kunnen ontregelen en op die manier de farmacokinetiek kunnen verstoren in chronische nierpatiënten.

Concluderend draagt dit proefschrift bij aan het uitbreiden van onze kennis betreffende de metabolieten die accumuleren tijdens chronische nierinsufficiëntie en laat het zien op welke wijze uremische toxines schadelijk kunnen zijn voor nierpatiënten. Dit verhoogde inzicht in het uremisch syndroom legt een goede fundering voor toekomstig onderzoek naar chronische nierinsufficiëntie.

References
Curriculum Vitae
List of Publications
Dankwoord

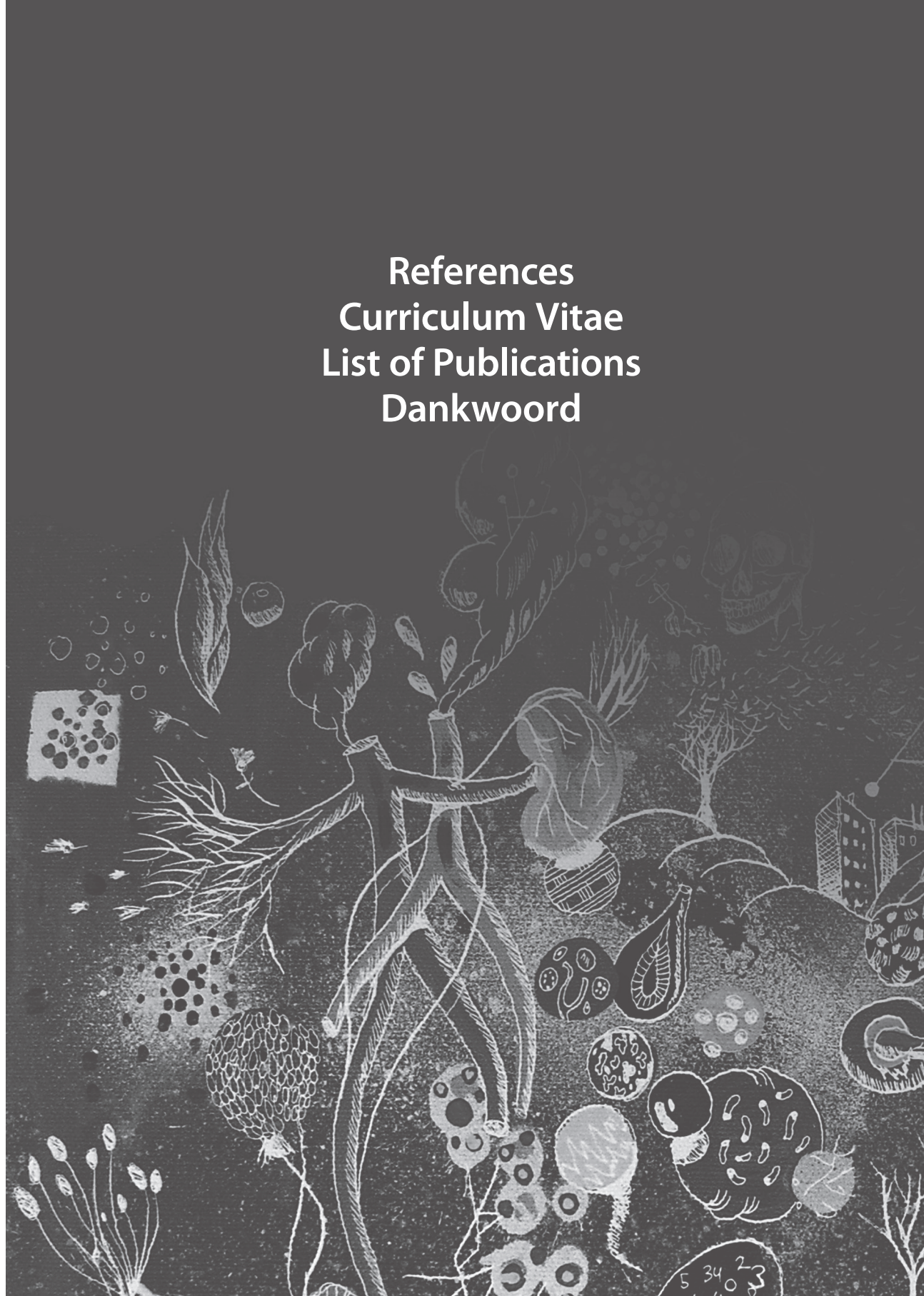

REFERENCES

1. Maio G (1999) The metaphorical and mythical use of the kidney in antiquity. Am J Nephrol 19: 101-106.
2. Salem ME, Eknoyan G (1999) The kidney in ancient Egyptian medicine: where does it stand? Am J Nephrol 19: 140-147.
3. Eknoyan G (2005) The kidneys in the Bible: what happened? J Am Soc Nephrol 16: 3464-3471.
4. Meyer TW, Hostetter TH (2007) Uremia. N Engl J Med 357: 1316-1325.
5. Lopez-Novoa JM, Martinez-Salgado C, Rodriguez-Pena AB, Lopez-Hernandez FJ (2010) Common pathophysiological mechanisms of chronic kidney disease: therapeutic perspectives. Pharmacol Ther 128: 61-81.
6. Barreto FC, Barreto DV, Liabeuf S, Drueke TB, Massy ZA (2009) Effects of uremic toxins on vascular and bone remodeling. Semin Dial 22: 433-437.
7. De Deyn PP, Vanholder R, Eloot S, Glorieux G (2009) Guanidino compounds as uremic (neuro)toxins. Semin Dial 22: 340-345.
8. Koppe L, Pillon NJ, Vella RE, Croze ML, Pelletier CC, et al. (2013) p-Cresyl sulfate promotes insulin resistance associated with CKD. J Am Soc Nephrol 24: 88-99.
9. Perlman RL, Finkelstein FO, Liu L, Roys E, Kiser M, et al. (2005) Quality of life in chronic kidney disease (CKD): a cross-sectional analysis in the Renal Research Institute-CKD study. Am J Kidney Dis 45: 658-666.
10. Hailpern SM, Melamed ML, Cohen HW, Hostetter TH (2007) Moderate chronic kidney disease and cognitive function in adults 20 to 59 years of age: Third National Health and Nutrition Examination Survey (NHANES III). J Am Soc Nephrol 18: 2205-2213.
11. Shinohara K, Shoji T, Emoto M, Tahara H, Koyama H, et al. (2002) Insulin resistance as an independent predictor of cardiovascular mortality in patients with end-stage renal disease. J Am Soc Nephrol 13: 1894-1900.
12. Jacobs C (2009) [Renal replacement therapy by hemodialysis: an overview]. Nephrol Ther 5: 306-312.
13. Kolff WJ, Higgins CC (1954) Dialysis in the treatment of uremia: artificial kidney. J Urol 72: 1082-1094.
14. Scribner BH, Buri R, Caner JE, Hegstrom R, Burnell JM (1960) The treatment of chronic uremia by means of intermittent hemodialysis: a preliminary report. Trans Am Soc Artif Intern Organs 6: 114-122.
15. Atkins RC, Leonard CD, Scribner BH (1971) Management of chronic renal failure. Dis Mon: 1-38.
16. Go AS, Chertow GM, Fan D, McCulloch CE, Hsu CY (2004) Chronic kidney disease and the risks of death, cardiovascular events, and hospitalization. N Engl J Med 351: 1296-1305.
17. Eknoyan G, Beck GJ, Cheung AK, Daugirdas JT, Greene T, et al. (2002) Effect of dialysis dose and membrane flux in maintenance hemodialysis. N Engl J Med 347: 2010-2019.
18. Smith HW (1951) The kidney: Structure and function in health and disease. New York: Oxford University Press. ISBN: 0195011406.
19. Kolff WJ (1972) Hemodialysis in the management of renal disease. Annu Rev Med 23: 321-332.
20. Vanholder R, De Smet R (1999) Pathophysiologic effects of uremic retention solutes. J Am Soc Nephrol 10: 1815-1823.
21. Vanholder R, De Smet R, Glorieux G, Argiles A, Baurmeister U, et al. (2003) Review on uremic toxins: classification, concentration, and interindividual variability. Kidney Int 63: 1934-1943.
22. Duranton F, Cohen G, De Smet R, Rodriguez M, Jankowski J, et al. (2012) Normal and pathologic concentrations of uremic toxins. J Am Soc Nephrol 23: 1258-1270.
23. Vanholder R, Van LS, Glorieux G (2008) What is new in uremic toxicity? Pediatr Nephrol 23: 1211-1221.
24. Johnson WJ, Hagge WW, Wagoner RD, Dinapoli RP, Rosevear JW (1972) Effects of urea loading in patients with far-advanced renal failure. Mayo Clin Proc 47: 21-29.
25. Vanholder R, Van Laecke S, Glorieux G (2008) The middle-molecule hypothesis 30 years after: lost and rediscovered in the universe of uremic toxicity? J Nephrol 21: 146-160.
26. Cheung AK, Rocco MV, Yan G, Leypoldt JK, Levin NW, et al. (2006) Serum beta-2 microglobulin levels predict mortality in dialysis patients: results of the HEMO study. J Am Soc Nephrol 17: 546-555.
27. Cheung AK, Greene T, Leypoldt JK, Yan G, Allon M, et al. (2008) Association between serum 2-microglobulin level and infectious mortality in hemodialysis patients. Clin J Am Soc Nephrol 3: 69-77.
28. Lesaffer G, De Smet R, Lameire N, Dhondt A, Duym P, et al. (2000) Intradialytic removal of protein-bound uraemic toxins: role of solute characteristics and of dialyser membrane. Nephrol Dial Transplant 15: 50-57.

29. Neirynck N, Vanholder R, Schepers E, Eloot S, Pletinck A, et al. (2013) An update on uremic toxins. Int Urol Nephrol 45: 139-150.
30. Vanholder R, Bammens B, de LH, Glorieux G, Meijers B, et al. (2011) Warning: the unfortunate end of p-cresol as a uraemic toxin. Nephrol Dial Transplant 26: 1464-1467.
31. Wishart DS, Knox C, Guo AC, Eisner R, Young N, et al. (2009) HMDB: a knowledgebase for the human metabolome. Nucleic Acids Res 37: D603-610.
32. Adijiang A, Goto S, Uramoto S, Nishijima F, Niwa T (2008) Indoxyl sulphate promotes aortic calcification with expression of osteoblast-specific proteins in hypertensive rats. Nephrol Dial Transplant 23: 1892-1901.
33. Chiu CA, Lu LF, Yu TH, Hung WC, Chung FM, et al. (2010) Increased levels of total P-Cresylsulphate and indoxyl sulphate are associated with coronary artery disease in patients with diabetic nephropathy. Rev Diabet Stud 7: 275-284.
34. Barreto FC, Barreto DV, Liabeuf S, Meert N, Glorieux G, et al. (2009) Serum indoxyl sulfate is associated with vascular disease and mortality in chronic kidney disease patients. Clin J Am Soc Nephrol 4: 1551-1558.
35. Motojima M, Hosokawa A, Yamato H, Muraki T, Yoshioka T (2003) Uremic toxins of organic anions up-regulate PAI-1 expression by induction of NF-kappaB and free radical in proximal tubular cells. Kidney Int 63: 1671-1680.
36. Gelasco AK, Raymond JR (2006) Indoxyl sulfate induces complex redox alterations in mesangial cells. Am J Physiol Renal Physiol 290: F1551-1558.
37. Peng YS, Lin YT, Chen Y, Hung KY, Wang SM (2012) Effects of indoxyl sulfate on adherens junctions of endothelial cells and the underlying signaling mechanism. J Cell Biochem 113: 1034-1043.
38. Yamamoto H, Tsuruoka S, Ioka T, Ando H, Ito C, et al. (2006) Indoxyl sulfate stimulates proliferation of rat vascular smooth muscle cells. Kidney Int 69: 1780-1785.
39. Enomoto A, Takeda M, Tojo A, Sekine T, Cha SH, et al. (2002) Role of organic anion transporters in the tubular transport of indoxyl sulfate and the induction of its nephrotoxicity. J Am Soc Nephrol 13: 1711-1720.
40. Nii-Kono T, Iwasaki Y, Uchida M, Fujieda A, Hosokawa A, et al. (2007) Indoxyl sulfate induces skeletal resistance to parathyroid hormone in cultured osteoblastic cells. Kidney Int 71: 738-743.
41. Sun CY, Chang SC, Wu MS (2012) Uremic toxins induce kidney fibrosis by activating intrarenal renin-angiotensin-aldosterone system associated epithelial-to-mesenchymal transition. PLoS One 7: e34026.
42. Lekawanvijit S, Adrahtas A, Kelly DJ, Kompa AR, Wang BH, et al. (2010) Does indoxyl sulfate, a uraemic toxin, have direct effects on cardiac fibroblasts and myocytes? Eur Heart J 31: 1771-1779.
43. Meert N, Schepers E, Glorieux G, Van Landschoot M, Goeman JL, et al. (2012) Novel method for simultaneous determination of p-cresylsulphate and p-cresylglucuronide: clinical data and pathophysiological implications. Nephrol Dial Transplant 27: 2388-2396.
44. Wu IW, Hsu KH, Hsu HJ, Lee CC, Sun CY, et al. (2012) Serum free p-cresyl sulfate levels predict cardiovascular and all-cause mortality in elderly hemodialysis patients--a prospective cohort study. Nephrol Dial Transplant 27: 1169-1175.
45. Liabeuf S, Barreto DV, Barreto FC, Meert N, Glorieux G, et al. (2010) Free p-cresylsulphate is a predictor of mortality in patients at different stages of chronic kidney disease. Nephrol Dial Transplant 25: 1183-1191.
46. Poveda J, Sanchez-Nino MD, Glorieux G, Sanz AB, Egido J, et al. (2013) p-Cresyl sulphate has pro-inflammatory and cytotoxic actions on human proximal tubular epithelial cells. Nephrol Dial Transplant: In Press.
47. Wu IW, Hsu KH, Lee CC, Sun CY, Hsu HJ, et al. (2011) p-Cresyl sulphate and indoxyl sulphate predict progression of chronic kidney disease. Nephrol Dial Transplant 26: 938-947.
48. Dreisbach AW (2009) The influence of chronic renal failure on drug metabolism and transport. Clin Pharmacol Ther 86: 553-556.
49. Sun H, Frassetto L, Benet LZ (2006) Effects of renal failure on drug transport and metabolism. Pharmacol Ther 109: 1-11.
50. Gibson GG, Skett P (1995) Pathways of drug metabolism. Introduction to drug metabolism. second ed. London: Chapman & Hall.
51. de Loor H, Bammens B, Evenepoel P, De Preter V, Verbeke K (2005) Gas chromatographic-mass spectrometric analysis for measurement of p-cresol and its conjugated metabolites in uremic and normal serum. Clin Chem 51: 1535-1538.
52. Agatsuma S, Sekino H, Watanabe H (1996) Indoxyl-beta-D-glucuronide and 3-indoxyl sulfate in plasma of hemodialysis patients. Clin Nephrol 45: 250-256.
53. Niwa T, Miyazaki T, Tsukushi S, Maeda K, Tsubakihara Y, et al. (1996) Accumulation of indoxyl-beta-D-glucuronide in uremic serum: suppression of its production by oral sorbent and efficient removal by hemodialysis. Nephron 74: 72-78.
54. Peters JC (1991) Tryptophan nutrition and metabolism: an overview. Adv Exp Med Biol 294: 345-358.
55. Stone TW, Darlington LG (2002) Endogenous kynurenines as targets for drug discovery and development. Nat Rev Drug Discov 1: 609-620.
56. Smith HW (1959) From fish to philosopher. Garden City, New York: Summit, N. J., CIBA Pharmaceutical Products Inc.
57. Beyenbach KW (1982) Direct demonstration of fluid secretion by glomerular renal tubules in a marine teleost. Nature 299: 54-56.
58. International Transporter C, Giacomini KM, Huang SM, Tweedie DJ, Benet LZ, et al. (2010) Membrane transporters in drug development. Nat Rev Drug Discov 9: 215-236.
59. Masereeuw R, Russel FG (2010) Therapeutic implications of renal anionic drug transporters. Pharmacol Ther 126: 200-216.
60. Toyohara T, Suzuki T, Morimoto R, Akiyama Y, Souma T, et al. (2009) SLCO4C1 transporter eliminates uremic toxins and attenuates hypertension and renal inflammation. J Am Soc Nephrol 20: 2546-2555.
61. Wang L, Sweet DH (2013) Renal organic anion transporters (SLC22 family): expression, regulation, roles in toxicity, and impact on injury and disease. AAPS J 15: 53-69.
62. Hook JB, Munro JR (1968) Specificity of the inhibitory effect of "uremic" serum on p-aminohippurate transport. Proc Soc Exp Biol Med 127: 289-292.
63. White AG (1966) Uremic serum inhibition of renal paraaminohippurate transport. Proc Soc Exp Biol Med 123: 309-310.
64. Deguchi T, Ohtsuki S, Otagiri M, Takanaga H, Asaba H, et al. (2002) Major role of organic anion transporter 3 in the transport of indoxyl sulfate in the kidney. Kidney Int 61: 1760-1768.
65. Motojima M, Hosokawa A, Yamato H, Muraki T, Yoshioka T (2002) Uraemic toxins induce proximal tubular injury via organic anion transporter 1-mediated uptake. Br J Pharmacol 135: 555-563.
66. Cropp CD, Komori T, Shima JE, Urban TJ, Yee SW, et al. (2008) Organic anion transporter 2 (SLC22A7) is a facilitative transporter of cGMP. Mol Pharmacol 73: 1151-1158.
67. Whitley AC, Sweet DH, Walle T (2005) The dietary polyphenol ellagic acid is a potent inhibitor of hOAT1. Drug Metab Dispos 33: 1097-1100.
68. VanWert AL, Sweet DH (2008) Impaired clearance of methotrexate in organic anion transporter 3 (Slc22a8) knockout mice: a gender specific impact of reduced folates. Pharm Res 25: 453-462.
69. Ichida K, Hosoyamada M, Kimura H, Takeda M, Utsunomiya Y, et al. (2003) Urate transport via human PAH transporter hOAT1 and its gene structure. Kidney Int 63: 143-155.
70. Hagos Y, Stein D, Ugele B, Burckhardt G, Bahn A (2007) Human renal organic anion transporter 4 operates as an asymmetric urate transporter. J Am Soc Nephrol 18: 430-439.
71. Anzai N, Miyazaki H, Noshiro R, Khamdang S, Chairoungdua A, et al. (2004) The multivalent PDZ domain-containing protein PDZK1 regulates transport activity of renal urate-anion exchanger URAT1 via its C terminus. J Biol Chem 279: 45942-45950.
72. Deguchi T, Kusuhara H, Takadate A, Endou H, Otagiri M, et al. (2004) Characterization of uremic toxin transport by organic anion transporters in the kidney. Kidney Int 65: 162-174.
73. Bahn A, Ljubojevic M, Lorenz H, Schultz C, Ghebremedhin E, et al. (2005) Murine renal organic anion transporters mOAT1 and mOAT3 facilitate the transport of neuroactive tryptophan metabolites. Am J Physiol Cell Physiol 289: C1075-1084.
74. Uwai Y, Honjo H, Iwamoto K (2012) Interaction and transport of kynurenic acid via human organic anion transporters hOAT1 and hOAT3. Pharmacol Res 65: 254-260.
75. Hagenbuch B, Stieger B (2013) The SLCO (former SLC21) superfamily of transporters. Mol Aspects Med 34: 396-412.
76. Mikkaichi T, Suzuki T, Onogawa T, Tanemoto M, Mizutamari H, et al. (2004) Isolation and characterization of a digoxin transporter and its rat homologue expressed in the kidney. Proc Natl Acad Sci U S A 101: 3569-3574.
77. Koepsell H (2013) The SLC22 family with transporters of organic cations, anions and zwitterions. Mol Aspects Med 34: 413-435.

78. Schophuizen CM, Wilmer MJ, Jansen J, Gustavsson L, Hilgendorf C, et al. (2013) Cationic uremic toxins affect human renal proximal tubule cell functioning through interaction with the organic cation transporter. Pflugers Arch 465: 1701-1714.
79. Kimura N, Masuda S, Katsura T, Inui K (2009) Transport of guanidine compounds by human organic cation transporters, hOCT1 and hOCT2. Biochem Pharmacol 77: 1429-1436.
80. Reznichenko A, Sinkeler SJ, Snieder H, van den Born J, de Borst MH, et al. (2013) SLC22A2 is associated with tubular creatinine secretion and bias of estimated GFR in renal transplantation. Physiol Genomics 45: 201-209.
81. Brown MH, Paulsen IT, Skurray RA (1999) The multidrug efflux protein NorM is a prototype of a new family of transporters. Mol Microbiol 31: 394-395.
82. van Veen HW (2010) Structural biology: Last of the multidrug transporters. Nature 467: 926-927.
83. Damme K, Nies AT, Schaeffeler E, Schwab M (2011) Mammalian MATE (SLC47A) transport proteins: impact on efflux of endogenous substrates and xenobiotics. Drug Metab Rev 43: 499-523.
84. Masereeuw R, Russel FG (2012) Regulatory pathways for ATP-binding cassette transport proteins in kidney proximal tubules. AAPS J 14: 883-894.
85. Schinkel AH, Jonker JW (2003) Mammalian drug efflux transporters of the ATP binding cassette (ABC) family: an overview. Adv Drug Deliv Rev 55: 3-29.
86. Laouari D, Yang R, Veau C, Blanke I, Friedlander G (2001) Two apical multidrug transporters, P-gp and MRP2, are differently altered in chronic renal failure. Am J Physiol Renal Physiol 280: F636-645.
87. van Aubel RA, Smeets PH, van den Heuvel JJ, Russel FG (2005) Human organic anion transporter MRP4 (ABCC4) is an efflux pump for the purine end metabolite urate with multiple allosteric substrate binding sites. Am J Physiol Renal Physiol 288: F327-F333.
88. Woodward OM, Kottgen A, Coresh J, Boerwinkle E, Guggino WB, et al. (2009) Identification of a urate transporter, ABCG2, with a common functional polymorphism causing gout. Proc Natl Acad Sci U S A 106: 10338-10342.
89. Mutsaers HA, van den Heuvel LP, Ringens LH, Dankers AC, Russel FG, et al. (2011) Uremic toxins inhibit transport by breast cancer resistance protein and multidrug resistance protein 4 at clinically relevant concentrations. PLoS One 6: e18438.
90. Rhee EP, Souza A, Farrell L, Pollak MR, Lewis GD, et al. (2010) Metabolite profiling identifies markers of uremia. J Am Soc Nephrol 21: 1041-1051.
91. Herget-Rosenthal S, Glorieux G, Jankowski J, Jankowski V (2009) Uremic toxins in acute kidney injury. Semin Dial 22: 445-448.
92. Aronov PA, Luo FJ, Plummer NS, Quan Z, Holmes S, et al. (2011) Colonic contribution to uremic solutes. J Am Soc Nephrol 22: 1769-1776.
93. Evenepoel P, Meijers BK, Bammens BR, Verbeke K (2009) Uremic toxins originating from colonic microbial metabolism. Kidney Int Suppl: S12-19.
94. Daykin CA, Foxall PJ, Connor SC, Lindon JC, Nicholson JK (2002) The comparison of plasma deproteinization methods for the detection of low-molecular-weight metabolites by (1)H nuclear magnetic resonance spectroscopy. Anal Biochem 304: 220-230.
95. Weiss RH, Kim K (2012) Metabolomics in the study of kidney diseases. Nat Rev Nephrol 8: 22-33.
96. Shah VO, Townsend RR, Feldman HI, Pappan KL, Kensicki E, et al. (2013) Plasma metabolomic profiles in different stages of CKD. Clin J Am Soc Nephrol 8: 363-370.
97. Feigenbaum J, Neuberg CA (1941) Simplified method for the preparation of aromatic sulfuric acid esters. Journal of the American Chemical Society 63: 3529-3530.
98. Wilmer MJ, Saleem MA, Masereeuw R, Ni L, van der Velden TJ, et al. (2010) Novel conditionally immortalized human proximal tubule cell line expressing functional influx and efflux transporters. Cell Tissue Res 339: 449-457.
99. Wittgen HGM, van den Heuvel JJMW, van den Broek PHH, Siissalo S, Groothuis GMM, et al. (2012) Transport of the coumarin metabolite 7-hydroxycoumarin glucuronide is mediated via Multidrug Resistance-Associated Proteins 3 and 4. Drug Metabolism and Disposition 40: 1076-1079.
100. Mutsaers HA, Wilmer MJ, Reijnders D, Jansen J, van den Broek PH, et al. (2013) Uremic toxins inhibit renal metabolic capacity through interference with glucuronidation and mitochondrial respiration. Biochim Biophys Acta 1832: 142-150.
101. Moghadasali R, Mutsaers HA, Azarnia M, Aghdami N, Baharvand H, et al. (2013) Mesenchymal stem cell-conditioned medium accelerates regeneration of human renal proximal tubule epithelial cells after gentamicin toxicity. Exp Toxicol Pathol 65: 595-600.
102. Wilmer MJ, Kluijtmans LA, van der Velden TJ, Willems PH, Scheffer PG, et al. (2011) Cysteamine restores glutathione redox status in cultured cystinotic proximal tubular epithelial cells. Biochim Biophys Acta 1812: 643-651.
103. Tiziani S, Emwas AH, Lodi A, Ludwig C, Bunce CM, et al. (2008) Optimized metabolite extraction from blood serum for 1H nuclear magnetic resonance spectroscopy. Anal Biochem 377: 16-23.
104. Williams KI, Burstein SH, Layne DS (1966) Dimethyl sulfone: isolation from human urine. Arch Biochem Biophys 113: 251-252.
105. Jacob SW, Herschler R (1983) Dimethyl sulfoxide after twenty years. Ann N Y Acad Sci 411: xiii-xvii.
106. Engelke UF, Tangerman A, Willemsen MA, Moskau D, Loss S, et al. (2005) Dimethyl sulfone in human cerebrospinal fluid and blood plasma confirmed by one-dimensional (1)H and two-dimensional (1)H-(13)C NMR. NMR Biomed 18: 331-336.
107. Williams KI, Burstein SH, Layne DS (1966) Dimethyl sulfone: isolation from cows' milk. Proc Soc Exp Biol Med 122: 865-866.
108. Silva Ferreira AC, Rodrigues P, Hogg T, Guedes De PP (2003) Influence of some technological parameters on the formation of dimethyl sulfide, 2-mercaptoethanol, methionol, and dimethyl sulfone in port wines. J Agric Food Chem 51: 727-732.
109. Layman DL, Jacob SW (1985) The absorption, metabolism and excretion of dimethyl sulfoxide by rhesus monkeys. Life Sci 37: 2431-2437.
110. Kloesch B, Liszt M, Broell J, Steiner G (2011) Dimethyl sulphoxide and dimethyl sulphone are potent inhibitors of IL-6 and IL-8 expression in the human chondrocyte cell line C-28/I2. Life Sci 89: 473-478.
111. Beilke MA, Collins-Lech C, Sohnle PG (1987) Effects of dimethyl sulfoxide on the oxidative function of human neutrophils. J Lab Clin Med 110: 91-96.
112. Layman DL (1987) Growth inhibitory effects of dimethyl sulfoxide and dimethyl sulfone on vascular smooth muscle and endothelial cells in vitro. In Vitro Cell Dev Biol 23: 422-428.
113. Shaykhutdinov RA, MacInnis GD, Dowlatabadi R, Weljie AM, Vogel HJ (2009) Quantitative analysis of metabolite concentrations in human urine samples using C-13{H-1} NMR spectroscopy. Metabolomics 5: 307-317.
114. Psychogios N, Hau DD, Peng J, Guo AC, Mandal R, et al. (2011) The human serum metabolome. PLoS One 6: e16957.
115. Dekant W, Bernauer U, Rosner E, Amberg A (2001) Toxicokinetics of ethers used as fuel oxygenates. Toxicol Lett 124: 37-45.
116. Amberg A, Rosner E, Dekant W (2001) Toxicokinetics of methyl tert-butyl ether and its metabolites in humans after oral exposure. Toxicol Sci 61: 62-67.
117. Li X, Xu Z, Lu X, Yang X, Yin P, et al. (2009) Comprehensive two-dimensional gas chromatography/time-of-flight mass spectrometry for metabonomics: Biomarker discovery for diabetes mellitus. Anal Chim Acta 633: 257-262.
118. Suhre K, Wallaschofski H, Raffler J, Friedrich N, Haring R, et al. (2011) A genome-wide association study of metabolic traits in human urine. Nat Genet 43: 565-569.
119. Meisinger C, Prokisch H, Gieger C, Soranzo N, Mehta D, et al. (2009) A genome-wide association study identifies three loci associated with mean platelet volume. Am J Hum Genet 84: 66-71.
120. Neirynck N, Eloot S, Glorieux G, Barreto DV, Barreto FC, et al. (2012) Estimated glomerular filtration rate is a poor predictor of the concentration of middle molecular weight uremic solutes in chronic kidney disease. PLoS One 7: e44201.
121. Eloot S, Schepers E, Barreto DV, Barreto FC, Liabeuf S, et al. (2011) Estimated glomerular filtration rate is a poor predictor of concentration for a broad range of uremic toxins. Clin J Am Soc Nephrol 6: 1266-1273.
122. Choi JY, Yoon YJ, Choi HJ, Park SH, Kim CD, et al. (2011) Dialysis modality-dependent changes in serum metabolites: accumulation of inosine and hypoxanthine in patients on haemodialysis. Nephrol Dial Transplant 26: 1304-1313.
123. Raj DS, Ouwendyk M, Francoeur R, Pierratos A (2000) Plasma amino acid profile on nocturnal hemodialysis. Blood Purif 18: 97-102.

124. Niwa T, Takeda N, Yoshizumi H (1998) RNA metabolism in uremic patients: accumulation of modified ribonucleosides in uremic serum. Technical note. Kidney Int 53: 1801-1806.
125. Schepers E, Glorieux G, Vanholder R (2010) The gut: the forgotten organ in uremia? Blood Purif 29: 130-136.
126. Burckhardt BC, Burckhardt G (2003) Transport of organic anions across the basolateral membrane of proximal tubule cells. Rev Physiol Biochem Pharmacol 146: 95-158.
127. van Aubel RA, Smeets PH, Peters JG, Bindels RJ, Russel FG (2002) The MRP4/ABCC4 gene encodes a novel apical organic anion transporter in human kidney proximal tubules: putative efflux pump for urinary cAMP and cGMP. J Am Soc Nephrol 13: 595-603.
128. Huls M, Brown CD, Windass AS, Sayer R, van den Heuvel JJ, et al. (2008) The breast cancer resistance protein transporter ABCG2 is expressed in the human kidney proximal tubule apical membrane. Kidney Int 73: 220-225.
129. Nakagawa T, Mazzali M, Kang DH, Sanchez-Lozada LG, Herrera-Acosta J, et al. (2006) Uric acid--a uremic toxin? Blood Purif 24: 67-70.
130. Matsuo H, Takada T, Ichida K, Nakamura T, Nakayama A, et al. (2009) Common defects of ABCG2, a high-capacity urate exporter, cause gout: a function-based genetic analysis in a Japanese population. Sci Transl Med 1: 5ra11.
131. Cohen G, Glorieux G, Thornalley P, Schepers E, Meert N, et al. (2007) Review on uraemic toxins III: recommendations for handling uraemic retention solutes in vitro--towards a standardized approach for research on uraemia. Nephrol Dial Transplant 22: 3381-3390.
132. El-Sheikh AA, van den Heuvel JJ, Koenderink JB, Russel FG (2007) Interaction of nonsteroidal anti-inflammatory drugs with multidrug resistance protein (MRP) 2/ABCC2- and MRP4/ABCC4-mediated methotrexate transport. J Pharmacol Exp Ther 320: 229-235.
133. El-Sheikh AA, van den Heuvel JJ, Krieger E, Russel FG, Koenderink JB (2008) Functional role of arginine 375 in transmembrane helix 6 of multidrug resistance protein 4 (MRP4/ABCC4). Mol Pharmacol 74: 964-971.
134. Imai Y, Asada S, Tsukahara S, Ishikawa E, Tsuruo T, et al. (2003) Breast cancer resistance protein exports sulfated estrogens but not free estrogens. Mol Pharmacol 64: 610-618.
135. Jourde-Chiche N, Dou L, Cerini C, gnat-George F, Vanholder R, et al. (2009) Protein-bound toxins--update 2009. Semin Dial 22: 334-339.
136. Jankowski J, van der Giet M, Jankowski V, Schmidt S, Hemeier M, et al. (2003) Increased plasma phenylacetic acid in patients with end-stage renal failure inhibits iNOS expression. J Clin Invest 112: 256-264.
137. Masereeuw R, Moons MM, Russel FG (1996) Renal excretion and accumulation kinetics of 2-methylbenzoylglycine in the isolated perfused rat kidney. J Pharm Pharmacol 48: 560-565.
138. Masereeuw R, Moons MM, Russel FG (1998) Disposition of 4-methylbenzoylglycine in rat isolated perfused kidney and effects of hippurates on renal mitochondrial metabolism. J Pharm Pharmacol 50: 1397-1404.
139. Borst P, de Wolf C, van de Wetering K (2007) Multidrug resistance-associated proteins 3, 4, and 5. Pflugers Arch 453: 661-673.
140. Lu H, Klaassen C (2008) Gender differences in mRNA expression of ATP-binding cassette efflux and bile acid transporters in kidney, liver, and intestine of 5/6 nephrectomized rats. Drug Metab Dispos 36: 16-23.
141. Huls M, van den Heuvel JJ, Dijkman HB, Russel FG, Masereeuw R (2006) ABC transporter expression profiling after ischemic reperfusion injury in mouse kidney. Kidney Int 69: 2186-2193.
142. Huang ZH, Murakami T, Okochi A, Yumoto R, Nagai J, et al. (2000) Expression and function of P-glycoprotein in rats with glycerol-induced acute renal failure. Eur J Pharmacol 406: 453-460.
143. Smith HW, Finkelstein N, Aliminosa L, Crawford B, Graber M (1945) The renal clearances of substituted hippuric acid derivatives and other aromatic acids in dog and man. J Clin Invest 24: 388-404.
144. Pick A, Klinkhammer W, Wiese M (2010) Specific inhibitors of the breast cancer resistance protein (BCRP). ChemMedChem 5: 1498-1505.
145. Hazai E, Bikadi Z (2008) Homology modeling of breast cancer resistance protein (ABCG2). J Struct Biol 162: 63-74.
146. Lee CT, Kuo CC, Chen YM, Hsu CY, Lee WC, et al. (2010) Factors associated with blood concentrations of indoxyl sulfate and p-cresol in patients undergoing peritoneal dialysis. Perit Dial Int 30: 456-463.
147. Brener ZZ, Kotanko P, Thijssen S, Winchester JF, Bergman M (2010) Clinical benefit of preserving residual renal function in dialysis patients: an update for clinicians. Am J Med Sci 339: 453-456.
148. Martinez AW, Recht NS, Hostetter TH, Meyer TW (2005) Removal of P-cresol sulfate by hemodialysis. J Am Soc Nephrol 16: 3430-3436.
149. Meijers BK, De Loor H, Bammens B, Verbeke K, Vanrenterghem Y, et al. (2009) p-Cresyl sulfate and indoxyl sulfate in hemodialysis patients. Clin J Am Soc Nephrol 4: 1932-1938.
150. Dankers AC, Sweep FC, Pertijs JC, Verweij V, van den Heuvel JJ, et al. (2012) Localization of breast cancer resistance protein (Bcrp) in endocrine organs and inhibition of its transport activity by steroid hormones. Cell Tissue Res 349: 551-563.
151. Meijers BK, Van Kerckhoven S, Verbeke K, Dehaen W, Vanrenterghem Y, et al. (2009) The uremic retention solute p-cresyl sulfate and markers of endothelial damage. Am J Kidney Dis 54: 891-901.
152. Sun CY, Chang SC, Wu MS (2012) Suppression of Klotho expression by protein-bound uremic toxins is associated with increased DNA methyltransferase expression and DNA hypermethylation. Kidney Int 81: 640-650.
153. Kim SH, Yu MA, Ryu ES, Jang YH, Kang DH (2012) Indoxyl sulfate-induced epithelial-to-mesenchymal transition and apoptosis of renal tubular cells as novel mechanisms of progression of renal disease. Lab Invest 92: 488-498.
154. Van der Eycken E, Terryn N, Goeman JL, Carlens G, Nerinckx W, et al. (2000) Sudan-β-d-glucuronides and their use for the histochemical localization of β-glucuronidase activity in transgenic plants. Plant Cell Reports 19: 966-970.
155. Wittgen HG, van den Heuvel JJ, van den Broek PH, Dinter-Heidorn H, Koenderink JB, et al. (2011) Cannabinoid type 1 receptor antagonists modulate transport activity of multidrug resistance-associated proteins MRP1, MRP2, MRP3, and MRP4. Drug Metab Dispos 39: 1294-1302.
156. George J, Struthers AD (2009) Role of urate, xanthine oxidase and the effects of allopurinol in vascular oxidative stress. Vasc Health Risk Manag 5: 265-272.
157. Schulz E, Gori T, Munzel T (2011) Oxidative stress and endothelial dysfunction in hypertension. Hypertens Res 34: 665-673.
158. Glantzounis GK, Tsimoyiannis EC, Kappas AM, Galaris DA (2005) Uric acid and oxidative stress. Curr Pharm Des 11: 4145-4151.
159. Mok Y, Lee SJ, Kim MS, Cui W, Moon YM, et al. (2012) Serum uric acid and chronic kidney disease: the Severance cohort study. Nephrol Dial Transplant 27: 1831-1835.
160. Hediger MA, Johnson RJ, Miyazaki H, Endou H (2005) Molecular physiology of urate transport. Physiology (Bethesda) 20: 125-133.
161. Saag KG, Choi H (2006) Epidemiology, risk factors, and lifestyle modifications for gout. Arthritis Res Ther 8 Suppl 1: S2.
162. Kim KY, Ralph Schumacher H, Hunsche E, Wertheimer AI, Kong SX (2003) A literature review of the epidemiology and treatment of acute gout. Clin Ther 25: 1593-1617.
163. Maalouf NM (2011) Metabolic syndrome and the genesis of uric acid stones. J Ren Nutr 21: 128-131.
164. Feig DI, Kang DH, Johnson RJ (2008) Uric acid and cardiovascular risk. N Engl J Med 359: 1811-1821.
165. Dehghan A, van HM, Sijbrands EJ, Hofman A, Witteman JC (2008) High serum uric acid as a novel risk factor for type 2 diabetes. Diabetes Care 31: 361-362.
166. Forman JP, Choi H, Curhan GC (2007) Plasma uric acid level and risk for incident hypertension among men. J Am Soc Nephrol 18: 287-292.
167. Feig DI, Kang DH, Nakagawa T, Mazzali M, Johnson RJ (2006) Uric acid and hypertension. Curr Hypertens Rep 8: 111-115.
168. Khosla UM, Zharikov S, Finch JL, Nakagawa T, Roncal C, et al. (2005) Hyperuricemia induces endothelial dysfunction. Kidney Int 67: 1739-1742.
169. Moe OW (2010) Posing the question again: does chronic uric acid nephropathy exist? J Am Soc Nephrol 21: 395-397.
170. Zhang L, Wang F, Wang X, Liu L, Wang H (2012) The association between plasma uric acid and renal function decline in a Chinese population-based cohort. Nephrol Dial Transplant 27: 1836-1839.
171. Chilappa CS, Aronow WS, Shapiro D, Sperber K, Patel U, et al. (2010) Gout and hyperuricemia. Compr Ther 36: 3-13.
172. Benedict JD, Forsham PH, Stetten D, Jr. (1949) The metabolism of uric acid in the normal and gouty human studied with the aid of isotopic uric acid. J Biol Chem 181: 183-193.
173. Vitart V, Rudan I, Hayward C, Gray NK, Floyd J, et al. (2008) SLC2A9 is a newly identified urate transporter influencing serum urate concentration, urate excretion and gout. Nat Genet 40: 437-442.

174. Anzai N, Kanai Y, Endou H (2007) New insights into renal transport of urate. Curr Opin Rheumatol 19: 151-157.
175. Ichida K, Matsuo H, Takada T, Nakayama A, Murakami K, et al. (2012) Decreased extra-renal urate excretion is a common cause of hyperuricemia. Nat Commun 3: 764.
176. Liu Y, Sun X, Di D, Quan J, Zhang J, et al. (2011) A metabolic profiling analysis of symptomatic gout in human serum and urine using high performance liquid chromatography-diode array detector technique. Clin Chim Acta 412: 2132-2140.
177. Liu Y, Yu P, Sun X, Di D (2012) Metabolite target analysis of human urine combined with pattern recognition techniques for the study of symptomatic gout. Mol Biosyst 8: 2956-2963.
178. Patschan D, Patschan S, Gobe GG, Chintala S, Goligorsky MS (2007) Uric acid heralds ischemic tissue injury to mobilize endothelial progenitor cells. J Am Soc Nephrol 18: 1516-1524.
179. Vecsei L, Szalardy L, Fulop F, Toldi J (2013) Kynurenines in the CNS: recent advances and new questions. Nat Rev Drug Discov 12: 64-82.
180. Noto Y, Okamoto H (1978) Inhibition by kynurenine metabolites of proinsulin synthesis in isolated pancreatic islets. Acta Diabetol Lat 15: 273-282.
181. Okamoto H (1975) Effect of quinaldic acid and its relatives on insulin-release from isolated Langerhans islets. Acta Vitaminol Enzymol 29: 227-231.
182. Pawlak D, Tankiewicz A, Buczko W (2001) Kynurenine and its metabolites in the rat with experimental renal insufficiency. J Physiol Pharmacol 52: 755-766.
183. Pawlak K, Mysliwiec M, Pawlak D (2010) Kynurenine pathway - a new link between endothelial dysfunction and carotid atherosclerosis in chronic kidney disease patients. Adv Med Sci 55: 196-203.
184. Barth MC, Ahluwalia N, Anderson TJ, Hardy GJ, Sinha S, et al. (2009) Kynurenic acid triggers firm arrest of leukocytes to vascular endothelium under flow conditions. J Biol Chem 284: 19189-19195.
185. Munn DH, Mellor AL (2013) Indoleamine 2,3 dioxygenase and metabolic control of immune responses. Trends Immunol 34: 137-143.
186. Opitz CA, Litzenburger UM, Sahm F, Ott M, Tritschler I, et al. (2011) An endogenous tumour-promoting ligand of the human aryl hydrocarbon receptor. Nature 478: 197-203.
187. Schroeder JC, Dinatale BC, Murray IA, Flaveny CA, Liu Q, et al. (2010) The uremic toxin 3-indoxyl sulfate is a potent endogenous agonist for the human aryl hydrocarbon receptor. Biochemistry 49: 393-400.
188. Watanabe I, Tatebe J, Namba S, Koizumi M, Yamazaki J, et al. (2013) Activation of aryl hydrocarbon receptor mediates indoxyl sulfate-induced monocyte chemoattractant protein-1 expression in human umbilical vein endothelial cells. Circ J 77: 224-230.
189. Doring A, Gieger C, Mehta D, Gohlke H, Prokisch H, et al. (2008) SLC2A9 influences uric acid concentrations with pronounced sex-specific effects. Nat Genet 40: 430-436.
190. Kolz M, Johnson T, Sanna S, Teumer A, Vitart V, et al. (2009) Meta-analysis of 28,141 individuals identifies common variants within five new loci that influence uric acid concentrations. PLoS Genet 5: e1000504.
191. Kottgen A, Albrecht E, Teumer A, Vitart V, Krumsiek J, et al. (2013) Genome-wide association analyses identify 18 new loci associated with serum urate concentrations. Nat Genet 45: 145-154.
192. Dreisbach AW, Lertora JJ (2008) The effect of chronic renal failure on drug metabolism and transport. Expert Opin Drug Metab Toxicol 4: 1065-1074.
193. Verbeeck RK, Musuamba FT (2009) Pharmacokinetics and dosage adjustment in patients with renal dysfunction. Eur J Clin Pharmacol 65: 757-773.
194. Yavuz A, Tetta C, Ersoy FF, D'Intini V, Ratanarat R, et al. (2005) Uremic toxins: a new focus on an old subject. Semin Dial 18: 203-211.
195. Meyer TW (2012) The removal of protein-bound solutes by dialysis. J Ren Nutr 22: 203-206.
196. Lohr JW, Willsky GR, Acara MA (1998) Renal drug metabolism. Pharmacol Rev 50: 107-141.
197. Simard E, Naud J, Michaud J, Leblond FA, Bonnardeaux A, et al. (2008) Downregulation of hepatic acetylation of drugs in chronic renal failure. J Am Soc Nephrol 19: 1352-1359.
198. Bateman DN, Gokal R, Dodd TR, Blain PG (1981) The pharmacokinetics of single doses of metoclopramide in renal failure. Eur J Clin Pharmacol 19: 437-441.
199. Verbeeck RK (1982) Glucuronidation and disposition of drug glucuronides in patients with renal failure. A review. Drug Metab Dispos 10: 87-89.

200. Howie MB, Bourke E (1979) Metabolism of p-aminobenzoic acid in the perfused livers of chronically uraemic rats. Clin Sci (Lond) 56: 9-14.
201. Osborne R, Joel S, Grebenik K, Trew D, Slevin M (1993) The pharmacokinetics of morphine and morphine glucuronides in kidney failure. Clin Pharmacol Ther 54: 158-167.
202. Kim YG, Shin JG, Shin SG, Jang IJ, Kim S, et al. (1993) Decreased acetylation of isoniazid in chronic renal failure. Clin Pharmacol Ther 54: 612-620.
203. Uchaipichat V, Mackenzie PI, Guo XH, Gardner-Stephen D, Galetin A, et al. (2004) Human udp-glucuronosyltransferases: isoform selectivity and kinetics of 4-methylumbelliferone and 1-naphthol glucuronidation, effects of organic solvents, and inhibition by diclofenac and probenecid. Drug Metab Dispos 32: 413-423.
204. Zhou J, Tracy TS, Remmel RP (2011) Correlation between bilirubin glucuronidation and estradiol-3-gluronidation in the presence of model UDP-glucuronosyltransferase 1A1 substrates/inhibitors. Drug Metab Dispos 39: 322-329.
205. Ohno S, Nakajin S (2009) Determination of mRNA expression of human UDP-glucuronosyltransferases and application for localization in various human tissues by real-time reverse transcriptase-polymerase chain reaction. Drug Metab Dispos 37: 32-40.
206. Bock KW (2010) Functions and transcriptional regulation of adult human hepatic UDP-glucuronosyl-transferases (UGTs): mechanisms responsible for interindividual variation of UGT levels. Biochem Pharmacol 80: 771-777.
207. Braun L, Kardon T, Puskas F, Csala M, Banhegyi G, et al. (1997) Regulation of glucuronidation by glutathione redox state through the alteration of UDP-glucose supply originating from glycogen metabolism. Arch Biochem Biophys 348: 169-173.
208. Kerdpin O, Knights KM, Elliot DJ, Miners JO (2008) In vitro characterisation of human renal and hepatic frusemide glucuronidation and identification of the UDP-glucuronosyltransferase enzymes involved in this pathway. Biochem Pharmacol 76: 249-257.
209. Yu C, Ritter JK, Krieg RJ, Rege B, Karnes TH, et al. (2006) Effect of chronic renal insufficiency on hepatic and renal udp-glucuronyltransferases in rats. Drug Metab Dispos 34: 621-627.
210. Hutter E, Renner K, Pfister G, Stockl P, Jansen-Durr P, et al. (2004) Senescence-associated changes in respiration and oxidative phosphorylation in primary human fibroblasts. Biochem J 380: 919-928.
211. Lash LH, Putt DA, Cai H (2008) Drug metabolism enzyme expression and activity in primary cultures of human proximal tubular cells. Toxicology 244: 56-65.
212. Schaaf GJ, de Groene EM, Maas RF, Commandeur JN, Fink-Gremmels J (2001) Characterization of biotransformation enzyme activities in primary rat proximal tubular cells. Chem Biol Interact 134: 167-190.
213. Wang P, Henning SM, Heber D (2010) Limitations of MTT and MTS-based assays for measurement of antiproliferative activity of green tea polyphenols. PLoS One 5: e10202.
214. Lancaster CR (2002) Succinate:quinone oxidoreductases: an overview. Biochim Biophys Acta 1553: 1-6.
215. Massudi H, Grant R, Guillemin GJ, Braidy N (2012) NAD+ metabolism and oxidative stress: the golden nucleotide on a crown of thorns. Redox Rep 17: 28-46.
216. Fukuwatari T, Morikawa Y, Hayakawa F, Sugimoto E, Shibata K (2001) Influence of adenine-induced renal failure on tryptophan-niacin metabolism in rats. Biosci Biotechnol Biochem 65: 2154-2161.
217. Owada S, Maeba T, Sugano Y, Hirayama A, Ueda A, et al. (2010) Spherical carbon adsorbent (AST-120) protects deterioration of renal function in chronic kidney disease rats through inhibition of reactive oxygen species production from mitochondria and reduction of serum lipid peroxidation. Nephron Exp Nephrol 115: e101-e111.
218. Dzurik R, Spustova V, Krivosikova Z, Gazdikova K (2001) Hippurate participates in the correction of metabolic acidosis. Kidney Int Suppl 78: S278-281.
219. Kitagawa A (2001) Effects of cresols (o-, m-, and p-isomers) on the bioenergetic system in isolated rat liver mitochondria. Drug Chem Toxicol 24: 39-47.
220. Riegel W, Ulrich C, Sauernheimer S, Deppisch RM, Kohler H (2001) Hepatotoxic substance(s) removed by high-flux membranes enhances the positive acute phase response. Kidney Int Suppl 78: S308-314.
221. Mutsaers HA, Wilmer MJ, van den Heuvel LP, Hoenderop JG, Masereeuw R (2011) Basolateral transport of the uraemic toxin p-cresyl sulfate: role for organic anion transporters? Nephrol Dial Transplant 26: 4149.

222. Saito A, Nagai R, Tanuma A, Hama H, Cho K, et al. (2003) Role of megalin in endocytosis of advanced glycation end products: implications for a novel protein binding to both megalin and advanced glycation end products. J Am Soc Nephrol 14: 1123-1131.
223. Leblond FA, Giroux L, Villeneuve JP, Pichette V (2000) Decreased in vivo metabolism of drugs in chronic renal failure. Drug Metab Dispos 28: 1317-1320.
224. Leblond F, Guevin C, Demers C, Pellerin I, Gascon-Barre M, et al. (2001) Downregulation of hepatic cytochrome P450 in chronic renal failure. J Am Soc Nephrol 12: 326-332.
225. Naud J, Michaud J, Beauchemin S, Hebert MJ, Roger M, et al. (2011) Effects of chronic renal failure on kidney drug transporters and cytochrome P450 in rats. Drug Metab Dispos 39: 1363-1369.
226. Sun H, Huang Y, Frassetto L, Benet LZ (2004) Effects of uremic toxins on hepatic uptake and metabolism of erythromycin. Drug Metab Dispos 32: 1239-1246.
227. Knights KM, Miners JO (2010) Renal UDP-glucuronosyltransferases and the glucuronidation of xenobiotics and endogenous mediators. Drug Metab Rev 42: 63-73.
228. Engelke UFH, Moolenaar SH, Hoenderop SMGC, Morava E, van der Graaf M, et al. (2007) Handbook of ^{1}H-NMR spectroscopy in inborn errors of metabolism: body fluid NMR spectrum and in vivo MR spectroscopy. Heilbronn: SPS Verlagsgesellschaft mbH.
229. Brautbar N (2004) Industrial solvents and kidney disease. Int J Occup Environ Health 10: 79-83.
230. Qin W, Xu Z, Lu Y, Zeng C, Zheng C, et al. (2012) Mixed organic solvents induce renal injury in rats. PLoS One 7: e45873.
231. vNemmar A, Al-Salam S, Zia S, Yasin J, Al Husseni I, et al. (2010) Diesel exhaust particles in the lung aggravate experimental acute renal failure. Toxicol Sci 113: 267-277.
232. Cummings JH (1983) Fermentation in the human large intestine: evidence and implications for health. Lancet 1: 1206-1209.
233. Schefold JC, Zeden JP, Fotopoulou C, VON HS, Pschowski R, et al. (2009) Increased indoleamine 2,3-dioxygenase (IDO) activity and elevated serum levels of tryptophan catabolites in patients with chronic kidney disease: a possible link between chronic inflammation and uraemic symptoms. Nephrol Dial Transplant 24: 1901-1908.
234. van Angelen AA, Glaudemans B, van der Kemp AW, Hoenderop JG, Bindels RJ (2013) Cisplatin-induced injury of the renal distal convoluted tubule is associated with hypomagnesaemia in mice. Nephrol Dial Transplant 28: 879-889.
235. Franch HA, Mitch WE (2009) Navigating between the Scylla and Charybdis of prescribing dietary protein for chronic kidney diseases. Annu Rev Nutr 29: 341-364.
236. Kewley RJ, Whitelaw ML, Chapman-Smith A (2004) The mammalian basic helix-loop-helix/PAS family of transcriptional regulators. Int J Biochem Cell Biol 36: 189-204.
237. Nguyen LP, Bradfield CA (2008) The search for endogenous activators of the aryl hydrocarbon receptor. Chem Res Toxicol 21: 102-116.
238. Denison MS, Nagy SR (2003) Activation of the aryl hydrocarbon receptor by structurally diverse exogenous and endogenous chemicals. Annu Rev Pharmacol Toxicol 43: 309-334.
239. DiNatale BC, Murray IA, Schroeder JC, Flaveny CA, Lahoti TS, et al. (2010) Kynurenic acid is a potent endogenous aryl hydrocarbon receptor ligand that synergistically induces interleukin-6 in the presence of inflammatory signaling. Toxicol Sci 115: 89-97.
240. Gondouin B, Cerini C, Dou L, Sallee M, Duval-Sabatier A, et al. (2013) Indolic uremic solutes increase tissue factor production in endothelial cells by the aryl hydrocarbon receptor pathway. Kidney Int 84: 733-744.
241. Hwang SJ, Hwang YJ, Yun MO, Kim JH, Oh GS, et al. (2013) Indoxyl 3-sulfate stimulates Th17 differentiation enhancing phosphorylation of c-Src and STAT3 to worsen experimental autoimmune encephalomyelitis. Toxicol Lett 220: 109-117.
242. Esser C, Rannug A, Stockinger B (2009) The aryl hydrocarbon receptor in immunity. Trends Immunol 30: 447-454.
243. Gramatzki D, Pantazis G, Schittenhelm J, Tabatabai G, Kohle C, et al. (2009) Aryl hydrocarbon receptor inhibition downregulates the TGF-beta/Smad pathway in human glioblastoma cells. Oncogene 28: 2593-2605.
244. Bui LC, Tomkiewicz C, Chevallier A, Pierre S, Bats AS, et al. (2009) Nedd9/Hef1/Cas-L mediates the effects of environmental pollutants on cell migration and plasticity. Oncogene 28: 3642-3651.
245. Trecherel E, Godin C, Louandre C, Benchitrit J, Poirot S, et al. (2012) Upregulation of BAD, a pro-apoptotic protein of the BCL2 family, in vascular smooth muscle cells exposed to uremic conditions. Biochem Biophys Res Commun 417: 479-483.
246. Sinha-Hikim I, Shen R, Kovacheva E, Crum A, Vaziri ND, et al. (2010) Inhibition of apoptotic signalling in spermine-treated vascular smooth muscle cells by a novel glutathione precursor. Cell Biol Int 34: 503-511.
247. Cohen G, Rudnicki M, Horl WH (2001) Uremic toxins modulate the spontaneous apoptotic cell death and essential functions of neutrophils. Kidney Int Suppl 78: S48-52.
248. Koopman WJ, Willems PH, Smeitink JA (2012) Monogenic mitochondrial disorders. N Engl J Med 366: 1132-1141.
249. Cardoso AR, Queliconi BB, Kowaltowski AJ (2010) Mitochondrial ion transport pathways: role in metabolic diseases. Biochim Biophys Acta 1797: 832-838.
250. Murphy MP, Holmgren A, Larsson NG, Halliwell B, Chang CJ, et al. (2011) Unraveling the biological roles of reactive oxygen species. Cell Metab 13: 361-366.
251. Spencer SL, Sorger PK (2011) Measuring and modeling apoptosis in single cells. Cell 144: 926-939.
252. Dowling TC, Briglia AE, Fink JC, Hanes DS, Light PD, et al. (2003) Characterization of hepatic cytochrome p4503A activity in patients with end-stage renal disease. Clin Pharmacol Ther 73: 427-434.
253. Dreisbach AW, Japa S, Gebrekal AB, Mowry SE, Lertora JJ, et al. (2003) Cytochrome P4502C9 activity in end-stage renal disease. Clin Pharmacol Ther 73: 475-477.
254. Turpeinen M, Koivuviita N, Tolonen A, Reponen P, Lundgren S, et al. (2007) Effect of renal impairment on the pharmacokinetics of bupropion and its metabolites. Br J Clin Pharmacol 64: 165-173.
255. Molanaei H, Stenvinkel P, Qureshi AR, Carrero JJ, Heimburger O, et al. (2012) Metabolism of alprazolam (a marker of CYP3A4) in hemodialysis patients with persistent inflammation. Eur J Clin Pharmacol 68: 571-577.
256. Nolin TD, Frye RF, Le P, Sadr H, Naud J, et al. (2009) ESRD impairs nonrenal clearance of fexofenadine but not midazolam. J Am Soc Nephrol 20: 2269-2276.
257. Michaud J, Nolin TD, Naud J, Dani M, Lafrance JP, et al. (2008) Effect of hemodialysis on hepatic cytochrome P450 functional expression. J Pharmacol Sci 108: 157-163.
258. Nolin TD, Appiah K, Kendrick SA, Le P, McMonagle E, et al. (2006) Hemodialysis acutely improves hepatic CYP3A4 metabolic activity. J Am Soc Nephrol 17: 2363-2367.
259. Tsujimoto M, Higuchi K, Shima D, Yokota H, Furukubo T, et al. (2010) Inhibitory effects of uraemic toxins 3-indoxyl sulfate and p-cresol on losartan metabolism in vitro. J Pharm Pharmacol 62: 133-138.
260. Liu Y (2010) New insights into epithelial-mesenchymal transition in kidney fibrosis. J Am Soc Nephrol 21: 212-222.
261. Kriz W, Kaissling B, Le Hir M (2011) Epithelial-mesenchymal transition (EMT) in kidney fibrosis: fact or fantasy? J Clin Invest 121: 468-474.
262. Zeisberg M, Duffield JS (2010) Resolved: EMT produces fibroblasts in the kidney. J Am Soc Nephrol 21: 1247-1253.
263. Kalluri R, Weinberg RA (2009) The basics of epithelial-mesenchymal transition. J Clin Invest 119: 1420-1428.
264. Hoffmann D, Adler M, Vaidya VS, Rached E, Mulrane L, et al. (2010) Performance of novel kidney biomarkers in preclinical toxicity studies. Toxicol Sci 116: 8-22.
265. Bolati D, Shimizu H, Higashiyama Y, Nishijima F, Niwa T (2011) Indoxyl sulfate induces epithelial-to-mesenchymal transition in rat kidneys and human proximal tubular cells. Am J Nephrol 34: 318-323.
266. Pallet N, Bouvier N, Bendjallabah A, Rabant M, Flinois JP, et al. (2008) Cyclosporine-induced endoplasmic reticulum stress triggers tubular phenotypic changes and death. Am J Transplant 8: 2283-2296.
267. Kitamura M (2008) Endoplasmic reticulum stress and unfolded protein response in renal pathophysiology: Janus faces. Am J Physiol Renal Physiol 295: F323-334.
268. Kawakami T, Inagi R, Wada T, Tanaka T, Fujita T, et al. (2010) Indoxyl sulfate inhibits proliferation of human proximal tubular cells via endoplasmic reticulum stress. Am J Physiol Renal Physiol 299: F568-576.
269. Westra IM, Pham BT, Groothuis GM, Olinga P (2013) Evaluation of fibrosis in precision-cut tissue slices. Xenobiotica 43: 98-112.
270. Bonventre JV, Vaidya VS, Schmouder R, Feig P, Dieterle F (2010) Next-generation biomarkers for detecting kidney toxicity. Nat Biotechnol 28: 436-440.
271. Katzberg RW, Buonocore MH, Low R, Hu B, Jain K, et al. (2009) MR determination of glomerular filtration rate in subjects with solitary kidneys in comparison to clinical standards of renal function: feasibility and preliminary report. Contrast Media Mol Imaging 4: 51-65.

272. Igarashi K, Ueda S, Yoshida K, Kashiwagi K (2006) Polyamines in renal failure. Amino Acids 31: 477-483.
273. van Zuilen AD, Bots ML, Dulger A, van der Tweel I, van Buren M, et al. (2012) Multifactorial intervention with nurse practitioners does not change cardiovascular outcomes in patients with chronic kidney disease. Kidney Int 82: 710-717.
274. Humes HD, Buffington DA, MacKay SM, Funke AJ, Weitzel WF (1999) Replacement of renal function in uremic animals with a tissue-engineered kidney. Nat Biotechnol 17: 451-455.
275. Kikuchi K, Itoh Y, Tateoka R, Ezawa A, Murakami K, et al. (2010) Metabolomic search for uremic toxins as indicators of the effect of an oral sorbent AST-120 by liquid chromatography/tandem mass spectrometry. J Chromatogr B Analyt Technol Biomed Life Sci 878: 2997-3002.
276. Ito S, Higuchi Y, Yagi Y, Nishijima F, Yamato H, et al. (2013) Reduction of indoxyl sulfate by AST-120 attenuates monocyte inflammation related to chronic kidney disease. J Leukoc Biol 93: 837-845.
277. Lekawanvijit S, Kompa AR, Manabe M, Wang BH, Langham RG, et al. (2012) Chronic kidney disease-induced cardiac fibrosis is ameliorated by reducing circulating levels of a non-dialysable uremic toxin, indoxyl sulfate. PLoS One 7: e41281.
278. Bolati D, Shimizu H, Niwa T (2012) AST-120 ameliorates epithelial-to-mesenchymal transition and interstitial fibrosis in the kidneys of chronic kidney disease rats. J Ren Nutr 22: 176-180.
279. Yamamoto S, Zuo Y, Ma J, Yancey PG, Hunley TE, et al. (2011) Oral activated charcoal adsorbent (AST-120) ameliorates extent and instability of atherosclerosis accelerated by kidney disease in apolipoprotein E-deficient mice. Nephrol Dial Transplant 26: 2491-2497.
280. Hida M, Aiba Y, Sawamura S, Suzuki N, Satoh T, et al. (1996) Inhibition of the accumulation of uremic toxins in the blood and their precursors in the feces after oral administration of Lebenin, a lactic acid bacteria preparation, to uremic patients undergoing hemodialysis. Nephron 74: 349-355.
281. Takayama F, Taki K, Niwa T (2003) Bifidobacterium in gastro-resistant seamless capsule reduces serum levels of indoxyl sulfate in patients on hemodialysis. Am J Kidney Dis 41: S142-145.
282. Taki K, Takayama F, Niwa T (2005) Beneficial effects of Bifidobacteria in a gastroresistant seamless capsule on hyperhomocysteinemia in hemodialysis patients. J Ren Nutr 15: 77-80.
283. de Zeeuw D (2008) Renal disease: a common and a silent killer. Nat Clin Pract Cardiovasc Med 5 Suppl 1: S27-35.
284. Bugnicourt JM, Godefroy O, Chillon JM, Choukroun G, Massy ZA (2013) Cognitive disorders and dementia in CKD: the neglected kidney-brain axis. J Am Soc Nephrol 24: 353-363.

CURRICULUM VITAE

Henricus Antonius Maria Mutsaers werd geboren op 14 februari 1985 te Oss. Aldaar, behaalde hij in 2003 zijn VWO-diploma aan het Titus Brandsma Lyceum. In datzelfde jaar begon hij aan de opleiding Biomedische Wetenschappen aan de Radboud Universiteit Nijmegen. Zijn eerste schreden in de wondere wereld van wetenschappelijk onderzoek nam hij in 2006, en onder de bezielende begeleiding van Dr. Alwin Scharstuhl en Dr. Frank Wagener voltooide hij zijn bacherlorstage, op het gebied van wondgenezing en littekenvorming, bij de afdeling Farmacologie & Toxicologie van het UMC St. Radboud in het Nijmegen Centre for Molecular Life Sciences (NCMLS). Deze samenwerking beviel goed en de eerste masterstage werd bij dezelfde groep voltooid, wat uiteindelijk resulteerde in enkele wetenschappelijke publicaties. Vervolgens heeft hij in 2008 zijn tweede masterstage gelopen bij de Division of Toxicology and Neurotoxicology, Institute of Environmental Medicine van het Karolinska Institutet in Zweden onder de begeleiding van Dr. Roshan Tofighi en Prof. Dr. Sandra Ceccatelli waar hij, mede dankzij een persoonlijke subsidie van de Hersenstichting Nederland, onderzoek deed naar het effect van stresshormonen op neurale stamcellen. En ook deze stage heeft geresulteerd in een publicatie. Aansluitend heeft hij voor de Minor Medische Microbiologie stage gelopen in Schotland bij het Institute of Immunology and Infection Research, School of Biological Sciences, University of Edinburgh onder de begeleiding van Dr. Peter Cook en Prof. Dr. Andrew MacDonald, alwaar hij de invloed van interleukine 25 op het functioneren van dendritische cellen heeft bestudeerd. In april 2009 startte hij zijn promotie onderzoek naar uremische toxines en chronische nierziekten bij de afdelingen Farmacologie & Toxicologie, Fysiologie en Kindergeneeskunde van het UMC St. Radboud te Nijmegen onder de begeleiding van Dr. Roos Masereeuw, Prof. Dr. Joost Hoenderop en Prof. Dr. Bert van den Heuvel. Het project werd gefinancierd door de Nederlandse Nierstichting en was nauw betrokken bij het BioKid project van het BioMedical Materials programma. Gedurende zijn promotieonderzoek heeft hij meerdere studenten begeleid en zijn werk op nationale en internationale congressen gepresenteerd. Bovendien heeft hij een prijs ontvangen voor het beste abstract van de American Association of Pharmaceutical Scientist (AAPS). Voorts heeft zijn onderzoek geresulteerd in meerdere artikelen en dit proefschrift. Kort na het einde van zijn promotieonderzoek heeft Rick, gefinancierd door een persoonlijke subsidie van de ERA-EDTA, onderzoek gedaan naar het expressie profiel van de FGF-receptor tijdens de ontwikkeling van de nier op het Institut National de la Santé et de la Recherche Médicale (INSERM), Unité 693 in Parijs onder leiding van Dr. Marc Lombès. Momenteel is Rick werkzaam als Postdoc op de afdeling Farmaceutische Technologie en Biofarmacie van de Rijksuniversiteit Groningen onder de supervisie van Dr. Peter Olinga, Prof. Dr. Harry van Goor en Prof. Dr. Ruud Bank alwaar hij onderzoek doet naar orgaan fibrose, met de nier als aandachtsgebied.

LIST OF PUBLICATIONS

Dankers ACA, Mutsaers HAM, Smolinska A, Pertijs JCLM, Verweij V, Sweep FCGJ, Veening JG, Wijmenga SS, Russel FGM, Masereeuw R. Breast cancer resistance protein (BCRP/ABCG2) influences brain energy metabolism by regulating kynurenic acid levels. Submitted.

Mutsaers HAM, Levtchenko EN, Martinerie L, Pertijs JCLM, Allegaert K, Devriendt K, Masereeuw R, Monnens LAH, Lombès M (2014) Switch in FGFR3 and -4 expression profile during human renal development may account for transient hypercalcemia in patients with Sotos syndrome due to 5q35 microdeletions. Accepted for publication in *J. Clin. Endocrinol. Metab.*

Jansen J*, Schophuizen CMS*, Wilmer MJ, Lahham SHM, Mutsaers HAM, Wetzels JFM, Bank RA, van den Heuvel LP, Hoenderop JG, Masereeuw R (2014) A morphological and functional comparison of proximal tubule cell lines established from human urine and kidney tissue. *Exp. Cell Res.* 323: 87-99.

Masereeuw R, Mutsaers HAM, Toyohara T, Abe T, Jhawar S, Sweet DH, Lowenstein J (2014) The kidney and uremic toxin removal: glomerulus or tubule? *Semin. Nephrol.* 34: 191-208. (Invited review).

Mutsaers HAM, Engelke UFH, Wilmer MJG, Wetzels JFM, Wevers, RA, van den Heuvel LP, Hoenderop JG, Masereeuw R (2013) Optimized metabolomic approach to identify uremic solutes in plasma of stage 3-4 chronic kidney disease patients. *PLoS ONE* 8: e71199.

Dankers ACA*, Mutsaers HAM*, Dijkman HBPM, van den Heuvel LP, Hoenderop JG, Sweep FCGJ, Russel FGM, Masereeuw R (2013) Hyperuricemia influences tryptophan metabolism via inhibition of multidrug resistance protein 4 (MRP4) and breast cancer resistance protein (BCRP). *Biochim. Biophys. Acta-Mol. Basis Dis.* 1832: 1715-1722.

Mutsaers HAM, Wilmer MJG, Reijnders D, Jansen J, van den broek PHH, Forkink M, Schepers E, Glorieux G, Vanholder R, van den Heuvel LP, Hoenderop JG, Masereeuw R (2013) Uremic toxins inhibit renal metabolic capacity through interference with glucuronidation and mitochondrial respiration, *Biochim. Biophys. Acta-Mol. Basis Dis.* 1832*:* 142-150.

Moghadasali R*, Mutsaers HAM*, Azarnia M, Aghdami N, Baharvand H, Torensma R, Wilmer MJG, Masereeuw R (2013) Mesenchymal stem cell-conditioned medium accelerates regeneration of human renal proximal tubule epithelial cells after gentamicin toxicity, *Exp. Toxicol. Pathol,* 65*:* 595-600.

Mutsaers HAM, Tofighi R (2012) Dexamethasone enhances oxidative stress-induced cell death in murine neural stem cells, *Neurotox. Res*. 22*:* 127-137.

Mutsaers HAM, van den Heuvel LP, Ringens LHJ, Dankers ACA, Russel FGM, Wetzels JFM, Hoenderop JG, Masereeuw R (2011) Uremic toxins inhibit transport by breast cancer resistance protein and multidrug resistance protein 4 at clinically relevant concentrations, *PLoS ONE* 6: e18438.

Scharstuhl A, Mutsaers HAM, Pennings SWC, Russel FGM, Wagener FADTG (2009) Involvement of VDAC, Bax and ceramides in the efflux of AIF from mitochondria during curcumin-induced apoptosis, *PLoS ONE* 4: e6688.

Scharstuhl A, Mutsaers HAM, Pennings SWC, Szarek WA, Russel FGM, Wagener FADTG (2009) Curcumin-induced fibroblast apoptosis and wound contraction can be regulated in vitro by antioxidants and heme oxygenase: implications for scar formation, *J. Cell. Mol. Med.* 13**:** 712-725**.**

*Both authors contributed equally to this work.

Letters and short items:

Mutsaers HAM, Masereeuw R, Olinga P (2014) Altered tryptophan metabolism and CKD-associated fatigue. Accepted for publication in *Kidney Int*.

Mutsaers HAM, Wilmer MJG, van den Heuvel LP, Hoenderop JG, Masereeuw R (2011) Basolateral transport of the uraemic toxin *p*-cresyl sulfate: role for organic anion transporters?, *Nephrol. Dial. Transplant.* 26*:* 4149.

Mutsaers R (2012) Beware of Janus-faced riddles, *Med. J. Aust.* 197*:* 672.

Mutsaers HAM (2012) Cryptography in modern-day medical science, *Med. J. Aust.* 197*:* 353.

Mutsaers HAM (2012) Unacceptable in the 80s, *J. Inherit. Metab. Dis*. 35*:* 728. (Print only).